Sensitivity and Robustness in Industrial Engineering - Methodologies and Applications to crash tests

Gengjian Qian

▶ **To cite this version:**

Gengjian Qian. Sensitivity and Robustness in Industrial Engineering - Methodologies and Applications to crash tests. Biomechanics [physics.med-ph]. Université Claude Bernard Lyon 1, 2017. English. NNT : . tel-01526187

HAL Id: tel-01526187
https://hal.science/tel-01526187

Submitted on 22 May 2017

HAL is a multi-disciplinary open access archive for the deposit and dissemination of scientific research documents, whether they are published or not. The documents may come from teaching and research institutions in France or abroad, or from public or private research centers.

L'archive ouverte pluridisciplinaire **HAL**, est destinée au dépôt et à la diffusion de documents scientifiques de niveau recherche, publiés ou non, émanant des établissements d'enseignement et de recherche français ou étrangers, des laboratoires publics ou privés.

N°d'ordre NNT : 2017LYSE1064

THESE de DOCTORAT DE L'UNIVERSITE DE LYON
opérée au sein de
l'Université Claude Bernard Lyon 1

Ecole Doctorale N° 162
MEGA (Mécanique, Energétique, Génie Civil, Acoustique)

Spécialité de doctorat : Mécanique

Soutenue publiquement le 05/04/2017, par :
Gengjian Qian

Analyse de sensibilité et robustesse dans le génie industriel - Méthodologies et applications aux essais de chocs

---

Devant le jury composé de :

MASSON, Catherine	Maître de conf	LBA IFSTTAR	Présidente
BOUHADDI, Noureddine	Professeur	Univ Franche Comté	Rapporteur
MARKIEWICZ, Eric	Professeur	Univ Valencienne	Rapporteur
LABESSE, Florence	Maître de conf	IUT Montluçon	Examinateurice
OTTENIO, Mélanie	Maître de conf	LBMC IFSTTAR	Examinateurice
MASSENZIO, Michel	Professeur	UCB Lyon1	Directeur de thèse
BRIZARD, Denis	Chercheur	LBMC IFSTTAR	Co-directeur de thèse
ICHCHOU, Mohamed	Professeur	Ecole Centrale Lyon	Co-directeur de thèse
BLOCH Jean	Docteur	TRANSPOLIS SAS	Invité
GOUBEL Clément	Docteur	GE Renewable Energy	Invité

Thesis reference number : 2017LYSE1064

PhD thesis

Sensitivity and Robustness in Industrial Engineering – Methodologies and Applications to crash tests

---

Presented and defended on 05/04/2017 at IUT Lyon1-Gratte-Ciel

A dissertation submitted in partial fulfillment of the requirements for the degree of

Doctor of University Claude Bernard Lyon 1
(Department of Mechanical Engineering)
By

Gengjian Qian

Graduate Committee :

MASSON, Catherine	Lecturer	LBA IFSTTAR	President
BOUHADDI, Noureddine	Professor	Univ Franche Comté	Reviewer
MARKIEWICZ, Eric	Professor	Univ Valencienne	Reviewer
LABESSE, Florence	Lecturer	IUT Montluçon	Examiner
OTTENIO, Mélanie	Lecturer	LBMC IFSTTAR	Examiner
MASSENZIO, Michel	Professor	UCB Lyon1	Advisor
BRIZARD, Denis	Researcher	LBMC IFSTTAR	Co-Advisor
ICHCHOU, Mohamed	Professor	Ecole Centrale Lyon	Co-Advisor
BLOCH Jean	Doctor	TRANSPOLIS SAS	Guest
GOUBEL Clément	Doctor	GE Renewable Energy	Guest

Foreword

This PhD was funded by the government of China under the State Scholarship Fund of CSC (China Scholarship Council) to study at LBMC (Laboratory of Biomechanics and Impact Mechanics – UMR_T9406), research unit with IFSTTAR (French Institute of science and technology for transport, development and networks) and Claude Bernard Lyon1 University.

This PhD report has been written in English in order to broaden the spectrum of readers and allow non French-speakers to join the PhD committee. A French summary can be found at the end of the document.

Analyse de sensibilité et robustesse dans le génie industriel - Méthodologies et applications aux essais de chocs

Mots clefs : dispositifs de retenue des véhicules, simulation d'impact, l'analyse de sensibilité, la conception robuste

Résumé

Plus d'un million de personnes meurent dans des accidents sur les routes du monde et beaucoup de millions sont gravement blessés chaque année. Selon les études, 'Run-Off-Road accidents (ROR)', c'est-à-dire que le véhicule a au moins une collision avec des équipements routiers, représentent environ 10% des accidents routières, mais 45% de tous les accidents mortels sont des ROR. Les dispositifs de retenue des véhicules (DDR) sont les infrastructures installées sur la route pour fournir un niveau de confinement du véhicule 'hors de contrôle'. La barrière de sécurité routière est un DDR continu installé à côté ou sur la réserve centrale d'une route pour empêcher les véhicules errants de s'écraser sur les obstacles routiers et de les conserver en toute sécurité. Les résultats statistique montrent que l'existence des barrières peut réduire les morts jusqu'à un facteur de 4 par rapport aux collisions contre d'autres obstacles routiers.

Les performances de sauvetage d'un DDR dépendent de la conception de l'appareil. Des normes telles que EN1317 ont normalisé les conditions des essais de chocs sous lesquelles une conception de DDR doit être testée et ont défini les critères pour l'évaluation des performances d'une conception.

En fait, un DDR ne puisse pas vraiment être optimisé: il existe des critères multiples pour l'évaluation de la performance d'un DDR et tous les critères ne peuvent pas être optimisés en même temps; les conditions de travail d'un DDR, c'est-à-dire les conditions d'impact d'un DDR avec un véhicule errant, sont nombreuses; les facteurs incertains du DDR peuvent dégrader les performances d'une conception.

La thèse vise à définir une approche qui peut servir : l'analyse de sensibilité (AS) et la conception robuste du DDR ; enrichissement des normes existantes dans la conception du DDR. Le cas d'une barrière de sécurité routière est spécifié dans l'étude : une barrière a été testée expérimentalement, le programme Ls-Dyna est utilisé pour la simulation de choc de l'appareil ; en tenant compte des propriétés du modèle de choc, les efficacités de différentes méthodes de l'AS ont été étudiées ; les influences des facteurs critiques dont les incertitudes contribuent le plus à l'instabilité de la barrière ont été quantifiées avec les approches d'AS sélectionnées ; compte tenu des incertitudes des facteurs critiques, l'optimisation robuste de multi-objectif de la barrière est réalisée ; des simulations d'impact de la barrière optimisée ont été effectuées sous des conditions d'impact différentes pour évaluer ses performances dans les véritables accidents.

Les approches présentées dans l'article peuvent être utiles pour la conception d'autres DDR ou plus largement d'autres systèmes d'ingénierie complexes. On peut espérer que l'analyse de robustesse et l'analyse de la généralisation (c'est-à-dire l'évaluation de la performance du DDR sous différentes conditions d'impact) du DDR pourraient enrichir les normes de la conception des DDR.

Sensitivity and Robustness in Industrial Engineering – Methodologies and Applications to crash tests

Keywords: Vehicle restraint systems, Crash simulation, Uncertainty and Sensitivity analysis, Robust design, Parameter studies

Summary:

More than 1 million people die in crashes on the world's roads and many millions are seriously injured each year. According to the studies: Run-Off-Road accidents (ROR), i.e. the vehicle run-off the road into the roadside and has at least one collision with either roadside equipment or the roadside itself, "represent about 10% of the total road accidents, while 45% of all fatal accidents are ROR". Vehicle Restraint Systems (VRS) are the infrastructures installed on the road to provide a level of containment for an errant vehicle. Safety barrier is "continuous VRS installed alongside, or on the central reserve, of a road to prevent errant vehicles from crashing on roadside obstacles, and to retain them safely". Statistic results show that "the existence of protective barriers on road can reduce fatalities up to a factor of 4 when compared to collisions against other road obstacles."

The life-saving performances of a VRS depend on the design of the device. Standards such as EN1317 normalized the impact conditions under which a design of VRS must be tested by crash tests, and defined the criteria for performance evaluation of a design. While a VRS cannot really be optimized: Multi-criteria exist for performance evaluation of a VRS and all the criteria cannot be optimized in the same time; the impact conditions of the VRS with the errant vehicle are numerous; uncertain factors of the VRS may degrade the performances of a design.

The thesis aims to define an approach that can serve: sensitivity analysis (SA) and robust design of the VRS; Enrichment for the existing standards in the design of VRS. The case of a safety barrier is specified in the study: a safety barrier has been test experimentally, the program Ls-Dyna was used for crash simulation of the device; considering properties of the crash model, efficiencies of different SA methods were studied and influences of the critical factors whose uncertainties contribute the most to the instability of the barrier were quantified with the selected SA approaches; considering the uncertainties of the critical factors, Multi-Objective robust optimization of the tested barrier were realized; under different impact conditions, crash simulations of the optimized barrier were carried out to evaluate its performances in the real crash accidents.

The approaches presented in the article can be useful for the design of other VRS or more broadly, other complex engineering systems. Hopefully, the robustness analysis and generalization analysis (i.e. performance evaluation of the VRS under different impact conditions) of the safety barrier could enrich the standards for the design of VRS.

Acknowledgments

Firstly, I would like to express my sincere gratitude to my advisors Michel Massenzio, Denis Brizard and Mohamed Ichchou for the continuous support of my Ph.D study and related research, for their patience, motivation, and immense knowledge. Their instructions helped me in all the last three years of research and writing of this thesis.

My thanks go to Sylvie Ronel, Eric Jacquelin for encouraging my research. Their persistent help and useful experience guide me when I encounter difficulties.

I would like to express my gratitude towards the company Transpolis. Specifically Clément Goubel, an ex-researcher at Transpolis and Ph.D of LBMC, who provided me the technical supports and based on whose thesis studies I developed my research.

I would like to my colleagues at LBMC, especially Philippe Vezin for welcoming me at the Laboratory and David Mitton, current director of the lab, for his patience and trust along the past years.

I would like to thank Professor Markiewicz and Professor Bouhaddi who kindly accepted to review my work and proposed valuable suggestions for the redaction of the dissertation. I would also like to thank Florence Labesse, Catherine Masson, Médanie Ottenio and Jean Bloch for taking part in the jury committee.

Thanks to the financing of my country, I am honored to continue my study in France and my achievement is inseparable from the support of my family. Last but not least, let me express my sincere thanks to my family and my country.

Table of content

Introduction 1
Chapter 1 State of the art 6
1.1 The Vehicle Restraint Systems (VRS) 7
1.1.1 Road safety and the role of VRS 7
1.1.2 VRS categories & aims 10
1.1.3 VRS performance analysis---European Norm EN 1317 12
1.1.4 VRS crash test Simulation 16
1.2 Uncertainty & Robust analysis in engineering models 22
1.2.1 Sensitivity Analysis 22
1.2.2 Robust analysis & multi-objective optimization 23
1.2.3 Discussion 24
1.3 VRS performance study and robust design 25
1.4 Conclusions 26
Chapter 2 Methods for sampling based Sensitivity Analysis 27
2.1 Overview of Methods 28
2.1.1 Local Methods 28
2.1.2 Correlation/ Regression Methods 29
2.1.3 Screening Analysis 31
2.1.4 Variance-Based Sensitivity Analysis---Sobol' indices 36
2.1.5 Other sensitivity analysis methods 40
2.1.6 Discussion 42
2.2 Sensitivity Analysis of dynamic three points bending test 45
2.2.1 Experimental test & numerical model 45
2.2.2 SA of dynamic model 46
2.3 Conclusions 53
Chapter 3 Sensitivity Analysis of a W-beam steel VRS 56
3.1 Crash test 57
3.1.1 Device details 57
3.1.2 Test results 59
3.2 Numerical model of the crash test 61
3.2.1 General settings of model 61

3.2.2 Vehicle model 66
3.2.3 VRS model 67
3.2.4 Model validations 72
3.2.5 Discussions 76
3.3 SA of the VRS 77
3.3.1 Uncertain factors & Outputs 77
3.3.2 Two-level screening---Orthogonal Array (OA) 79
3.3.3 Multi-level Screening---Morris Analysis (MA) 80
3.3.4 VBSA---Sobol' indices 81
3.4 Conclusions 83
Chapter 4 Optimization of VRS 84
4.1 Multi-Objective Non-deterministic Optimization (MONO) 85
4.1.1 Multi-Objective Optimization 85
4.1.2 Approaches for MONO 86
4.2 Optimization of VRS 90
4.2.1 Parameters of the optimization process 90
4.2.2 Creation of surrogate model 91
4.2.3 Optimization calculation 92
4.3 Generalization of impact conditions 96
4.4 Conclusions 99
General Conclusions 100
Reference 106
Appendix I Details for Sensitivity analysis of the three points bending test model 112
Appendix II Failure modes of the VRS 116
Appendix III Deformations of the VRS 118
Appendix IV Data for Morris Analysis of the VRS 121
Appendix V Automation of design for VRS 124
Appendix VI French summary 126

List of Figures

Figure I- 1 Redirection of the errant vehicle with the safety barrier 3

Figure 1- 1 Road fatalities per 100 000 inhabitants, 2014 7
Figure 1- 2 Road deaths and the measures taken to reduce accidents in France 8
Figure 1- 3 Fail of a VRS regarding rail continuity 9
Figure 1- 4 Redirection of vehicle by barrier 10
Figure 1- 5 Soft steel permanent VRS and rigid concrete temporary VRS 11
Figure 1- 6 Envelope of combined tolerances for angle and speed 12
Figure 1- 7 Measurement of *THIV* 14
Figure 1- 8 Measurement of W_m and D_m 15
Figure 1- 9 Model of 1991 GM Saturn and 1995 Ford fiesta 17
Figure 1- 10 Reduced Geometro FE model with coarse mesh 17
Figure 1- 11 Detailed Toyota Yaris FE model 17
Figure 1- 12 Multi-Body model segment for the safety barrier 18
Figure 1- 13 Simulation of bolt pull-out: the bolt at the center of the hole 19
Figure 1- 14 Simulation of bolt pull-out: the bolt offset from the center of the hole 19
Figure 1- 15 Multi-body Models of Bolted Connections of safety barrier 19
Figure 1- 16 Detailed modeling of bolts connection of safety barrier 20
Figure 1- 17 Cylindrical soil block aspect of VRS model 20
Figure 1- 18 Simulation of soil-post interaction 21
Figure 1- 19 Boundary constraints' simplifications of the VRS 21
Figure 1- 20 System uncertainties in different science fields 22

Figure 2- 1 Sampling trajectories for Morris analysis 35
Figure 2- 2 Example of box plots 41
Figure 2- 3 Example of scatterplots, with the smoothed estimation lines 41
Figure 2- 4 Compute of *KS* 42
Figure 2- 5 Selection of SA methods 44
Figure 2- 6 SA strategies for different kind of models 44
Figure 2- 7 Bending test of steel reinforced wood beam 45
Figure 2- 8 Numerical model of the bending test 45
Figure 2- 9 Dimensions of the steel reinforced wood beam 46
Figure 2- 10 Moisture Content effect – wood tensile test simulation results 46
Figure 2- 11 Temperature effect – wood tensile test simulation results 47
Figure 2- 12 Deceleration results experimental test 48
Figure 2- 13 Deceleration results simulation analysis 48
Figure 2- 14 Velocity of impactor during bending test 49
Figure 2- 15 Simulation of bending test 49
Figure 2- 16 Parameters screening with FD 51
Figure 2- 17 Parameters screening with HFFD 52
Figure 2- 18 Parameters screening with OA 52
Figure 2- 19 Uncertainties management and SA 54

Figure 3- 1 General view of the VRS crash test 57
Figure 3- 2 Components connections of the VRS 58

Figure 3- 3 Profiles of VRS components 58
Figure 3- 4 Simplified view of the crash test 58
Figure 3- 5 Vehicle trajectory in crash test of the barrier 59
Figure 3- 6 Damage of the barrier and vehicle 59
Figure 3- 7 Deformation parameters of the device 60
Figure 3- 8 Hourglass modes of shell elements 61
Figure 3- 9 Hourglass modes of solid elements 62
Figure 3- 10 Statistic characteristics of material S235 steel 63
Figure 3- 11 S235 steel properties definition 63
Figure 3- 12 Tire side slip/friction curves 64
Figure 3- 13 Typical longitudinal tire/road friction profiles 65
Figure 3- 14 Vehicle model of L.I.E.R. mesh refinement of the right-front part 66
Figure 3- 15 Modification of sharp corner of vehicle model 66
Figure 3- 16 Vehicle damages after crash test 67
Figure 3- 17 Meshes of the VRS components 67
Figure 3- 18 Bolts pull out failure of post-spacer connection 68
Figure 3- 19 Characterization of spring elements to connect the bolts and nuts 69
Figure 3- 20 VRS modeling 69
Figure 3- 21 Bolts pull out failure simulation 70
Figure 3- 22 Deformations of post and ground in real test and simulation 70
Figure 3- 23 Numerical barrier crash model 71
Figure 3- 24 Characterization of spring elements at two ends of barrier model 71
Figure 3- 25 VRS crash test & simulation visual comparison 73
Figure 3- 26 Right front wheel contact with Post at t=0.55s 74
Figure 3- 27 Vehicle velocity during the crash test simulation 75
Figure 3- 28 Energy distribution during crash analysis 75
Figure 3- 29 ASI(t) with accelerations estimated by average value in 50ms 78
Figure 3- 30 ASI(t) with acceleration filtered by the filter 79
Figure 3- 31 ME & Interaction effect with both *THIV* and *D* as criteria for MA 81
Figure 3- 32 Scatterplots of inputs *RT*, *PT*, *PY* and the outputs *THIV*, *D* 82
Figure 3- 33 Evolution of Sobol' indices against sample data size 82

Figure 4- 1 Failure of Pareto efficient design selection with surrogate model 88
Figure 4- 2 Validation of the surrogate model for multi-objective optimization 89
Figure 4- 3 Failure of vehicle redirection when H and E decrease greatly 90
Figure 4- 4 Scatter plot of uncertain factors *PT*, *PY* and outputs *THIV*, *D* 92
Figure 4- 5 Pareto efficient solution of VRS MONO 93
Figure 4- 6 Scatter plot of input *H* and outputs of Pareto efficient solutions 94
Figure 4- 7 Scatter plot of input *E* and outputs of Pareto efficient solutions 94
Figure 4- 8 Scatter plot of input *A* and outputs of Pareto efficient solutions 94
Figure 4- 9 Scatter plot of input *B* and outputs of Pareto efficient solutions 94
Figure 4- 10 Optimal designs obtained with MOD and with MON 95
Figure 4- 11 Optimal designs of VRS obtained with different methods 95
Figure 4- 12 Relationship between impact angle and velocity with *THIV* 98
Figure 4- 13 Relationship between impact angle and velocity with W_m 98

Figure A- 1 DOE with Isight for sensitivity analysis of the beam 113
Figure A- 2 Rail no.4(a)-8(e) after impact 120
Figure A- 3 Auto-optimization of the VRS 125

Figure A- 4 Un modèle d'essai de choc de la barrière 130
Figure A- 5 Synthèse des méthodes d'AS 132
Figure A- 6 Diagramme de decision pour le choix de la méthode d'AS 133
Figure A- 7 Le modèle numérique de l'essai de flexion 134
Figure A- 8 Simulation de l'essai de flexion 134
Figure A- 9 L'essai de choc de la barrière et trajectoire du véhicule 135
Figure A- 10 Profils des composants de la barrière et les maillages des composants 136
Figure A- 11 Le modèle du véhicule de LIER et raffinement des maillages 136
Figure A- 12 Le modèle d'essai de choc de la barrière 137
Figure A- 13 L'essai de choc et la simulation 137
Figure A- 14 *ME* et *Inter* avec *THIV* et *D* comme critères pour Morris criblage 139
Figure A- 15 Evolution des Sobol' indices 140
Figure A- 16 Échec de la réorientation du véhicule 141
Figure A- 17 Des solutions optimales de MONO de la barrière 142
Figure A- 18 Les valeurs d'entrée des solutions optimales 142
Figure A- 19 Relation entre l'angle et la vitesse d'impact avec *THIV* 143
Figure A- 20 Relation entre l'angle et la vitesse d'impact avec *W* 144

List of Tables

Table I- 1 Road fatalities by road user group (France) 2

Table 1- 1: Accident against fixed obstacles in France 2009 9
Table 1- 2: People killed in crash accident with fixed obstacles in France 2014 9
Table 1- 3: Crash tests for performances evaluations of safety barriers 12
Table 1- 4: Different containment levels of the barriers and the relative crash tests 13
Table 1- 5: Severity classes of VRS 15
Table 1- 6: Working width (W_n) classes 16

Table 2- 1 A two-level HFFD for 4 parameters 33
Table 2- 2 Orthogonal Array L8 33
Table 2- 3 Comparison of different SA methods 43
Table 2- 4 Distribution of noisy factors for bending test 47
Table 2- 5 SA of bending test model for $V_{0.02}$ as output criterion 51
Table 2- 6 SA of bending test model for V_{∞} as output criterion 51

Table 3- 1 Test conditions boundaries of TB32 and real test conditions 57
Table 3- 2 Quantitative criteria of VRS performances 60
Table 3- 3 Permanent deformations of the safety barrier 60
Table 3- 4 Comparison of results from the simulation and the test 74
Table 3- 5 Uncertainties on VRS input variables 77
Table 3- 6 OA sampling and simulation outputs of the crash model 79
Table 3- 7 Main effect of OA screening 80
Table 3- 8 Sensitivity analysis of the VRS model in three steps 83

Table 4- 1 Intervals of design variables 90
Table 4- 2 Criteria of initial and the optimized design *e* 99

Table A- 1 Two-level DOE of the bending test 115
Table A- 2 Failure modes analysis of the VRS 117
Table A- 3 Sampling of MA and outputs of results 123
Table A- 4 EN1317 Définition des conditions d'impact 128
Table A- 5 EN1317 indices de sévérité 128
Table A- 6 EN1317 Largeur de fonctionnement 129
Table A- 7 Comparaison des méthodes de l'AS différentes 132
Table A- 8 Comparaison des résultats de l'essai et de la simulation 137
Table A- 9 Les facteurs incertains de la barrière 138
Table A- 10 *ME* des facteurs cribler par OA 139
Table A- 11 L'AS de la barrière en trois étapes 140
Table A- 12 Les intervalles des variables de conception 141

Introduction

Context

Each year, about 1.2 million people die in crashes on the world's roads and many millions are seriously injured. Table I- 1 lists the road fatalities of traffic accident in France [1]: compared to the road fatalities data of 2010, great reductions were observed for car occupants (-68.6%) in 2014, but still the car occupants death contribute the most to the facilities of traffic accidents.

	1990	2000	2010	2013	2014	2014 % change from			
						2013	2010	2000	1990
Cyclists	429	273	147	147	159	8.2	8.2	-41.1	-63.6
Moped users	702	461	248	159	165	3.8	-33.5	-63.8	-77.0
Motorcyclists	1011	947	704	631	625	-1.0	-11.2	-33.3	-39.4
Car occupants	6729	5351	2117	1612	1663	3.2	-21.4	-68.6	-75.8
Pedestrians	496	848	485	465	499	7.3	2.9	-40.5	-67.5
Others	1632	290	291	254	273	7.5	-6.2	-5.2	-57.0
Total	10999	8170	3992	3268	3384	3.5	-15.2	-58.1	-69.8

Table I- 1 Road fatalities by road user group (France) [1]

In France, one third of the people dying on the roads are killed after impacting against a hazard. More than 90% of these accidents are caused because of driver-related reasons, such as 'driver distraction ', 'fast speed', 'drink driving', 'sleeping/actually asleep', etc. Large efforts have been paid to 'driver education'. On the other hand, the development of the passive roadside safety infrastructures, i.e. the Vehicle Restraint Systems (VRS) installed on the road to provide a level of containment for an errant vehicle, can reduce economic costs and save lives when a run-off-road collision happens.

Different categories of the VRS exist for different kinds of purposes. The safety barrier is a continuous VRS installed alongside, or on the central reserve, of a road to stop 'out of control' vehicles from leaving the road and hitting roadside hazards or from crossing into the path of on-coming vehicles. On one hand, the safety barrier stops an errant vehicle from rushing into the sloping ground on the roadside by restraining the vehicle on the road. On the other hand, the barrier protects the roadside facilities and avoids the direct crash of the errant vehicle with rigid fix hazards (trees, parapets, embankments, etc.). Figure I- 1 illustrates the numerical simulation of a vehicle with a safety barrier [2]. Almost all the kinetic energy will be converted into vehicle internal energy in a short time when vehicle collides with rigid fixed objects. The safety barrier 'absorbs' the impact energy with its deformations, redirects the errant vehicle and extends the collision time, which will greatly reduce the impact severity.

The common senses for the design of safety barrier are: "the barrier should contain and redirect the vehicle; the vehicle should not penetrate, underride or override the installation, and should remain upright during and after collision; detached elements should not cause serious injuries to the occupant" [13]. In fact, a safety barrier can't really be 'optimized':

- Minimization of accident severity and minimization of the device deformations are the two antagonistic main objectives in the design of a safety barrier. Soft devices 'absorb' the impact energy with large deformations and prolong the impact period,

which greatly reduce the injuries to the occupants. While the rigidity of a device need to be increased in order to minimize the deformation of the barrier.

- The working conditions of the barrier, i.e. impact conditions of the barrier with the errant vehicle, are numerous: the errant vehicle could be a mini car, a heavy car, a pickup truck or a lorry; a crash accident may occur at straight/curve road; the ground of the road might be flat/slope; the icing of the road could reduce the grip of the tires and influence the performances of the barriers; the crash accidents are at different impact speeds and angles, etc.
- Uncertain factors widely exist in engineering devices and may degrade performance of a nominal design.

In the early days, development of structures aiming to restrain an errant vehicle used to be made using common sense, engineering judgment and many crash tests.

Nowadays, the rules (such as EN1317 [12] [13] in Europe and National Cooperative Highway Research Program report (NCHRP) [3] in the USA) for crash tests and performance evaluations of the VRS are defined. With the development of Computer-aided engineering (CAE) technology, numerical simulations help to reduce economic costs and to analyze the factors that could not be studied with real tests in the design of the VRS.

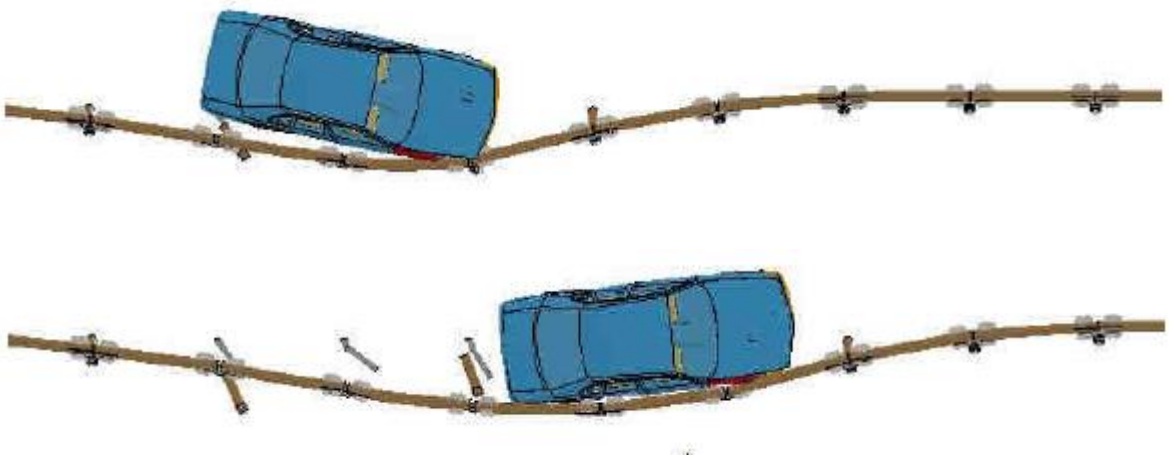

Figure I- 1 Redirection of the errant vehicle with the safety barrier [2]

Aims

The present thesis aims to define an approach that can serve two purposes:

- Methodology for the uncertainty analysis and robust design of the VRS;
- Enrichment for the existing standards in the design of VRS.

Different categories of the VRS exist and the case of a safety barrier is specified in the study: uncertainty analysis and the robust optimization of the selected barrier are realized with CAE. Although all the factors that may influence the performances of the barrier can't be analyzed, the approaches presented in the dissertation can be useful for the design of other VRS or more broadly, other complex engineering systems.

The working conditions of the VRS are numerous and standards are used for the normalization of the design of VRS. For the case of the safety barrier, only one or two crash test under the impact conditions specified in the standards are used for the performance evaluation of a design. Hopefully, the robustness analysis and generalization analysis (i.e. performance evaluation of the VRS under different impact conditions) of the safety barrier could enrich the standards in the design of VRS.

Challenges

Some questions arise from this context analysis:

- Though economically feasible, the design and evaluation of the VRS with CAE usually requires thousands of samples and model runs. While a single crash simulation of a vehicle with a VRS may require several days of CPU time.
- Uncertain factors exist in the VRS and the robustness of a design should be tested.
- The optimization of the VRS is a multi-objective design process: in the design of a safety barrier, the main object is to reduce occupants' injuries in the crash accident; the magnitude of the device deformations should be within acceptable level; and it is preferable to minimize the manufacturing and installation cost of the VRS in the meantime.
- A VRS can only be optimized under the standardized crash test conditions. An optimized device might be infeasible to restrain the vehicle on the road under other crash conditions.

Methodology

Methodology corresponding to the challenges of this research is:

- The numerical model of the studied VRS should be simplified in order to reduce the CPU time of a single simulation.
- Sensitivity analysis (SA) is used to identify qualitatively/quantitatively the inputs whose uncertainties greatly influence the outputs, i.e. the robustness of a model. The proper methods for SA should be chosen in order to quantify influences of the uncertain factors with acceptable number of model runs. SA of the VRS helps to identify the influential factors and quantify their influences on the robustness of the model.
- Considering the influence of the uncertain factors on the model outputs, multi-objective optimization of the VRS will be carried out and the optimized design will be evaluated numerically under different crash conditions.

Document organization

The main tasks of this study include simulation of the VRS crash test, SA methods study for robustness analysis of the model, multi-objective optimization of the device. The organization of the document is as follows:

- The background of the study is given in chapter 1: the VRS is one of the three pillars of the road safety triangle (i.e. driver, vehicle, roadside safety infrastructures such as

the VRS). Uncertainties in the VRS influence the robustness of a design, and complicate the optimization process. In addition, multiple objectives need to be considered in the optimization of the VRS.

- Many sampling-based SA methods have been developed in the literature and they have their advantages and disadvantages. Process for SA of complex engineering systems is studied in chapter 2: the SA methods are presented; SA of a simple engineering model is carried out to test the efficiency of different SA methods; strategy for SA of the VRS and many other complex models is proposed.
- The SA of a VRS is carried out in chapter 3: the performances of a steel VRS has been evaluated through crash test in accordance with EN1317 standard [12] [13]. Real crash test provide a view of the failure modes of the device with one set of parameters. The finite element program LS-DYNA [4] is used for the simulation of the crash test. Numerical model for the crash test is created which includes a vehicle and a VRS, and it has a high accuracy and relatively low calculation cost; SA of the VRS is realized with the numerical model by the strategy summarized in chapter 2.
- The few influential uncertain factors of VRS are identified after SA. Uncertainties reductions of these factors can greatly increase model robustness. Optimization procedure helps to construct VRS of higher performances and of lower economic cost. Multi-objective non-deterministic optimization of the VRS under the specified working conditions is realized in chapter 4. Test vehicles and impact conditions specified in test standards, meant to give an in-service evaluation of roadside safety features performances, are harmonized in order to compare and classify safety performance. The optimized VRS is also tested numerically under varied impact conditions.
- General conclusions are given in the last part of the dissertation.

Chapter 1 State of the art

1.1 The Vehicle Restraint Systems (VRS)

1.1.1 Road safety and the role of VRS

More than 1 million people die in crashes on the world's roads each year, Figure 1- 1 [1] lists road fatalities of the 32 International Road Traffic and Accident Database (IRTAD) member countries in 2014. Half of these countries constitute the league of relatively well-performing countries with fatality rates per 100 000 inhabitants of five or less. Increasing road safety requires acting on the three pillars of the road safety triangle, i.e. Driver education, Vehicle design and Infrastructure design:

- Fatal traffic accidents are mainly due to bad behaviors of the road user. In France 2014 [1]: "inappropriate or excessive speed was the main cause in 26% of fatal crashes; It is estimated that alcohol is the main cause of 19% of fatalities and a contributing factor in 28% of fatal crashes; illegal drugs were a factor in 23% of fatalities and were the main cause of more than 5% of fatal crashes; sickness/fatigue is a contributing factor in 9% of fatal crashes; Not wearing a seat belt or a helmet will also increase the accident severity." Figure 1- 2 illustrated the diminution of road accidents deaths and the measures taken for controlling drink driving and reducing speed in France [5];
- Vehicle design, which takes account of the behavioral and physical limitations of road users, can address a range of risk factors and help to reduce exposure to risk, crash involvement and crash injury severity [6];
- Roadside infrastructures promote safe and informed driving. Infrastructures such as center and edge line striping, drainage systems, lighting, signs and signals helps to create good driving conditions; the Vehicle Restraint Systems (VRS) such as the safety barrier are passive safety equipment aiming at reducing the costs when an accident happens.

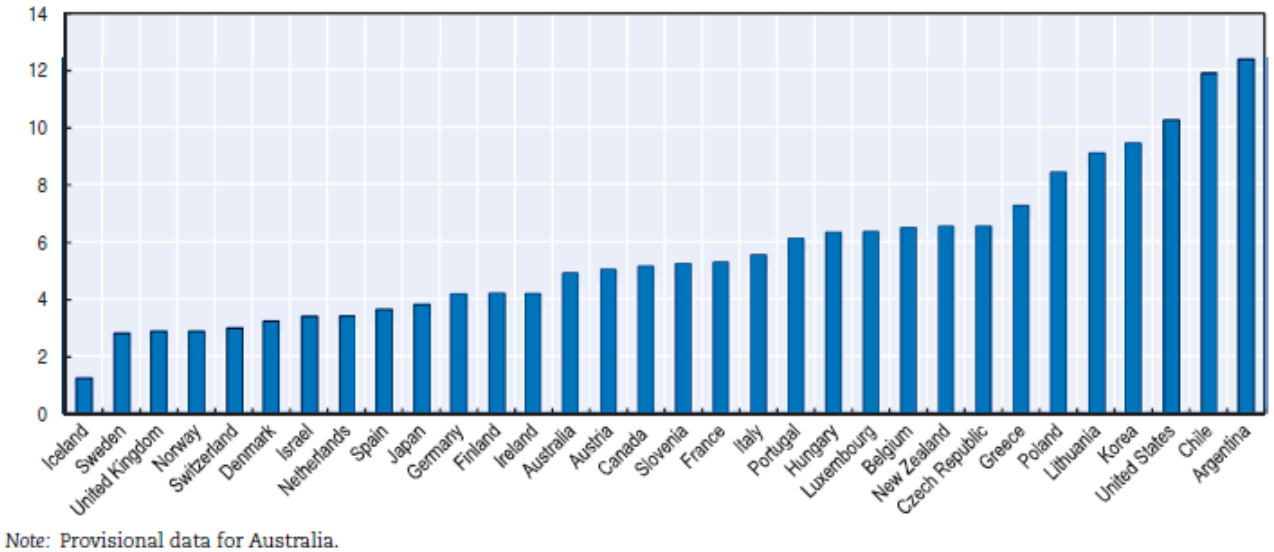

Note: Provisional data for Australia.

Figure 1- 1 Road fatalities per 100 000 inhabitants, 2014 [1]

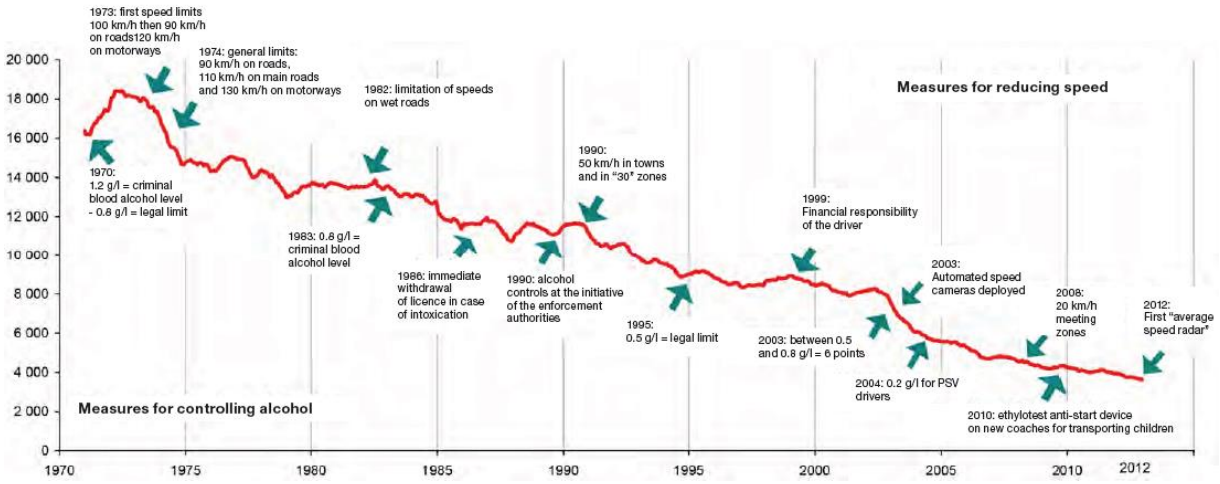

Figure 1- 2 Road deaths in mainland France and the measures taken to reduce speeding and drink driving – 1970 to 2012 [5]

Significant resources have been devoted to developing new vehicle technologies and enforcement campaigns, while the efforts in road safety often neglect the role of passive roadside safety infrastructures. Acting on the driver and on the vehicle surely has its role to play, the European Union Road Federation believes that "investing in road safety infrastructure can offer fast and cost-effective solutions that can reduce fatalities and related health care costs" [7].

The general nature of a Run-Off-Road accident (ROR) is that the vehicle will run-off the road into the roadside and has at least one collision with either roadside equipment. According to the Roadside Infrastructure for Safer European Roads (RISER) project report [8], "ROR represent about 10% of the total road accidents for the respective countries, while 45% of all fatal accidents are ROR". In the design of roads, the placement of certain objects (such as sign posts, trees, slopes, etc.) in the roadside can often not be avoided. Therefore, one of the main factors which determine the severity of these types of accidents is the layout of roadside and the type of objects present which potentially could become collision hazards. "Due to the poor energy-absorbing qualities of many roadside objects, an impact would result in serious damage to the vehicle and more severe injuries to occupants" [9].

Vehicle Restraint Systems (VRS) are the infrastructures installed on the side of the road to provide a level of containment for an errant vehicle. They are an essential component of a modern road infrastructure and constitute one of the most important life-saving devices. Further evidence of the effectiveness of VRS in reducing accidents can be found in the 2009 Annual Road Safety Report in France [10] published by the 'Observatoire National Interministériel de Sécurité Routière'. According to the data available in the report (see Table 1- 1), "the existence of safety barriers on road can reduce fatalities up to a factor of 4 when compared to collisions against other road obstacles". Actually, the presence of a VRS appears to offer the highest level of protection compared to accidents against other fixed obstacles.

Table 1- 2 listed the number of people killed in crash accident with VRS and other roadside fixed obstacles in France 2014 [11]. VRS can avoid the direct crash of a runaway vehicle with roadside fixed obstacles and greatly decrease crash severity. But still 86% of ROR death is caused by directly crash with roadside fixed obstacles. Promotion of the VRS represent an immediately available solution that can, in addition to saving lives, significantly reduce the accident related health care cost.

A well designed VRS could save lives when traffic accident happens, while it is not

always the case. The VRS in Figure 1- 3 fail to restrain the errant vehicle and fatal injuries are caused to the passengers. The design of the VRS plays a role important in the life saving of traffic accidents.

Mainland France	Vehicles involved		Persons killed		Gravity (fatalities/100 vehicle involved)
	Num.	%	Num.	%	
Safety Barriers (one type of VRS)	2811	17.9	185	11	6.6
Trees	1830	11.6	513	30.4	28
Walls, bridge piers	1533	9.7	212	12.6	13.8
Parapets	142	0.9	18	1.1	12.7
Posts	1302	8.3	202	12	15.5
Ditches, slopes, rocky road sides	2249	14.3	316	18.7	14.1
Signs-street furniture	740	4.7	52	3.1	7
Urban obstacles (calming islands, stationed vehicles, other obstacles on the road side)	5156	32.9	208	12.2	4
Totality	15721	100	1688	100	10.7

Table 1- 1: Accident against fixed obstacles in France 2009 [10]

	Urban	Non-urban	Highway	Total
Roadside fixed obstacles	299	670	40	1009
VRS	21	70	72	163
Total	320	740	112	1172

Table 1- 2: People killed in crash accident with VRS and other roadside fixed obstacles in France 2014 [11]

source: http://www.crashforensics.com/papers.cfm?PaperID=53

Figure 1- 3 Fail of a VRS regarding rail continuity

1.1.2 VRS categories & aims

Along with Pedestrian Restrain Systems (i.e. Pedestrian Parapets), the VRS are the main component of road safety infrastructures. An errant vehicle could be a motorcycle, a small car, a bus or a heavy truck; the impact conditions of a vehicle with the VRS are numerous. The VRS are considered as the most "flexible safety device" to withstand a crash from different kind of vehicles in different conditions.

The kinetic energy will be converted into vehicle internal energy in a short time and great damages will be caused to the passengers when vehicle collides with rigid fixed objects (trees or rocks on the roadside for example). The VRS reduce the severity of crash accidents by "dissipate" the initial vehicle kinetic energy and prolong the period of impact. Aiming firstly at reducing the consequences of accidents of an errant vehicle that has lost control of its trajectory, the safety barrier is one of the VRS. The Figure 1- 4 shows how a safety barrier works: the errant vehicle is redirected and its kinetic energy is retained after the impact (top right line A); only a small part of the initial vehicle kinetic energy is transformed into internal energy (top right line B) of the vehicle and barrier (lower right line A and B); the crash process of the vehicle with the barrier is much longer than that with the fixed rigid objects.

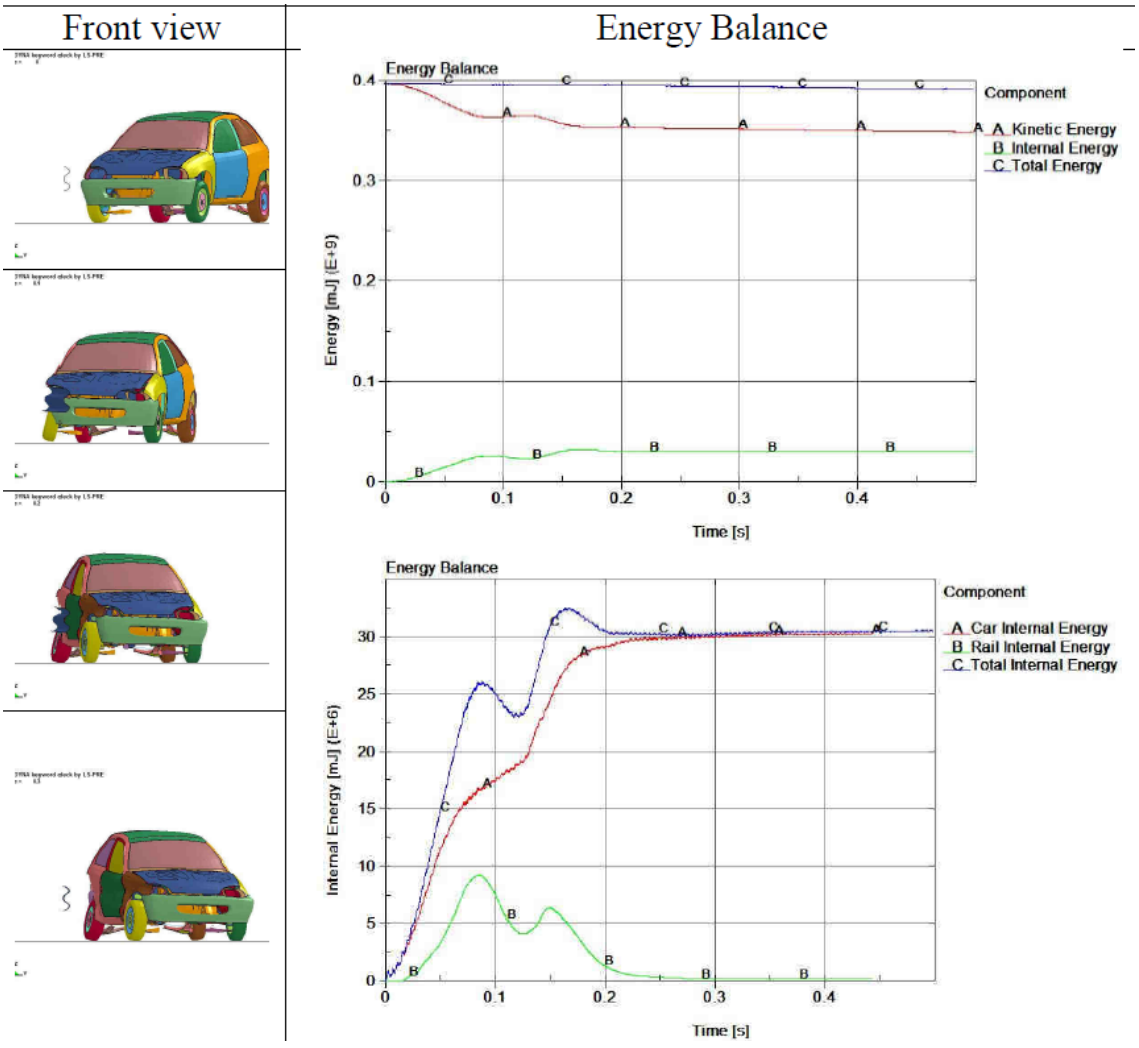

Figure 1- 4 Redirection of vehicle by barrier and energy distributions in impact process [2]

Different types of VRS exist with distinct goals. The VRS are divided into the following categories in the European Norm EN1317 [12]:

- **Safety Barrier** : "continuous VRS installed alongside, or on the central reserve, of a road to prevent errant vehicles from crashing on roadside obstacles, and to retain them safely";
- **Terminal**: "end treatment of a safety barrier, which is to avoid barrier ends from becoming dangerous points for vehicle crash accidents";
- **Transition**: "connection of two safety barriers of different designs and/or performances to guarantee structural continuity and secure the passage of the first barrier to the following one without creating black spots in critical points";
- **Removable barrier section**: "section of a barrier connected at both ends to permanent barriers in order to be removed or displaced wholly or in parts that allows a horizontal opening to be provided";
- **Crash cushion**: "road vehicle energy absorption device installed in front of one or more hazards to reduce the severity of impact and safely stop the vehicle without worse consequences";
- **Vehicle parapet**: "safety barrier installed on the side of a bridge or on a retaining wall or similar structure where there is a vertical drop and which can include additional protection and restraint for pedestrians and other road users";
- **Motorcycles protections systems**: "MPS represent an integrated system or an upgrade which, if applied on a road safety barrier, can reduce the consequence of impact for a motorcyclist after falling".

The VRS can also be classified according to their utilities. Figure 1- 5 shows the soft and rigid VRS. VRS deformations in crash accident are generally inverse to its rigidity, and the impact severity is proportional to rigidity of the VRS. When the risk of VRS crossing is considered acceptable and when the space behind the VRS is compatible with its working width, soft devices are preferred because of their high performance in the reduction of crash severity; In contrast, rigid devices are preferred when the deflection of the device (when impacted by a vehicle) has to be minimized e.g. bridges or highways median strip. Steel beams or even wire ropes are used for fabrication of soft devices, and rigid devices usually consist of concrete or strong steel structures which are able to restrain buses and/or heavy trucks.

The case of safety barrier will be studied in this subject. Without special instructions, the VRS presented in the rest of the dissertation is the safety barrier.

Figure 1- 5 Soft steel permanent VRS and rigid concrete temporary VRS (safety barrier)

1.1.3 VRS performance analysis---European Norm EN 1317

Before being installed on the roadsides, crash tests are needed in order to evaluate the performances of VRS. The European Norm EN 1317-1 [12] describes the general criteria to assess the performance of VRS. In this thesis, we focus on road side safety barrier structural analysis. EN 1317-2 [13] details the performance evaluation of safety barriers. It defines: the testing procedures for the barriers; which test a product should undergo; what are the safety levels and the classes of performance.

1.1.3.a Normalized impact conditions

Table 1- 3 lists the crash test conditions for VRS performance evaluation. Figure 1- 6 shows the maximum deviation allowed for impact speed and angle in the tests.

Test	Vehicle Type	Mass(kg)	Speed(km/h)	Angle(°)
TB11	Car	900	100	20
TB21	Car	1300	80	8
TB22	Car	1300	80	15
TB31	Car	1500	80	20
TB32	Car	1500	110	20
TB41	Rigid Truck	10000	70	8
TB42	Rigid Truck	10000	70	15
TB51	Bus	13000	70	20
TB61	Rigid Truck	16000	80	20
TB71	Rigid Truck	30000	65	20
TB81	Articulated Truck	38000	65	20

Table 1- 3: Crash tests for performances evaluations of safety barriers

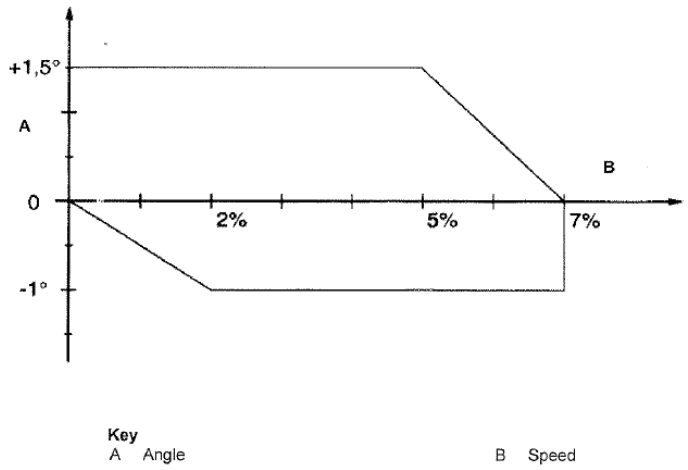

Figure 1- 6 Envelope of combined tolerances for angle and speed [13]

1.1.3.b Criteria of the barriers

A new barrier usually needs to be tested by both a light vehicle and a heavier vehicle to detect its performances to restrain vehicles of different kinds. All performance criteria of the VRS --- which include the containment level, the impact severity level and the deformation level --- will be evaluated through the defined crash tests.

Containment levels

Containment levels, i.e. containment capacities of the VRS are ranked by the increasing impact energy of the heavier vehicle crash test. Table 1- 4 listed the containment levels of the barriers and the relative crash tests a device needs to withstand. To 'pass' the crash tests, a safety barrier needs to fulfill a series of requirements (see EN1317-Part 2 [13]):

- "The safety barrier shall contain and redirect the vehicle without complete breakage of the principal longitudinal elements of the system";
- "Elements of the safety barrier shall not penetrate the passenger compartment of the vehicle";
- "Deformations of, or intrusion into the passenger compartment that can cause serious damage are not permitted";
- "The gravity center of the vehicle shall not cross the center line of the deformed system";
- "The vehicle must not roll over (including rollover of the vehicle onto its side) during or after impact, although rolling pitching and yawing are acceptable";
- "For tests with Heavy Good Vehicles, no more than 5% of the mass of the ballast shall become detached or be split during the test, until the vehicle comes to rest";
- "Following impact into the safety barrier or parapet, the vehicle when bouncing back is not permitted to cross a line parallel to the initial traffic face of the system".

	Level	Tests
Normal	N1	TB31
	N2	TB32+TB11
High	H1	TB42+TB11
	H2	TB51+TB11
	H3	TB61+TB11
Very High	H4a	TB71+TB11
	H4b	TB81+TB11

Table 1- 4: Different containment levels of the barriers and the relative crash tests

Impact Severity levels

Impact Severity is an index to evaluate the injuries caused to the vehicle users in a traffic accident. Its levels are measured by assessing two components [12]:

1) Acceleration Severity Index (*ASI*): non-dimensional acceleration quantity computed using eq. (1-1):

$$ASI = \max\left(\sqrt{\left(\frac{\bar{a}_x(t)}{12g}\right)^2 + \left(\frac{\bar{a}_y(t)}{9g}\right)^2 + \left(\frac{\bar{a}_z(t)}{10g}\right)^2}\right) \tag{1-1}$$

with

$$\bar{a}_{x,y,z} = \frac{1}{\delta}\int_t^{t+\delta} a_{x,y,z}\, dt, \quad \delta = 0.05s \tag{1-2}$$

where g is gravity acceleration and $a_{x,y,z}$ are the acceleration at the mass center of the vehicle in the three directions along the impact time. Acceleration signals are with background noises: eq. (1-2) calculates the $\bar{a}_{x,y,z}$ by taking the moving average over a time interval of 0.05s; filtering of acceleration with a four-pole phaseless Butterworth digital filter can also be used for calculation of $\bar{a}_{x,y,z}$ to removes some unwanted signal.

ASI is calculated to at least two decimal places and reported to one decimal place by mathematical rounding, i.e. 1.14=1.1, 1.15=1.2.

2) The Theoretical Head Impact Velocity (*THIV*): the impact velocity of passenger's head with the vehicle calculated by supposing the head continues moving freely, as the vehicle changes its speed in the crash, until it strikes the interior of the vehicle. The magnitude of the *THIV* is considered to be a measure of the impact severity. The vehicle accelerations and yaw rate are needed for the measurement of *THIV* and its calculation is detailed in EN 1317-Part1 [12] (see Figure 1- 7).

THIV is calculated to at least one decimal place and reported to zero decimal place by mathematical rounding, i.e. 22.4=22, 22.5=23.

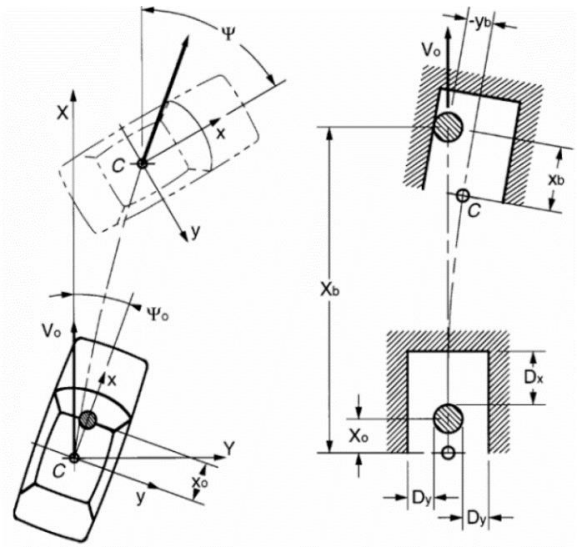

Figure 1- 7 Measurement of *THIV* [12]

The impact severity is divided in 3 levels with level **A** affords a great level of safety and level **C** implies a bad safety level. Table 1- 5 shows the different levels of impact severity as well as the maximum *ASI*/*THIV* permissible values.

Severity Levels	Criteria		
A	*ASI*≤1.0		*THIV*≤33km/h
B	*ASI*≤1.4	And	
C	*ASI*≤1.9		

Table 1- 5: Severity classes of VRS

Deformation of the restraint system

The Figure 1- 8 shows the measurement of the two main criteria of the barrier's deformations during the crash: Dynamic deflection (D_m) and Working width (W_m). W_m is "the maximum lateral distance between any part of the barrier on the undeformed traffic side and the maximum dynamic position of any part of the barrier [13]". It is used to evaluate the space needed behind the barrier for the device to work properly. D_m is calculated as "the distance between the traffic face of the system in its initial condition and it maximum displacement". Normalized Dynamic Deflection (D_n) and Normalized Working Width (W_n) are calculated:

$$D_n = D_m \times \sqrt{\frac{M_s \times \left(V_s \times \sin\alpha_s\right)^2}{M_m \times \left(V_m \times \sin\alpha_m\right)^2}} \tag{1-3}$$

$$W_n = W_u + \left[\left(W_m - W_u\right) \times \sqrt{\frac{M_s \times \left(V_s \times \sin\alpha_s\right)^2}{M_m \times \left(V_m \times \sin\alpha_m\right)^2}}\right] \tag{1-4}$$

where D_m, W_m are measured dynamic deflection and working width, W_u is undeformed width of the system, M_s, V_s, α_s specified vehicle mass, impact velocity, and impact angle in EN1317, M_m, V_m, α_m measured vehicle mass, impact velocity, and impact angle in real tests. Tolerance for the measurement has to be inferior to$d = \pm 0.05\text{m} + 0.1 \times Measure$.

W_n is divided into 8 classes from *W1* to *W8* according to the growing of system deformation (see Table 1- 6). D_n is up to relative regulations (not the EN 1317). While, in fact, the two criteria have positive linear correlation.

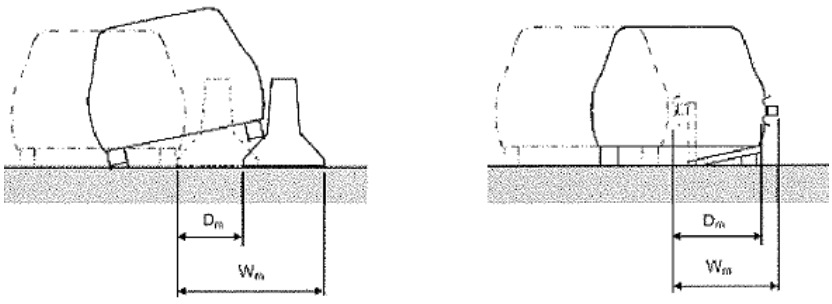

Figure 1- 8 Measurement of W_m and D_m for rigid barriers (left) and soft barriers (right) [13]

W_n classes	Value (m)
W1	*W1*≤0.6
W2	0.6<*W2*≤0.8
W3	0.8<*W3*≤1.0
W4	1.0<*W4*≤1.3
W5	1.3<*W5*≤1.7
W6	1.7<*W6*≤2.1
W7	2.1<*W7*≤2.5
W8	2.5<*W8*≤3.5

Table 1- 6: Working width (W_n) classes

1.1.4 VRS crash test Simulation

Crash testing is commonly associated to the development of new device. But it provides a view of the performance of the device of only one set of parameters. One cannot know how robust the design is because the repetition of crash test is economically infeasible and the system uncertainties (such as uncertainties in material mechanical properties, tolerances of manufacture) cannot be controlled. Numerical simulation tools utilizing nonlinear Finite Element analysis (such as program LS-DYNA) allow the evaluation of the robustness of a design taking into account all these variations.

1.1.4.a Vehicle modeling

Computational Mechanics (CM) has been used for a long time, and restrained by computer calculation capabilities, simple analytical models using beams, masses and springs were developed to examine vehicle dynamics while impacting a road barrier in the early stages. In the 1990s, following codes and computer development, more advanced models emerged but still looked like soap boxes (Figure 1- 9).

National Crash Analysis Centre (NCAC) provides the vehicle and VRS models on their web page [http://www.ncac.gwu.edu/vml/models.html]. Figure 1- 10 and Figure 1- 11 illustrate the reduced and detailed vehicle models that are widely used in current vehicle crash simulations. Detailed models with intensive meshes will no doubt increase the crash simulation accuracy, and they are primarily used in vehicle structure performance studies in crash simulations. To reduce the calculation cost, reduced vehicle models have advantage over detailed models in crash studies where the deformations of the vehicle are not of critical importance and where large numbers of model runs are needed. As for the case of the VRS crash test simulation, detailed models might be used to simulate precisely the crash process, but large number of model runs are needed for the sampling-based parameters studies such as model uncertainty analysis and structural robust design, and the simplified vehicle models are usually needed. Rigid vehicle models are even used when vehicle deformations are of little influence in crash simulations of the VRS [14].

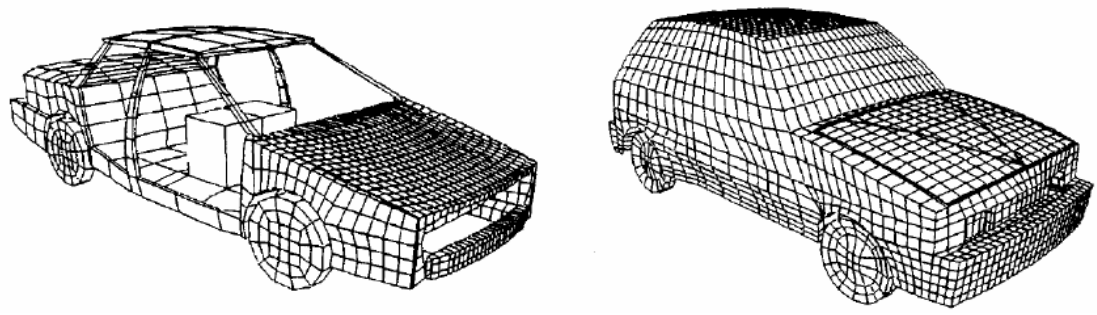

Figure 1- 9 Model of 1991 GM Saturn and 1995 Ford fiesta

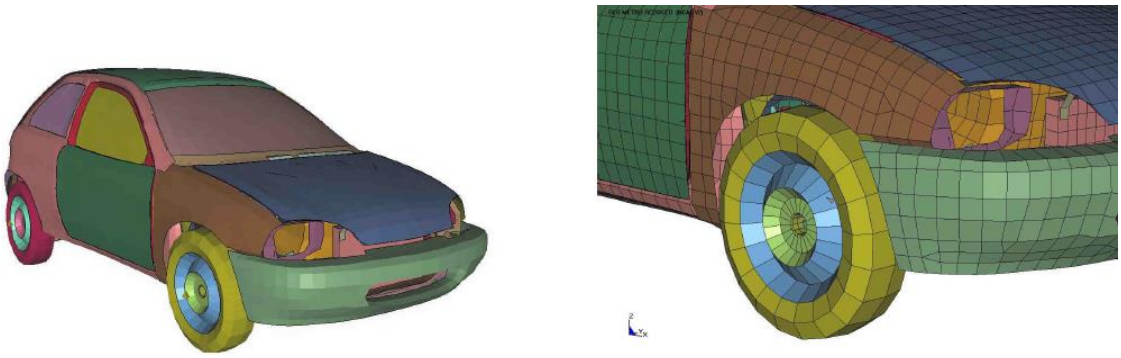

Figure 1- 10 Reduced Geometro FE model with coarse mesh

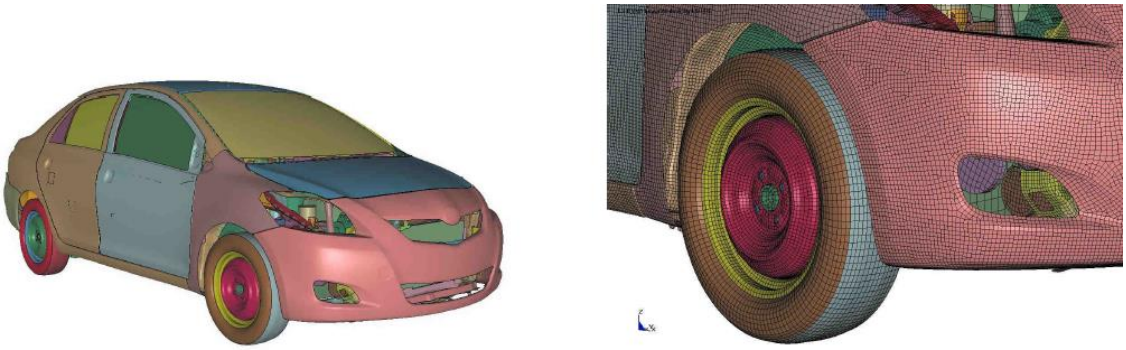

Figure 1- 11 Detailed Toyota Yaris FE model

1.1.4.b VRS models

The modelling of the roadside barrier as well as of the vehicle demands for great accuracy and high skills. By dividing the complex structure into simple subsystems, multibody-system modelling has been used for safety barrier simplifications (see Figure 1- 12) [14]: the VRS was divided into the substructure posts, brackets and rail beams; stiffness, viscosity, friction and impact are captured directly by internal force elements like springs, dampers and contacts.

A. Tabiei and J. Wu [15] summarized the three major issues for safety barrier modelling: bolt connections, soil-post dynamic interaction and effect of barrier ends.

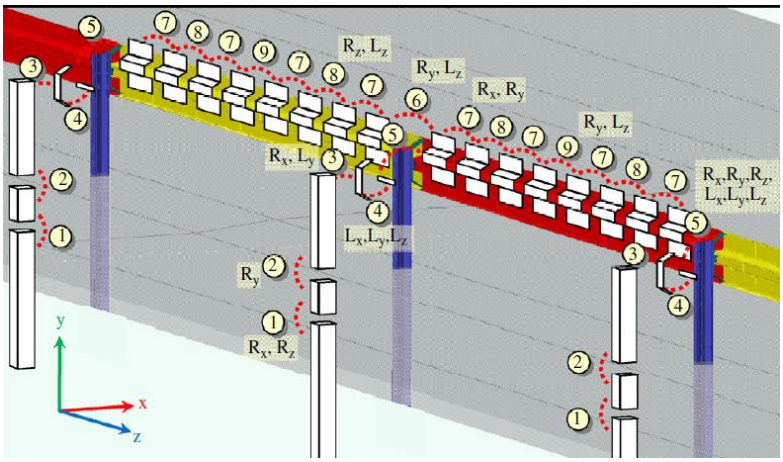

Figure 1- 12 Multi-Body model segment for the safety barrier [14]

Bolt connection

The VRS components (the Posts of support, the Rails of the barrier and the Spacers between the Posts and the Rails) are connected with bolts through slotted holes. In the experimental testing of the VRS, it is observed that some bolt connections are subjected too very high forces that cause the bolts to shear through the rail, spacer or post. This behaviour is very important for accurate simulation of the impact event and influences the redirection of the vehicle. Four different approaches are available to simulate the bolt connection:

- Bolt connection simplification: the bolt connections can be modelled by merging the nodes of the two parts [16]. However, this method does not accurately represent the behaviour of the connections, especially when bolt connection failure happens;
- '*Tied Nodes Sets with Failure*' option in LS-DYNA simulation: this method does not allow any separation of the nodes until failure has occurred. In the actual connection, however, the slotted hole and bolt allow some movement prior to failure;
- Nonlinear Spring elements: Tabiei [15] modelled the VRS components with slotted holes and the bolts in detail and tested the bolt pull-out load curve for force-displacement which characterized the stiffness of the nonlinear springs (see Figure 1- 13, Figure 1- 14). Considering components degree of freedom in bolt connections, Neuenhaus [17] modelled the bolts connection through the multi-body approach (see Figure 1- 15): the shear between the Post and Spacer and the Spacer and Rail were restrained with spring $S_{yz\text{-}shear}$; the tensile bolt load between the Post and Spacer and the Spacer and Rail beam were modelled with spring $S_{x\text{-}tensile}$; the vertical slip of the slotted hole between the Post and Spacer and the horizontal slip of the slotted hole between the Rail and the Spacer were restrained with spring $S_{y\text{-}slot}$ and $S_{x\text{-}slot}$. The challenges of this approach are: the bolt positions relative to the slotted hole might be changed during crash test which influence the spring load Force-Displacement definition (see Figure 1- 13, Figure 1- 14); large efforts are needed to tune the springs in order to simulation precisely the displacement freedoms of the components.
- The bolts can be modelled in detail as depicted in Figure 1- 16: this method is realistic and would yield the best results. However, it is very expensive. Even if the bolts are assumed to be rigid for saving computation time there is still need to have a fine mesh in the vicinity of the bolts. The bolted joints were simulated by modelling the slotted holes and pre-loaded bolt & nut in [18, 19, 20] for detailed analysis.

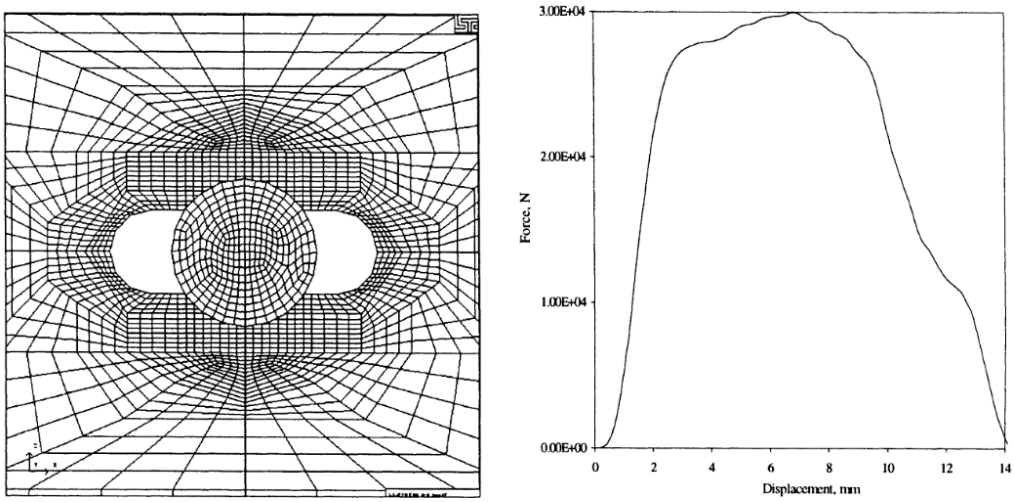

Figure 1- 13 Simulation of bolt pull-out: the bolt at the center of the hole [15]

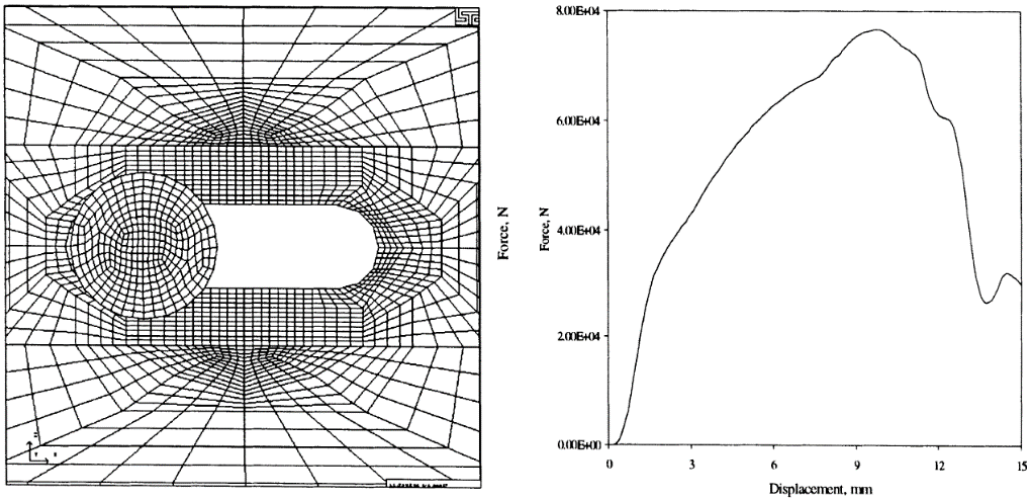

Figure 1- 14 Simulation of bolt pull-out: the bolt offset from the center of the hole [15]

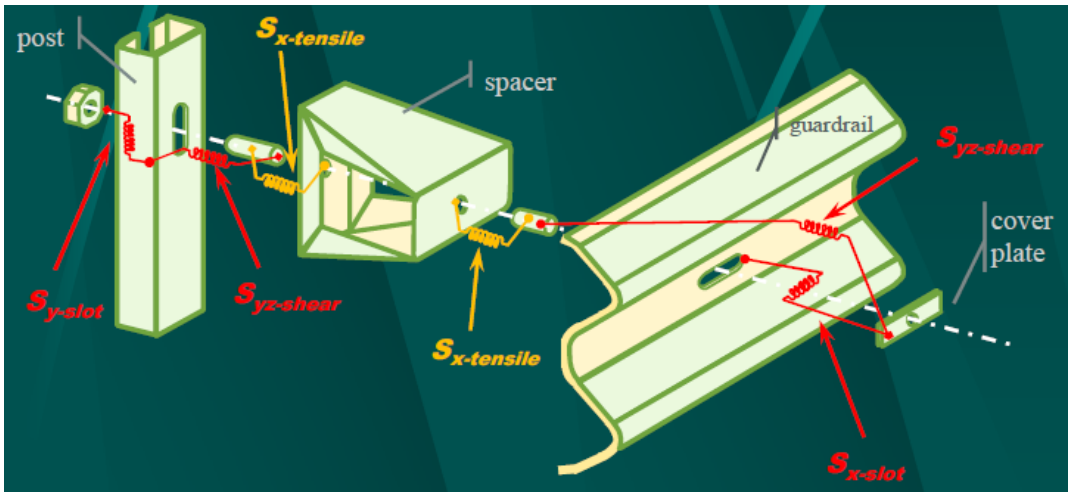

Figure 1- 15 Multi-body Models of Bolted Connections of safety barrier [14]

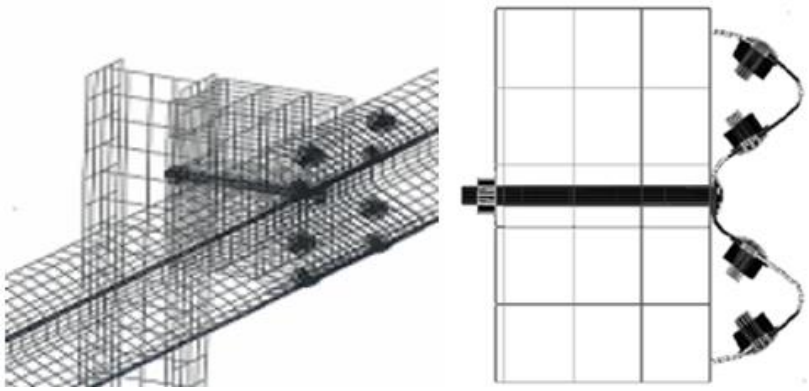

Figure 1- 16 Detailed modeling of bolts connection of safety barrier [19]

Soil simulation

The Posts of the safety barrier are fixed to the ground. The simulation of the Soil-Post interaction, which obviously plays a vital role in the response of the barrier during an impact event, is a complex and important issue. To evaluate the soil material model, it is important that actual physical tests of the soil be simulated. Soil solid materials in LS-DYNA for roadside safety hardware crash test simulations have been developed and solid elements were used to simulate soil in barrier crash test modelling in [19, 20, 21] (Figure 1- 17). Since it is computationally expensive to include the soil FE model in the impact simulation, nonlinear spring elements were used to simulate the soil's response during crash simulation of barriers in [22, 23] (see Figure 1- 18). The soil stiffness can be simulated using normal nonlinear axial springs and nonlinear torsional springs and the force-deflection curves (load curves) of these springs can be obtained from component simulations.

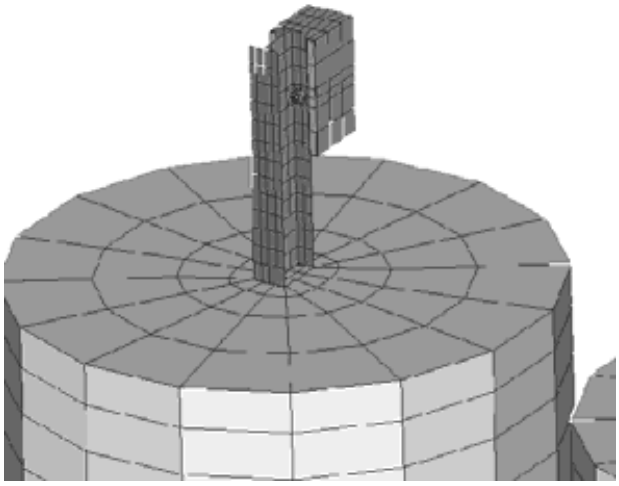

Figure 1- 17 Cylindrical soil block aspect of VRS model to simulate soil-post interaction [19]

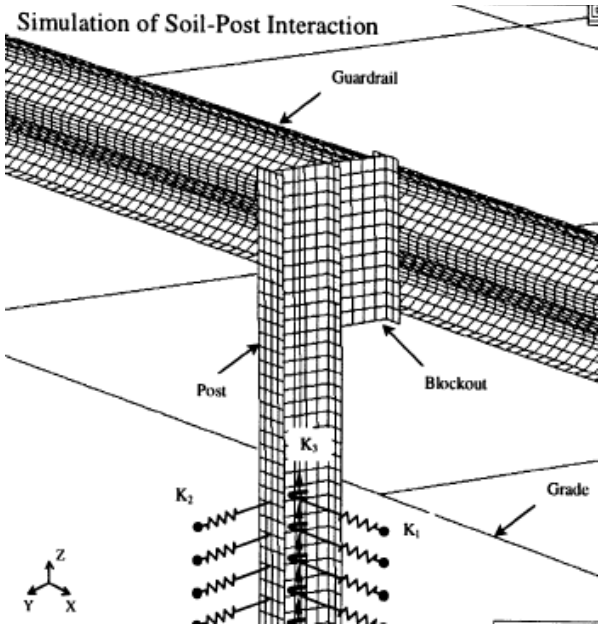

Figure 1- 18 Simulation of soil-post interaction [22]

Barrier continuation loads

The length of the safety barrier being tested shall be sufficient to demonstrate the full performance characteristic of any longer installations. A tested VRS might measure up to a hundred meters in length, and the use of FE model of the entire system is impractical and computationally inefficient. Generally, only the parts in the middle of the barrier will be modelled, and a simulated end effect is included in the proposed FE model. Simulation of the VRS is very much dependent on the accurate representation of the unmodeled portions. Since the barrier redirects impacting vehicles primarily through rail tension, continuations of the barrier were modelled with spring elements to reduce the length of the device in [15, 22, 23] (see Figure 1- 19). The stiffness of the springs can be define through analytical analysis by supposing the stiffness of the spring proportional to the modulus of the material and cross-section of the beam, and inversely proportional to the length of the unmodeled portion of the beam. The springs elements can also be characterized through simulations.

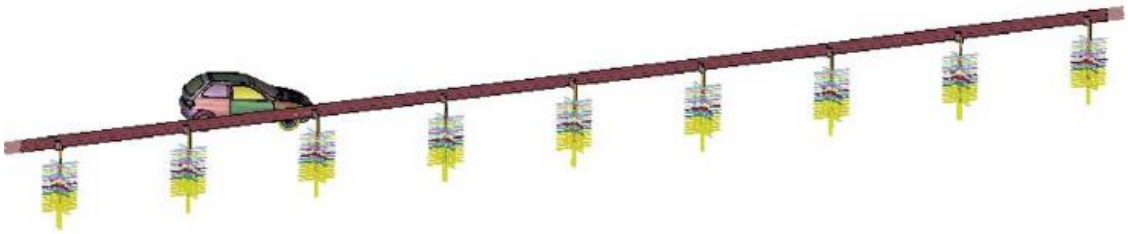

Figure 1- 19 Boundary constraints' simplifications of the VRS with spring elements [15]

1.2 Uncertainty & Robust analysis in engineering models

1.2.1 Sensitivity Analysis

Uncertainties exist in almost every engineering system and "What makes modeling and scientific inquiry in general so painful is uncertainty" [25]. Figure 1- 20 [24] shows the systems uncertainty exist in different science fields. The propagation of uncertainty gives rise to complexities in the simulation of structural behavior.

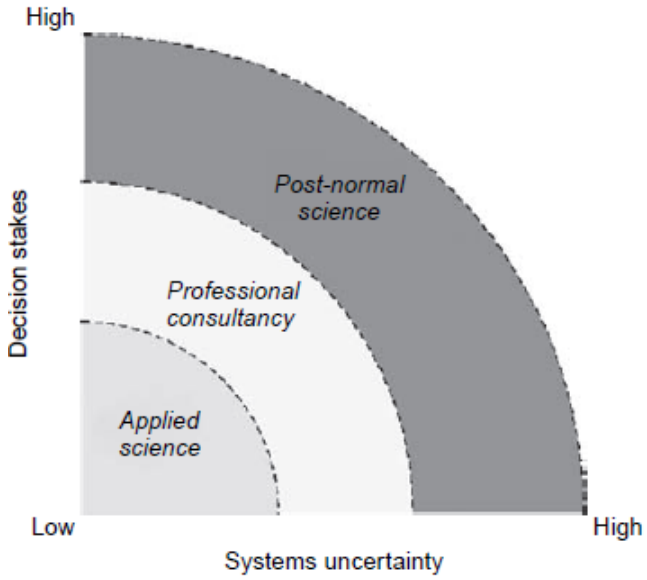

Figure 1- 20 System uncertainties in different science fields [24]

Uncertainty analysis focuses on quantifying uncertainty in model output. "Sensitivity Analysis (SA) is the study of how the uncertainty in the output of a model (numerical or otherwise) can be apportioned to different sources of uncertainty in the model input" [25]. It can be useful for a range of purposes, including [26]:

- "Testing the robustness of the results of a model or system in the presence of uncertainty";
- "Increased understanding of the relationships between input and output variables in a system or model";
- "Uncertainty reduction: identifying model inputs that cause significant uncertainty in the output and should therefore be the focus of attention if the robustness is to be increased";
- "Searching for errors in the model";
- "Model simplification";
- "Enhancing communication from modelers to decision makers";
- "Finding regions in the space of input factors for which the model output is either maximum or minimum or meets some optimum criterion".

Most of the SA methods met in the literature are based on derivatives [27], and indeed the derivative $\partial Y_j / \partial X_i$ of an output Y_j versus an input X_i can be thought as the definition of

the sensitivity of Y_j versusX_i. The derivative-based method is efficient as the model needs to be executed only few times. But this approach can only be used for SA of linear models and derivatives are only informative at local position where they are computed. Models in all science fields are usually nonlinear systems, global SA methods [28], which are based on exploring the full space of the input factors, are developed for qualitative and quantitative parameter studies of such models. Some methods (such as Regression analysis, correlation ratio…) [29] are simple and have a low computational cost for models or systems with special characteristics. Rather than exactly quantifying sensitivity, screening methods [30] tends to have a relatively low computational cost when compared to quantitative approaches, and can be used in a preliminary analysis to weed out non-influential variables before applying a more informative analysis to the remaining set. Variance-based SA methods [28] can measure the main and total sensitivity index quantitatively, but the main constraint of these methods is high calculation cost, especially for models with many variables.

In short, uncertainties widely exist in models of all science fields, and they are inevitable in model evaluations and can significantly degrade the performance of a design. Large number of uncertain parameters may exist in a model, but generally only a few of them are influential. The SA are necessary to determine which input uncertain factors contribute the most to the variability of outputs and well understand the interactions between the uncertain factors. Different methods exist for SA and they have both advantages and disadvantages. Efficient methods are developed for models with known properties. But properties are unknown for many engineering models, sampling–based screening methods are generally used for qualitative analysis of such models and variance-based methods are used for quantitative analysis.

1.2.2 Robust analysis & multi-objective optimization

An optimization problem is to maximize or minimize the model outputs (objectives) by choosing inputs (design variables) values from a set (constraints). Many engineering design problems have multiple conflicting objectives, e.g. it is usually not achievable to minimize the economic cost and optimize the system performance in the same time. Uncertain factors exist in the engineering systems: the model parameters such as mechanical properties of material can't be defined exactly; in addition, influenced by fabrication accuracy, tolerance of the design variables contribute to the model uncertainty. Optimizations considering multi-objective and the uncertain factors of the system are called "Multi-Objective Non-deterministic Optimization (MONO)". These problems intend to obtain design solutions as "best" as possible by weight the importance of different objectives, and at the same time constrain variations in their objectives and constraint functions due to factors uncertainties within an acceptable range.

Approaches have been proposed in the literature to define the objectives and constraints in MONO problems, and methods have been developed for the realization of the optimization:

- Considering uncertainties' influence on both design objectives and the constraints of the design, the optimization approach can be classified into two types [31]: "objective robustness" and "feasibility robustness". Creation of these robustness criteria have been realized by the literature studies.
- Optimization methods such as Genetic Algorithm (GA) are developed to obtain the optimal solutions of multi-objective problems.

1.2.3 Discussion

Sensitivity Analysis (SA) is a natural previous & next step of robust optimization. On one hand, for a model of many uncertain factors, robust optimization taking into considerations of all parameters' uncertainties might be computationally unrealizable, especially when model single run is of high calculation cost. SA helps to identity the few influential parameters among the many uncertain factors that should be focus on in structural robust analysis, and the reduction of uncertain factors greatly reduce the calculation cost of robust optimization. On the other hand, after performing a robust optimization and obtaining a set of optimal and robust solutions, a deeper analysis of the effects of individual parameters could be investigated to determine if any opportunities exist for further reduction in system uncertainty.

1.3 VRS performance study and robust design

Numerous factors such as vehicle types (vehicle dimension, mass, etc.), impact speed & angle, impact point, and uncertainties of material mechanical characteristic have an effect towards device performances and have to be taken into account during numerical simulation process, the challenges include:

- A vehicle may contain thousands of components and a tested VRS may be hundreds of meters in length. The crash simulation of a vehicle with a VRS is commonly of high calculation cost.
- Like many engineering systems, numerous variables exist in a VRS model that may influence its performances. Parameter studies of such models therefore require a large number of model runs.

The variables can be classified into three categories:

- Uncertain input factors: the overall strength of a structure is based on the nominal values of basic strength variables, both material and geometric, such as yield strength and modulus of elasticity of the material, plate thickness. The actual values of these variables are often different from the nominal values and their random variability can cause the strength of the VRS to vary beyond acceptable levels. Due to aging and human factors, the installation conditions of the VRS are also factors with uncertainties.
- Design Variables: the dimensions of the VRS components.
- Working conditions: the goal of a VRS is to redirect an errant vehicle and the impact conditions of a vehicle with the VRS (such as vehicle types, impact velocity & angle, friction between road and tires) are uncountable.

The main tasks for the parameter studies of the VRS are:

- Crash modeling of the VRS with the vehicle: an accurate crash model with relatively low calculation cost is essential for sampling-based parameter studies.
- SA of the VRS to identify the influential uncertain factors and quantify their influences: the performances of a VRS are influenced by its uncertain factors. SA can quantify the influences of uncertain factors and identify influential ones which contribute most to the uncertainty of the VRS performances. Only the influential factors will be focused on in robust analysis and structural optimization of the VRS. Quantitative SA may need thousands of model runs and the research on efficiently quantifying the influences of the uncertain factors is one task of this study.
- Robust optimization to increase the performances of the VRS considering the influences of uncertain factors: dimensions of the VRS components can be treated as design variables and Multi-objective robust optimization of VRS will be realized.
- Performances of a VRS are tested under standardized impact conditions. The crash conditions are unknown in real crash accidents. Optimized VRS needs to be evaluated under different crash conditions.

1.4 Conclusions

The main missions of the thesis are: the methodology study for uncertainty analysis and robust design of the VRS; and enrichment for the performance evaluations procedure of the VRS.

- "Investing in road infrastructure can offer fast and cost-effective solutions that can reduce fatalities and related health care costs [7]." The VRS are roadside passive safety infrastructure aiming to restrain or contain an errant vehicle and can effectively reduce road accident costs. Different categories of the VRS exist for different kinds of purposes. Before being installed on the roadside, the performance of a VRS must be evaluated according to specific standards (EN 1317 in Europe for example) through crash test.
- Engineering systems are characterized by uncertainty. Performances of the VRS can be influenced by many uncertain factors. Experimental crash test can't be multiplied and are economically infeasible for the uncertainty study of VRS. Numerical simulations are widely used in engineering system performance evaluation and structural design, and computational mechanics is being used for crash simulation of the VRS. SA can be used to clarify the influences of uncertainties in the model inputs on outputs' variability.
- Engineering systems commonly have multiple performance criteria. Considering uncertainties of noisy factors, multi-objective robust optimization could be used for design of such models.
- The case of the continuous VRS --- safety barrier --- will be studied. Uncertainty analysis and the robust optimization of the selected barrier will be the main tasks of the thesis, and the methodologies presented in the article can be useful for the design of other VRS or more broadly, other complex engineering systems.

Chapter 2 Methods for sampling based Sensitivity Analysis

2.1 Overview of Methods

Sampling-based approaches to uncertainty and sensitivity analysis are both effective and widely used. There are five basic steps underlying the implementation of a sampling-based uncertainty and Sensitivity Analysis (SA) [29]:

a) "Definition of probability distributions to characterize epistemic uncertainty in analysis inputs";
b) "Generation of samples from uncertain analysis inputs";
c) "Propagation of sampled inputs through an analysis" (e.g. numerical simulation);
d) "Presentation of uncertainty analysis results";
e) "Determination of sensitivity analysis results".

Definition of the inputs' distributions is one of the most important parts for SA of a system as these distributions influence both the uncertainties in outputs and the sensitivity of outputs to the inputs. Many sampling methods are available, including random sampling, Fractional Factorial Sampling, Latin hypercube sampling, etc., and sampling strategies need to be chosen according to the demand of SA methods. Numerical simulation of the engineering system helps to create the relationship between model inputs and outputs, and it is often the most computationally demanding part for the SA. A surrogate model may need to be developed to approximate the complex original model. The relationship between inputs and outputs will be studied through SA. SA strategies---local methods, regression methods, screening analyses, Variance-based methods---are presented.

2.1.1 Local Methods

In the case of large models, calculations of sensitivities across the whole inputs space (i.e. global methods) are computationally prohibitive, local sensitivities [27] can provide useful information on the behavior of the model near the nominal values of parameters.

For model $y=f(\mathbf{k})$, where y is the output and $\mathbf{k}$ is the m-vector of parameters. The solution changes when the values of parameters $\mathbf{k}$ change, and the new solution can be obtained through a Taylor series expansion:

$$y(\mathbf{k}+\Delta\mathbf{k}) = y(\mathbf{k}) + \sum_{j=1}^{m} \frac{\partial y}{\partial k_j}\Delta k_j + \frac{1}{2}\sum_{l=1}^{m}\sum_{j=1}^{m} \frac{\partial^2 y}{\partial k_l \partial k_j}\Delta k_l \Delta k_j + \ldots \tag{2-1}$$

The partial derivatives $\frac{\partial y}{\partial k_j}$ are called first-order local sensitivities, $\frac{\partial^2 y}{\partial k_l \partial k_j}$ are second-order local sensitivities, and so on.

As for the analysis of output variance, suppose $y = f(\mathbf{x})$ in the approximating model of Taylor series

$$y(\mathbf{x}) \stackrel{\text{def}}{=} f(\mathbf{x_0}) + \sum_{j=1}^{nX}\left[\frac{\partial f(\boldsymbol{x_0})}{\partial x_j}\right]\left[x_j - x_{j0}\right] + \cdots \tag{2-2}$$

where $\mathbf{x_0} = [x_{10}, x_{20}, \ldots, x_{nX,0}]$ are the base values for the x_j(e.g. for j=1,2,…,nX, $E(x_j) =$

x_{j0}). And

$$E(y) \stackrel{\text{def}}{=} y(\mathbf{x_0}) + \sum_{j=1}^{nX}\left[\frac{\partial f(\mathbf{x_0})}{\partial x_j}\right] E\left[x_j - x_{j0}\right] + \cdots = y(\mathbf{x_0}) \tag{2-3}$$

If x_j are uncorrelated:

$$V(y) \stackrel{\text{def}}{=} \sum_{j=1}^{nX}\left[\frac{\partial f(\mathbf{x_0})}{\partial x_j}\right]^2 V\left(x_j\right) \tag{2-4}$$

Then the fractional first order contribution of x_j to the variance of y can be approximated by

$$V(y|x_j) \stackrel{\text{def}}{=} \left[\frac{\partial f(\mathbf{x_0})}{\partial x_j}\right]^2 V\left(x_j\right)/V(y) \tag{2-5}$$

with $\sum_{j=1}^{nX} V\left(x_j\right) = 1$ if x_j are uncorrelated.

If x_j are correlated:

$$V(y) \stackrel{\text{def}}{=} \sum_{j=1}^{nX}\left[\frac{\partial f(\mathbf{x_0})}{\partial x_j}\right]^2 V\left(x_j\right) + 2\sum_{j=1}^{nX}\sum_{k=j+1}^{nX}\left[\frac{\partial f(\mathbf{x_0})}{\partial x_j}\right]\left[\frac{\partial f(\mathbf{x_0})}{\partial x_k}\right] Cov\left(x_j, x_k\right) + \cdots \tag{2-6}$$

where $\sum_{j=1}^{nX}\left[\frac{\partial f(\mathbf{x_0})}{\partial x_j}\right]^2 V\left(x_j\right)$ represents the first order contribution of x_j to the variance of y, and the remaining terms represent high order contribution of x_j to the variance of y which are due to the interaction of input parameters x_j.

2.1.2 Correlation/ Regression Methods [32]

2.1.2.a Correlation

Correlation provides a measure of the strength of the linear relationship between x_j and y. Specifically, Correlation Coefficient (CC) $c\left(x_j, y\right)$ between x_j and y is defined by

$$c\left(x_j, y\right) = \frac{\sum_{i=1}^{nS}\left(x_{ij} - \bar{x}_j\right)\left(y_i - \bar{y}\right)}{\left[\sum_{i=1}^{nS}\left(x_{ij} - \bar{x}_j\right)^2\right]^{1/2}\left[\sum_{i=1}^{nS}\left(y_i - \bar{y}\right)^2\right]^{1/2}}$$

where (2-7)

$$\bar{x}_j = \sum_{i=1}^{nS} x_{ij}/nS, \bar{y} = \sum_{i=1}^{nS} y_i/nS$$

$c\left(x_j, y\right)$ has a value between -1 and 1, with a positive correlation indicating that x_j and y tend to increase and decrease together and a negative correlation indicating that x_j and y tend to move in opposite directions. The absolute value of the CC corresponds to a trend

from no linear relationship between x_j and y (with $|c(x_j, y)| \approx 0$) to an linear relationship (with $|c(x_j, y)| \approx 1$).

2.1.2.b Regression

For systems with $|c(x_j, y)| \approx 1$, i.e. linear models, regression analysis can be used to predict the relationship between model inputs and outputs. Supposing y_i is the estimated value of output y_i :

$$\begin{aligned} &SS_{tot} = SS_{reg} + SS_{res} \\ &with \\ &SS_{tot} = \sum_{i=1}^{nS}\left(y_i - \bar{y}\right)^2, SS_{reg} = \sum_{i=1}^{nS}\left(y_i - \bar{y}\right)^2, SS_{res} = \sum_{i=1}^{nS}\left(y_i - y_i\right)^2 \end{aligned} \tag{2-8}$$

The ratio

$$R^2 = SS_{reg} / SS_{tot}, 0 \le R^2 \le 1 \tag{2-9}$$

provides a measure of the extent to which the regression model can match the observed data.

When $R^2 \approx 1$, $SS_{tot} = SS_{reg} + SS_{res} \approx SS_{reg} \Rightarrow SS_{res}$ is small relative to SS_{reg} , which indicates that the regression model is of good accuracy. Conversely, $R^2 \approx 0$ indicates that the regression model is not successful.

The linear models $y = b_0 + \sum_{j=1}^{nX} b_j x_j$ can be reformulated as

$$\begin{aligned} &Y = \sum_{j=1}^{nX} B_j X_j \\ &where \\ &\hat{s} = \left[\sum_{i=1}^{nS}\left(y_i - \bar{y}\right)^2 / \left(nS-1\right)\right]^{1/2}, \hat{s}_j = \left[\sum_{i=1}^{nS}\left(x_{ij} - \bar{x}_j\right)^2 / \left(nS-1\right)\right]^{1/2} \\ &Y = \left(y - \bar{y}\right)/\hat{s}, X_j = \left(x_j - \bar{x}_j\right)/\hat{s}_j, B_j = b_j \hat{s}_j / \hat{s} \end{aligned} \tag{2-10}$$

the unit of Y, X_j, B_j is 1. B_j represent the influence of X_j on the output Y, and it is defined as the standardized regression coefficient (SRCs).

2.1.2.c Rank regression

As for nonlinear regression in sensitivity analysis, the major challenge is the determination of a suitable form for the nonlinear model. A rank transformation can be used to convert a nonlinear but monotonic relationship into a linear relationship. “With this transformation, the values for x_j and y are replaced by their corresponding ranks. Specifically,

the smallest value for a variable is assigned a rank of 1; the next smallest value is assigned a rank of 2; tied values are assigned their average rank; and so on up to the largest value, which is assigned a rank of nS [29]". The main effect of the rank transformation was shown to be a forced linearization of the system, by an artificial increase in the relative weight of the first order terms. And parameters of great 'interaction effect' may be overlooked in the analysis based on the ranks.

2.1.3 Screening Analysis

In dealing with models that are computationally expensive to evaluate and have a large number of input parameters, screening methods can be used to identify the influential parameters that control the output variability (with low computational effort). This is based on the experience that only a few of the input parameters have a significant effect on the model output. "As a drawback, these 'economical' methods tend to provide qualitative sensitivity measure, i.e. they rank the input factors in order of importance, but do not quantify how much more important a given factor is than another"[33]. Design of Experiment (DOE) is used to take samples according to the requirements of the screening analyses.

2.1.3.a Two-level Design of Experiment [34]

Two-level screening, namely two values for each input variables are taken during DOE. The main effect $ME_r(Y)$ of parameter x_r on Y is obtained by taking half the difference of average Y values for x_r at the two levels:

$$ME_r(\mathrm{Y}) = \frac{1}{2}\left(\frac{1}{k_1} \sum_{x_{jr}=1} y_j - \frac{1}{k_0} \sum_{x_{jr}=0} y_j \right) \quad (2\text{-}11)$$

where the number of samples with x_r at level '1' is k_1, the number of samples with x_r at level '0' is k_0. SA analysis with inputs' at only two levels can greatly reduce the samples required, but no information is obtained about the linearity or continuity of the model and it can only be used for the analysis of monotonous models.

Parameter Study (PS)

The most evident way to take samples is to vary each factor independently over the two levels, holding all others at the specified baseline design. Small number of samples is used, but it does not account for interactions among factors and as it takes only one sample for each factor at each level, output uncertainties are largely influenced by single calculation result.

One-at-a-Time (OAT)

The value of only one parameter is changed between two consecutive simulations. This sampling strategy is efficient for linear model analysis. Supposing a polynomial model

$$Y = b_0 + \sum_{r=1}^{k} b_r X_r{}^{i_r}, i_r \geq 1 \tag{2-12}$$

with the OAT sampling :

$$\begin{bmatrix} 1 & 0 & 0 & 0 & \cdots & 0 \\ 1 & 1 & 0 & 0 & \cdots & 0 \\ 1 & 1 & 1 & 0 & \cdots & 0 \\ 1 & 1 & 1 & 1 & \cdots & 0 \\ \vdots & \vdots & \vdots & \vdots & \ddots & \vdots \\ 1 & 1 & 1 & 1 & \cdots & 1 \end{bmatrix} \begin{pmatrix} b_0 \\ b_1 \\ \vdots \\ b_k \end{pmatrix} = \begin{pmatrix} y_1 \\ y_2 \\ \vdots \\ y_{k+1} \end{pmatrix} \tag{2-13}$$

where every variable X_i takes only two values, 0 and 1, and only one variable changes its value between each pair of consecutive sampling (i.e. between two consecutive lines in the matrix). The quantity $\Delta y_i = y_{i+1} - y_i$ is an estimate of the effect on Y of changing X_i from 0 to 1, yielding:

$$\begin{bmatrix} 1 & 0 & 0 & 0 & \cdots & 0 \\ 0 & 1 & 0 & 0 & \cdots & 0 \\ 0 & 0 & 1 & 0 & \cdots & 0 \\ 0 & 0 & 0 & 1 & \cdots & 0 \\ \vdots & \vdots & \vdots & \vdots & \ddots & \vdots \\ 0 & 0 & 0 & 0 & \cdots & 1 \end{bmatrix} \begin{pmatrix} b_0 \\ b_1 \\ \vdots \\ b_k \end{pmatrix} = \begin{pmatrix} y_1 \\ y_2 - y_1 \\ \vdots \\ y_{k+1} - y_k \end{pmatrix} \tag{2-14}$$

The estimated average values of Y are :

$$y_{X_i=0} = \frac{1}{i}\sum_{j=1}^{i} y_j \quad y_{X_i=1} = \frac{1}{k+1-i}\sum_{j=i+1}^{k+1} y_j \tag{2-15}$$

through which we can determine the influence of a parameter X_i on Y.

Factorial Designs (FD) & Fractional Factorial Designs (FFD)

To take into consideration of all the combinations of all k factors at the 2 levels, 2^k samples are taken for full Factorial Design (FD). Therefore the main disadvantage of using a FD is the enormous number of simulations required, especially for models with many uncertain factors. Fractional Factorial Designs (FFD), consisting of a carefully chosen fraction of the full factorial design, can greatly decrease the number of samples.

Table 2- 1 shows a two-level Half-Fractional Factorial Design (HFFD) for 4 parameters (values of X_1,X_2,X_3 are obtained through two-level full factorial design), where '-1' represents low value and '1' represents high value. Note that half the values in each column are 1, and the other half are -1. Any two columns $(X_i, X_j)_{i \neq j}$ have the property that the four combinations (1,1), (1,-1), (-1,1), (-1,-1) each occur the same number of times. Instead of the FD for 4 parameters, of which 2^4 samples are needed, we realize a design with only 2^3 samples by HFFD. Similarly, only 2^{k-n} samples are required with $1/2^n$-FFD from the all 2^k combinations, with $2^{k-n}>k$. There are also other ways to achieve FFD, for example, the

Hadamard matrix can be used to decide the values of parameters and construct a similar parameter table.

X_1	X_2	X_3	$X_4=X_1X_2X_3$
1	1	1	1
-1	1	1	-1
1	-1	1	-1
-1	-1	1	1
1	1	-1	-1
-1	1	-1	1
1	-1	-1	1
-1	-1	-1	-1

Table 2- 1 A two-level HFFD for 4 parameters

Orthogonal Array

Although with relatively low accuracy, DOE with Orthogonal Arrays (OA) [35] is one of the most efficient sampling methods for FFD. Table 2- 2 listed the OA for a two-level DOE of seven factors (A-G), any two columns of the array are orthogonal, and only 8 samples are chosen for SA of a model with 7 factors.

A	B	C	D	E	F	G
+1	+1	+1	+1	+1	+1	+1
+1	+1	+1	-1	-1	-1	-1
+1	-1	-1	+1	+1	-1	-1
+1	-1	-1	-1	-1	+1	+1
-1	+1	-1	+1	-1	+1	-1
-1	+1	-1	-1	+1	-1	+1
-1	-1	+1	+1	-1	-1	+1
-1	-1	+1	-1	+1	+1	-1

Table 2- 2 Orthogonal Array L8

2.1.3.b Cotter's Design

Cotter's Design (CD), i.e. systematic fractional replicate design [30], does not require any prior assumptions about interactions. It requires the following $2k+2$ runs for k factors:

- One initial run with all factors at their low levels;
- k runs with each factor in turn at its upper level, while all other k-1 factors remain at their low levels;
- k runs with each factor in turn at its low level, while all other factors remain at

their upper levels;

- One run with all factors at their upper levels.

Denote the resulting outputs by $y_0, y_1, ..., y_k, y_{k+1}, ..., y_{2k}, y_{2k+1}$. The following equations can be used to estimate the order of importance for the factors:

$$M(j) = |C_e(j)| + |C_o(j)|$$
$$\text{with}$$
$$C_e(j) = \frac{1}{4}\left[\left(y_{2k+1} - y_{k+j}\right) - \left(y_j - y_0\right)\right] \tag{2-16}$$
$$C_o(j) = \frac{1}{4}\left[\left(y_{2k+1} - y_{k+j}\right) + \left(y_j - y_0\right)\right]$$

A major problem of CD is that an important factor may remain undetected. In fact, when a factor has effects that cancel each other out, the measures may fail. Moreover, this design has the disadvantage of lack of precision.

2.1.3.c Multi-level screening--- Morris Analysis

Morris Analysis (MA), i.e. Elementary Effect Method [28, 36], is a multi-level screening method based on the concept of two successive points within a trajectory differing from each other only in one dimension by a fixed amount of Δ. Consider a model with *k* independent inputs which varies in the *k*-dimensional unit cube across *p* selected levels. The Elementary Effect of the *i*th input factor EE_i is defined as

$$EE_i = \frac{\left[Y\left(X_1, X_2, ..., X_{i-1}, X_i + \Delta, ..., X_k\right) - Y\left(X_1, X_2, ..., X_k\right)\right]}{\Delta} \tag{2-17}$$

where *Y* represents the model under study and *k* is the number of model parameters. One *EE* per parameter is produced from each trajectory. It estimates at different points in the input space the main effect of a factor by computing *r* trajectories with *k*+1 model evaluations for each trajectory, and then taking their average.

MA begins by creating the trajectories with the highest spread. There are many strategies that can be used to choose these trajectories. The distance d_{ml} between a pair of trajectories *m* and *l* and the total distance $D_{ijkl...}$ of the all selected trajectories are defined in equations (2-18) and (2-19). Large number of $D_{ijkl...}$ means high spread of the trajectories. The *r* trajectories $\{i, j, k, l, ...\}$ with the highest value of $D_{ijkl...}$ are chosen.

$$d_{ml} = \sum_{i=1}^{k+1}\sum_{j=1}^{k+1}\sqrt{\sum_{z=1}^{k}\left[X_z^{(i)}(m) - X_z^{(j)}(l)\right]^2}, m \neq l \tag{2-18}$$

$$D_{ijkl...} = \sqrt{d_{ij}^2 + d_{ik}^2 + d_{il}^2 + ... + d_{jk}^2 + d_{jl}^2 + ... + d_{kl}^2 + ...} \tag{2-19}$$

Elementary effect of the *j*th trjectory in their *i*th component is:

$$EE_i^j\left(x^{(l+1)}\right)=\frac{\left[y\left(x^{(l)}\right)-y\left(x^{(l+1)}\right)\right]}{\Delta} \tag{2-20}$$

To analyze the sensitivity of each factor, the main effect μ_i and the interaction effect σ_i of input X_i are defined as:

$$\mu_i=\frac{1}{r}\sum_{j=1}^{r}EE_i^j \tag{2-21}$$

$$\sigma_i^2=\frac{1}{r-1}\sum_{j=1}^{r}\left(EE_i^j-\mu\right)^2 \tag{2-22}$$

However, μ_i may not detect some parameters to be influential due to positive and negative EE_i values canceling each other for non-monotonous models. Instead of μ_i, the mean of the absolute values of EE_i , μ_i* [37] is recommended for main effect calculation of a factor.

$$\mu_i^*=\frac{1}{r}\sum_{j=1}^{r}|\,EE_i^j\,| \tag{2-23}$$

	X_1	X_2	X_3	X_4	X_5	X_6
	0	2/3	1	0	0	1/3
	0	2/3	1	0	0	1
	0	0	1	0	0	1
t_1	2/3	0	1	0	0	1
	2/3	0	1	2/3	0	1
	2/3	0	1/3	2/3	0	1
	2/3	0	1/3	2/3	2/3	1
	0	1/3	1/3	1	1	2/3
	0	1	1/3	1	1	2/3
	0	1	1	1	1	2/3
t_2	2/3	1	1	1	1	2/3
	2/3	1	1	1	1	0
	2/3	1	1	1	1/3	0
	2/3	1	1	1/3	1/3	0
	1	2/3	0	2/3	1	0
	1	2/3	0	0	1	0
	1/3	2/3	0	0	1	0
t_3	1/3	2/3	0	0	1/3	0
	1/3	0	0	0	1/3	0
	1/3	0	2/3	0	1/3	0
	1/3	0	2/3	0	1/3	2/3
	1	1/3	2/3	1	0	1/3
	1	1/3	2/3	1	0	1
	1	1/3	0	1	0	1
t_4	1	1/3	0	1/3	0	1
	1	1/3	0	1/3	2/3	1
	1	1	0	1/3	2/3	1
	1/3	1	0	1/3	2/3	1

Figure 2- 1 Sampling trajectories for Morris analysis [28]

Figure 2- 1 shows an example of sampled trajectories of 4 trajectories and 6 input parameters with $p=4, \Delta=2/3$. We chose firstly a base value for input vector $\boldsymbol{X}$, we increase or decrease one parameter of input vector $\boldsymbol{X}$ by Δ to form another sample point.

MA is of relatively low computational cost. The design requires about one model evaluation per computed elementary effect, and a number r of elementary effects are computed for each factor. And the number of runs N is linear function of the number of examined factors k: $N = r \times (k+1)$.

MA can determine which input factors could be considered to have effects which are negligible, linear and additive, or nonlinear or involved in interactions with other factors. This method is ideal when the number of input factors is too large to allow the computationally expensive quantitative analysis. It helps to identify the few factors that are influential. The main disadvantage of the method is that individual interactions among factors cannot be estimated. The method can only provide an 'overall' measure of the interactions of a factor with the rest of the model.

2.1.4 Variance-Based Sensitivity Analysis---Sobol' indices

Working within a probabilistic framework, Variance-Based Sensitivity Analysis (VBSA) [38] decomposes the variance of the output of the model into fractions which can be attributed to inputs or sets of inputs. The VBSA measure sensitivity across the whole input space can deal with nonlinear responses, and measure the effect of interactions in non-additive systems.

For a model $Y=f(X_1, X_2,\ldots, X_k)$, we fix factor X_i at a particular value x_i^*, let $V_{X_{\sim i}}(Y \mid X_i)$ be the resulting variance of Y, take over $X_{\sim i}$ (all factors but X_i). $V_{X_{\sim i}}(Y \mid X_i)$ ignores the influence of X_i. The smaller $V_{X_{\sim i}}(Y \mid X_i)$, the greater the influence of X_i. It measures the sensitivity on the position of x_i^*. We take instead the average of $V_{X_{\sim i}}(Y \mid X_i)$ over input interval of x_i, i.e. $E_{X_i}\left(V_{X_{\sim i}}(Y \mid X_i)\right)$, the dependence on x_i^* will disappear. The smaller $E_{X_i}\left(V_{X_{\sim i}}(Y \mid X_i)\right)$, the more important a factor, and the main effect index S_i:

$$S_i = 1 - \frac{E_{X_i}\left(V_{X_{\sim i}}(Y \mid X_i)\right)}{V(Y)} = \frac{V_{X_i}\left(E_{X_{\sim i}}(Y \mid X_i)\right)}{V(Y)}, 0 \le S_i \le 1 \qquad (2\text{-}24)$$

with

$$E_{X_i}\left(V_{X_{\sim i}}(Y \mid X_i)\right) + V_{X_i}\left(E_{X_{\sim i}}(Y \mid X_i)\right) = V(Y) \qquad (2\text{-}25)$$

For model of independent parameters, we can use the main effect index to measure the influence of X_i on Y, and a high value of S_i signals an important variable.

In a model which has interactions between its k input parameters. The full analysis is composed of

$$\sum_i S_i + \sum_i \sum_{j>i} S_{ij} + \sum_i \sum_{j>i} \sum_{l>j} S_{ijl} + \ldots + S_{123\ldots k} = 1$$

with

$$S_{ij} = \frac{V_{X_i,X_j}\left(E_{X_{\sim i,\sim j}}\left(Y \mid X_i, X_j\right)\right)}{V(Y)} - S_i - S_j$$

$$S_{ijl} = \frac{V_{X_i,X_j,X_j}\left(E_{X_{\sim i,\sim j,\sim l}}\left(Y \mid X_i, X_j, X_l\right)\right)}{V(Y)} - S_{ij} - S_{jl} - S_{il} - S_i - S_j - S_l \quad (2\text{-}26)$$

...

where $S_{ij}, S_{ijl}, \ldots, S_{123\ldots k}$ represent the high order influence of parameter interactions on sensitivity analysis of Y. The sensitivity indices are 2^k-1 and it is complicate to compute all these indices. Instead, we can evaluate the importance of parameter with the first order sensitivity index and the total effects index of a parameter. The total effects of X_i is:

$$S_{T_i} = \left(1 - \frac{V_{X_{\sim i}}\left(E_{X_i}\left(Y \mid X_{\sim i}\right)\right)}{V(Y)}\right) = \frac{E_{X_{\sim i}}\left(V_X\left(Y \mid X_{\sim i}\right)\right)}{V(Y)} = S_i + \sum_{j \neq i} S_{ij} + \sum_{j \neq i} \sum_{l \neq j, l \neq i} S_{ijl} + \ldots + S_{123\ldots k} \quad (2\text{-}27)$$

The total normalized influence minus the influence of all variables except X_i, which means the total effects that contain the influence of X_i. A factor X_i is non-influential only when its total effect is 0.

Computation of Sobol' indices:

Instead of computing directly S_i and S_{Ti}, we tend to evaluate their values with some approximations which will greatly reduce the calculation cost.

Substituted-column method [28]

Generate a (N, $2k$) matrix of random numbers (k is the number of inputs) and define two matrices of data (**A** and **B**), each containing half of the sample. Define a matrix $\mathbf{C_i}$ formed by all columns of **B** except the ith column, which is taken from **A**:

$$\mathbf{A} = \begin{bmatrix} x_1^{(1)} & x_2^{(1)} & \cdots & x_i^{(1)} & \cdots & x_k^{(1)} \\ x_1^{(2)} & x_2^{(2)} & \cdots & x_i^{(2)} & \cdots & x_k^{(2)} \\ \vdots & \vdots & \ddots & \vdots & \ddots & \vdots \\ x_1^{(N-1)} & x_2^{(N-1)} & \cdots & x_i^{(N-1)} & \cdots & x_k^{(N-1)} \\ x_1^{(N)} & x_2^{(N)} & \cdots & x_i^{(N)} & \cdots & x_k^{(N)} \end{bmatrix} \quad (2\text{-}28)$$

$$\mathbf{B} = \begin{bmatrix} x_{k+1}^{(1)} & x_{k+2}^{(1)} & \cdots & x_{k+i}^{(1)} & \cdots & x_{2k}^{(1)} \\ x_{k+1}^{(2)} & x_{k+2}^{(2)} & \cdots & x_{k+i}^{(2)} & \cdots & x_{2k}^{(2)} \\ \vdots & \vdots & \ddots & \vdots & \ddots & \vdots \\ x_{k+1}^{(N-1)} & x_{k+2}^{(N-1)} & \cdots & x_{k+i}^{(N-1)} & \cdots & x_{2k}^{(N-1)} \\ x_{k+1}^{(N)} & x_{k+2}^{(N)} & \cdots & x_{k+i}^{(N)} & \cdots & x_{2k}^{(N)} \end{bmatrix} \tag{2-29}$$

$$\mathbf{C_i} = \begin{bmatrix} x_{k+1}^{(1)} & x_{k+2}^{(1)} & \cdots & x_{i}^{(1)} & \cdots & x_{2k}^{(1)} \\ x_{k+1}^{(2)} & x_{k+2}^{(2)} & \cdots & x_{i}^{(2)} & \cdots & x_{2k}^{(2)} \\ \vdots & \vdots & \ddots & \vdots & \ddots & \vdots \\ x_{k+1}^{(N-1)} & x_{k+2}^{(N-1)} & \cdots & x_{i}^{(N-1)} & \cdots & x_{2k}^{(N-1)} \\ x_{k+1}^{(N)} & x_{k+2}^{(N)} & \cdots & x_{i}^{(N)} & \cdots & x_{2k}^{(N)} \end{bmatrix} \tag{2-30}$$

Compute the model output for all the input values in the sample matrices **A**, **B**, and $\mathbf{C_i}$, obtaining three vectors of model outputs of dimension N ×1:

$$y_{\mathbf{A}} = f(\mathbf{A}), y_{\mathbf{B}} = f(\mathbf{B}), y_{\mathbf{C_i}} = f(\mathbf{C_i}) \tag{2-31}$$

We have

$$\begin{aligned} V_{X_i}\left[E_{X_{\sim i}}(Y \mid X_i)\right] &= \int E_{X_{\sim i}}^2(Y \mid X_i)\,dX_i - \left(\int E_{X_{\sim i}}(Y \mid X_i)\,dX_i\right)^2 \\ &= \int \left\{ \iint f(X_1, X_2, ..., X_i, ..., X_k) \times f\left(X_1', X_2', ..., X_i, ..., X_k'\right) dX_{\sim i} dX_{\sim i}' \right\} dX_i - \left(E(\mathrm{Y})\right)^2 \\ &= \iint f(X_1, X_2, ..., X_i, ..., X_k) \times f\left(X_1', X_2', ..., X_i, ..., X_k'\right) dX dX_{\sim i}' - f_0^2 \\ &\approx (1/N) \sum_{j=1}^{N} y_{\mathbf{A}}^j y_{\mathbf{C_i}}^j - f_0^2 \\ V(Y) &= \int E^2(Y)\,dX - \left(E(Y)\right)^2 \\ &= \int f(X_1, X_2, ..., X_i, ..., X_k) \times f(X_1, X_2, ..., X_i, ..., X_k)\,dX - f_0^2 \\ &\approx (1/N) \sum_{j=1}^{N} \left(y_{\mathbf{A}}^j\right)^2 - f_0^2 \end{aligned} \tag{2-32}$$

with $\quad f_0^2 = \left(\frac{1}{N} \sum_{j=1}^{N} y_{\mathbf{A}}^j\right)^2$

First order sensitivity indices are than as follows:

$$S_i = \frac{V\left[E(Y \mid X_i)\right]}{V(Y)} = \frac{y_{\mathbf{A}} . y_{\mathbf{C_i}} - f_0^2}{y_{\mathbf{A}} . y_{\mathbf{A}} - f_0^2} \approx \frac{(1/N) \sum_{j=1}^{N} y_{\mathbf{A}}^j y_{\mathbf{C_i}}^j - f_0^2}{(1/N) \sum_{j=1}^{N} (y_{\mathbf{A}}^j)^2 - f_0^2} \tag{2-33}$$

Similarly, the total-effect indices are as follows

$$S_{T_i} = 1 - \frac{V\left[E\left(Y \mid X_{\sim i}\right)\right]}{V(Y)} = 1 - \frac{y_{\mathbf{B}} \cdot y_{\mathbf{C_i}} - f_0^2}{y_{\mathbf{A}} \cdot y_{\mathbf{A}} - f_0^2} \approx 1 - \frac{(1/N)\sum_{j=1}^{N} y_{\mathbf{B}}^j y_{\mathbf{C_i}}^j - f_0^2}{(1/N)\sum_{j=1}^{N} \left(y_{\mathbf{A}}^j\right)^2 - f_0^2} \quad (2\text{-}34)$$

The improvements for the calculation of S_i and S_{Ti} have been proposed. The following formulas have higher accuracy according to the research of Saltelli al. [39]:

$$\begin{aligned} S_i &\approx \frac{(1/N)\sum_{j=1}^{N} y_{\mathbf{A}}^j \left(y_{\mathbf{C_i}}^j - y_{\mathbf{B}}^j\right)}{(1/N)\sum_{j=1}^{N} y_{\mathbf{A}}^j (y_{\mathbf{A}}^j - y_{\mathbf{B}}^j)} = \frac{\sum_{j=1}^{N} y_{\mathbf{A}}^j \left(y_{\mathbf{C_i}}^j - y_{\mathbf{B}}^j\right)}{\sum_{j=1}^{N} y_{\mathbf{A}}^j (y_{\mathbf{A}}^j - y_{\mathbf{B}}^j)} \\ S_{T_i} &\approx \frac{(1/2N)\sum_{j=1}^{N} \left(y_{\mathbf{B}}^j - y_{\mathbf{C_i}}^j\right)^2}{(1/N)\sum_{j=1}^{N} y_{\mathbf{A}}^j (y_{\mathbf{A}}^j - y_{\mathbf{B}}^j)} = \frac{\sum_{j=1}^{N} \left(y_{\mathbf{B}}^j - y_{\mathbf{C_i}}^j\right)^2}{2\sum_{j=1}^{N} y_{\mathbf{A}}^j (y_{\mathbf{A}}^j - y_{\mathbf{B}}^j)} \end{aligned} \quad (2\text{-}35)$$

Space-partition approach [40]

To make best use of the sample runs and in turn reduce the cost, Plischke al. [41] proposed a "space-partition" method to estimate the moment-independent importance measure. Suppose the sample space of X_i is (b_1, b_2), and it is partitioned into s successive subintervals [$a_{k\text{-}1}$, a_k), where $b_1 = a_0 < a_1 < \cdots < a_k < a_s = b_2$. Instead of calculating $E_{X_i}(V(Y|X_i))$, we use $V(Y|X_i \in [a_{k-1}, a_k))$ and calculate $E_{X_i}(V(Y|X_i \in [a_{k-1}, a_k)))$ to estimate S_i. Obviously, we have

$$\lim_{(a_k - a_{k-1}) \to 0} E_{X_i}(V(Y|X_i \in [a_{k-1}, a_k))) = E_{X_i}(V(Y|X_i)) \quad (2\text{-}36)$$

Similarly, this method can be used to calculate higher order sensitivity indices. The advantage of this method is that we can calculate all the S_i with only one sampling process, which will greatly reduce the number of samples required.

There are contradictions for the partition process of parameters. Suppose that we have N samples in total, we distribute these samples into s successive subintervals of X_i with N/s samples in each subinterval. In order to improve the accuracy of S_i, we need to increase s and N/s in the same time. But evidently, s inversely proportional to N/s for a given N. Zhai [40] discussed this contradiction in his resent research, and found that Space-partition method outperforms the traditional substituted Colum method.

Dimension reduction method

With the dimension reduction method, the model $y = f\left(x_1, x_2, ..., x_k\right)$ is written with

reference to a fixed input point, i.e, **x**=**c**:

$$y = f(\mathbf{x}) \approx {f_0}^{1-k} \prod_{i=1}^{k} f(x_i, \mathbf{c}_{-i}) \tag{2-37}$$

with $f_0 = f(\mathbf{c}) = f(c_1, c_2, \dots, c_k)$, $f(x_i, \mathbf{c}_{-i}) = f(c_1, c_2, \dots, c_{i-1}, x_i, c_{i+1}, \dots, c_k)$.

We use this formula to reduce the dimension of $f(\boldsymbol{x})$. Finally, after the derivation process, we have

$$S_i \approx \frac{\theta_i / \rho_i^2 - 1}{\left(\prod_{j=1}^{k} \theta_j / \rho_j^2 \right) - 1} \qquad S_{T_i} \approx \frac{1 - \rho_i^2 / \theta_i}{1 - \left(\prod_{j=1}^{k} \rho_j^2 / \theta_j \right)} \qquad \text{with} \quad \begin{aligned} \rho_j &= E_j\left[f\left(x_j, \mathbf{c}_{-j}\right) \right] \\ \theta_j &= E_j\left\{ \left[f\left(x_j, \mathbf{c}_{-j}\right) \right]^2 \right\} \end{aligned} \tag{2-38}$$

This method requires kN function evaluations only in the SA of a function of k random variables and N samples for each variable, which implies that the proposed method significantly reduces the number of functional evaluations required for the SA. And the multiplicative dimensional reduction method provides a simple and efficient alternative for global SA in a practical setting according to the research of Zhang [42].

2.1.5 Other sensitivity analysis methods

2.1.5.a Graphical Methods

The present possibilities to display the results associated with the already calculated mapping$[X_i, Y(X_i)]$, i=1,2,…,n, include Cumulative Distribution Function (CDF), scatter plot and box plots. Large amount of uncertainty information is lost in the calculation of means and standard deviations, and CDF or box plots are usually preferable. Box plots help to display and compare the uncertainty. An example of box plot is given in Figure 2- 2, the endpoints of the boxes are formed by the lower and upper quartiles of the data, that is, $X_{0.25}$ and $X_{0.75}$. The vertical line within the box represents the median, $X_{0.50}$. The mean is identified by the large dot. The bar on the right of the box extends to the minimum of $X_{0.75}$+1.5($X_{0.75}$-$X_{0.25}$) and the maximum value. Similarly, the bar on the left extends to the maximum of $X_{0.25}$-1.5($X_{0.75}$-$X_{0.25}$) and the minimum value. The observations falling outside of these bars are shown in crosses. The box plots help to summarize outputs distributions and facilitate comparisons of these distributions.

"A simple but useful tool is scatterplots of the output variable against individual input variables, after (randomly) sampling the model over its input distributions and gives a direct visual indication of sensitivity [43]". Scatterplots help to understand the relationships between the uncertainty in model inputs and variability of the results, Figure 2- 3 illustrated an example of scatterplots.

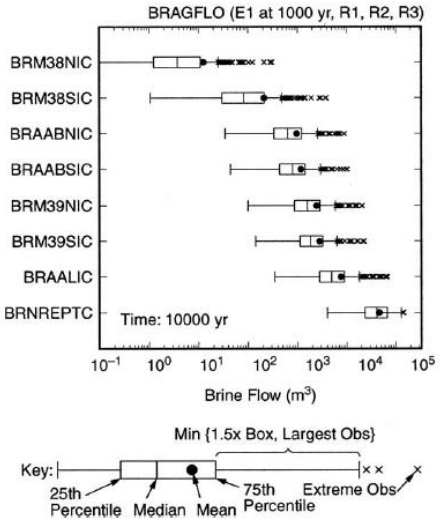

Figure 2- 2 Example of box plots (abscissa: output values; ordinate: input parameters) [29]

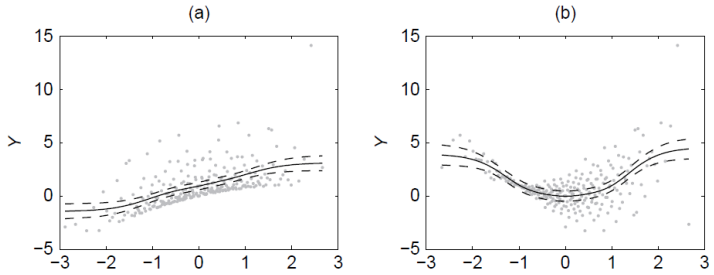

Figure 2- 3 Example of scatterplots, with the smoothed estimation lines [28]

2.1.5.b Group screening designs

Group screening designs [28] is available when there are hundreds of parameters and the model output is determined by only a few highly influential factors. When there are hundreds of parameters in a model, one way to reduce the number of simulations is to apply group designs. Group screening allows the analyst to generate fewer runs n than there are factors k: $n < k$. It can still isolate the main effects, quadratic effects, and two-factor interactions of influential factors.

2.1.5.c Output distribution based method

Pianosi, al.[44] characterize the conditional and unconditional distributions by their Cumulative Distribution Functions (CDFs). More specifically, "the sensitivity to input x_i is measured by the distance between the unconditional probability distribution of y that is obtained when all inputs vary simultaneously, and the conditional distributions that are obtained when varying all inputs but x_i (i.e. x_i is fixed at a nominal value)".

As a measure of distance between unconditional and conditional CDFs, $KS(x_i)$ is defined as

$$KS(x_i) = \max_y \left| F_y(y) - F_{y|x_i}(y) \right| \tag{2-39}$$

Figure 2- 4 illustrate the calculation of *KS*. In this example, CDF of the output *y* is measured (solid line), the input x_i is fixed, and conditional CDF of output is measured (dotted line). *KS* is the maximum distance between the two lines.

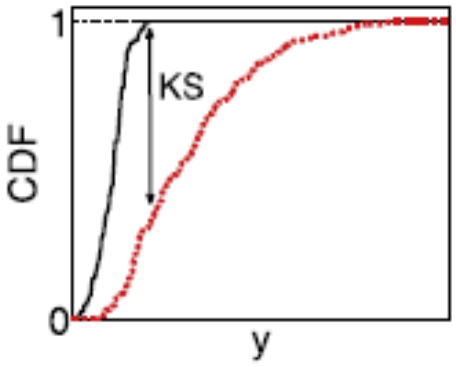

Figure 2- 4 Compute of *KS* [44]

2.1.5.d Fourier Amplitudes Sensitivity Test (FAST)

FAST is one of the most commonly used uncertainty and SA techniques. "It uses a periodic sampling approach and a Fourier transformation to decompose the variance of a model output into partial variances contributed by different model parameters and to evaluate both main effects and interaction effects of parameters [45]".

In fact, both the Sobol' indices and the FAST are quantitative SA methods based on calculation of variance, and the influence indices calculated by the two methods have the same meanings. Compare to the Sobol' indices, FAST has advantages in terms of efficiency. But the realization of FAST requires high skills and difficulties exist in encoding it.

2.1.6 Discussion

The method selection for SA is shown in Figure 2- 5 [46]. Model complexity (linearity, monotonicity, interaction, etc.) and the number of variables are the two factors that should be considered. The advantages and disadvantages of the SA methods are listed in Table 2- 3.

As a starting point, Graphical Methods give an intuitive view of the complexity of the model. Correlation method and Regression analysis are the methods that could be used in relationship study between inputs and outputs of linear models. With bias acceptable, Rank transformations method linearize the SA of nonlinear but monotonic models. Differential-based local method reduces the samples by estimating model input and output relationship only at specified local position. Generally, we don't have much information on the behavior of an engineering system, screening analyses basing on two-level DOE is efficient for SA of monotonic model. Multi-level screening, Morris' analysis, can be used for SA of non-monotonic systems and parameters' interactions can be studied qualitatively with this approach. Regardless of the linearity and monotonicity of the system, variance-based methods are commonly used for quantitative SA method to evaluate both the main effects

and total effects of the factors: the FAST explores the multidimensional space of the input factors by a search curve; similar to FAST, the Sobol' indices assumes the total variance of the model output to be made up of terms of increasing dimensionality, and is superior to FAST in that the computation of the sensitivity indices are easy to encoding. Metamodel [47] (such as Response Surface Method, Kriging interpolation, etc.) is needed to create low calculation cost surrogate model for calculation of the Sobol' indices as it requires thousands of model evaluations. Group sampling allows the analyst to generate smaller designs that can still isolate influential parameters and their effects, even with the number of samples less than the number of parameters, and are proposed only when the number of inputs is huge.

Different methods might be needed for the SA of a complex model, Figure 2- 6 [48] illustrates the strategy for SA of complex model. For the VRS being studied, model simulation is of high calculation cost; a dozen uncertain factors are to be analyzed. The Sobol' indices can be used for quantitative SA of such models; screening analysis is preferred to identity the influential uncertain factors and reduce the number of the input factors before quantitative analysis.

SA methods	**Advantages**	**Disadvantage**
Graphical methods	Intuitive method	Lack of evaluation criteria
Regression/correlation	Efficient for correlation evaluation of model inputs and outputs	Only be used for SA of Linear models
Rank regression	Linearization of the nonlinear but monotonous models	Approximation on sacrificing computational accuracy
Differential-based method	Efficient for input/output relationship study of linear model	Local method that can only be used for linear model
Two-level DOE	Efficient for SA of monotonous model	No information is obtained about the internal correlation
Morris	Main and interactions effects studies of non-monotonic models	Qualitative method with high number of samples
Variance-based SA	Quantitative methods regardless of model properties.	High number of samples required

Table 2- 3 Comparison of different SA methods

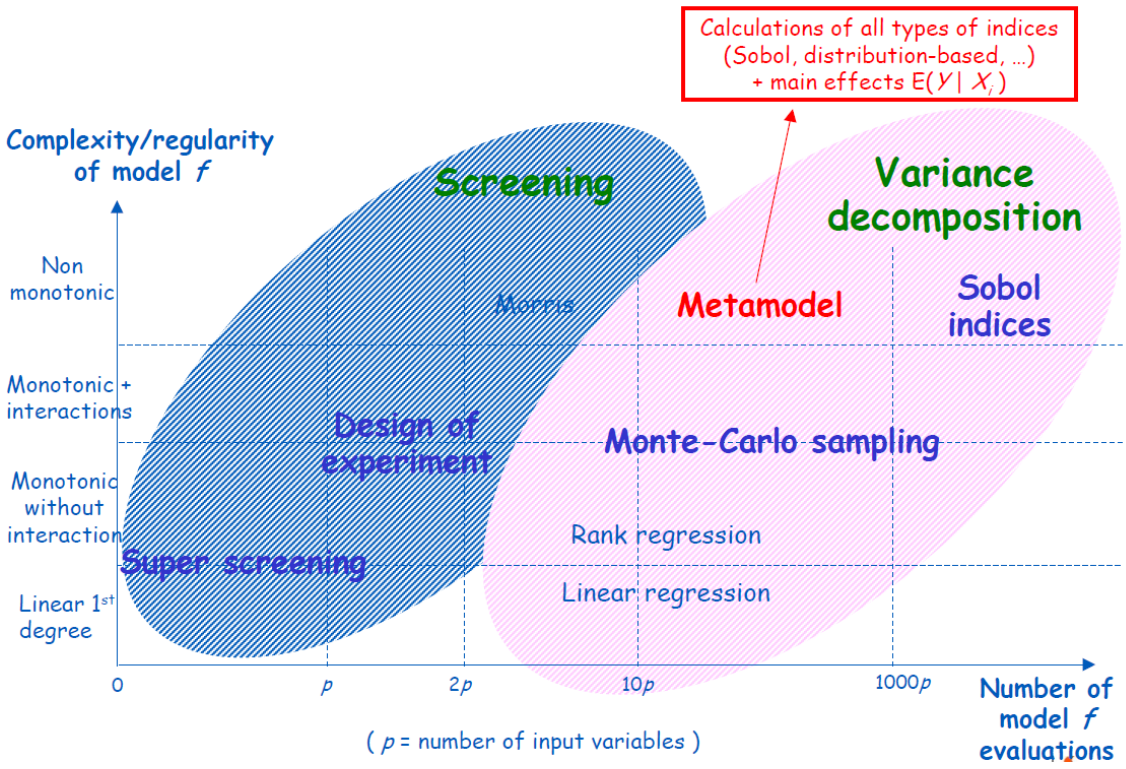

Figure 2- 5 Selection of SA methods [46]

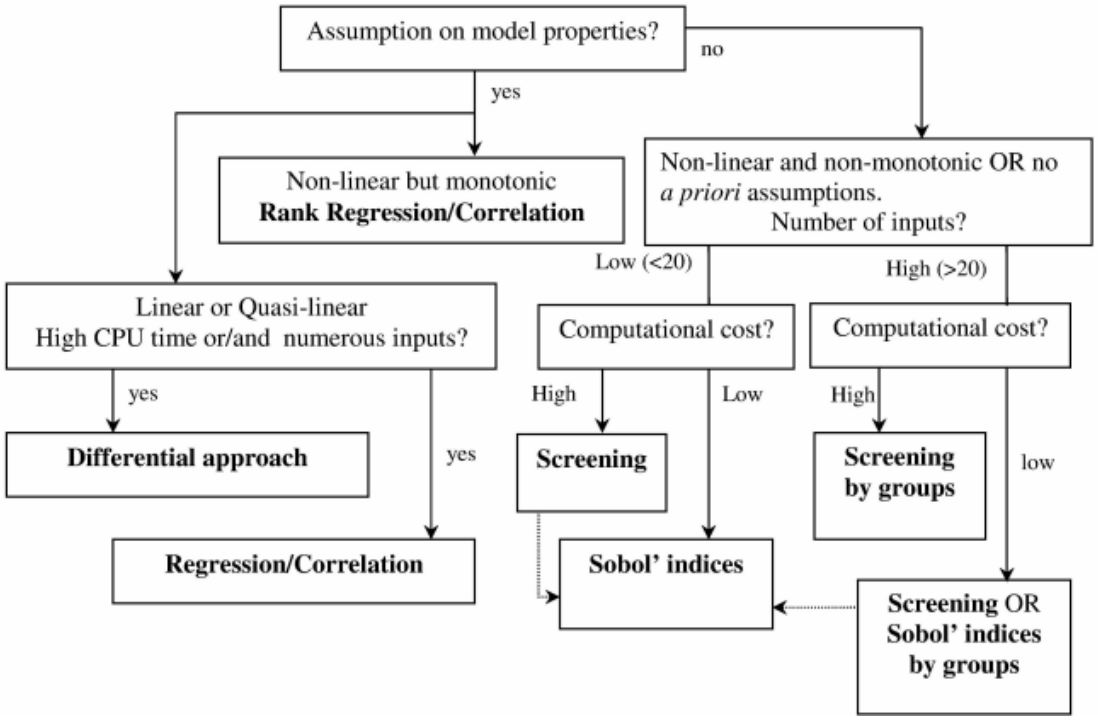

Figure 2- 6 SA strategies for different kind of models [48]

2.2 Sensitivity Analysis of dynamic three points bending test

The sampling-based sensitive analysis methods are presented in the previous section. Instead of analyze directly the VRS model whose simulation cost is high and who is with many uncertain factors, different screening methods and Sobol' indices are used for SA of a simple dynamic model. The efficiency and accuracy of screening methods are studied and the strategy for SA of the VRS and many other complex engineering systems are discussed.

The simple model studied is a three points dynamic bending test of a steel reinforced wood beam, which concerns a subset of a VRS and studies the deformations and the rupture of the structure.

2.2.1 Experimental test & numerical model

The dynamic three points bending experimental test of a steel reinforced wood beam was realized (see Figure 2- 7) and the corresponding numerical model of the crash test was fabricated (see Figure 2- 8) by Goubel [49] . The wood beams consisted in cylinders of 200mm in diameter and of two meters length, with the rear side machined and reinforced with a plate of 100mm×5mm×2000mm made of S235 steel (see Figure 2- 9). A rigid impactor of 2000 kg impacts the beam at a speed of 20 km/h.

Figure 2- 7 Bending test of steel reinforced wood beam [49]

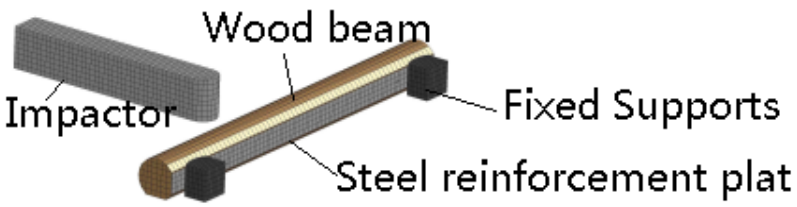

Figure 2- 8 Numerical model of the bending test [49]

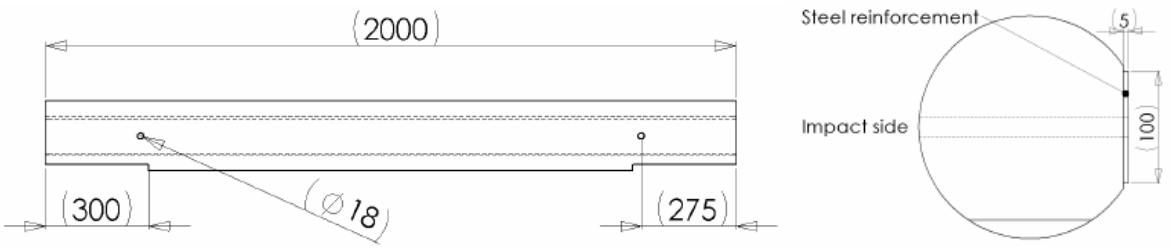

Figure 2- 9 Dimensions of the steel reinforced wood beam [49]

2.2.2 SA of dynamic model

2.2.2.a Uncertain factors

Wood is a complex material. The mechanical properties in the radial and tangential directions are much lower than the one in the longitudinal direction, and wood can be considered as a transverse isotropic material. Wood mechanical properties are influenced by many factors such as wood nature (hard or soft), density, water content of wood fibers, temperature, defects, etc. Influenced by manufacturing process and many other uncontrolled factors, uncertainties exist in mechanical properties of S235 steel. Referring to the study of Goubel [49], six uncertain factors are chosen. The wood mechanical properties are influenced by its Moisture Content (*MC*) (see Figure 2- 10), Temperature (*T*) (Figure 2- 11) and wood Grade (*G*), i.e. the assessment of wood defects [50]; Uncertainties of mechanical properties of the reinforcement plate, Yield strength (*Y*), Young's Modulus (*MY*), Tangent Modulus (*MT*), are considered [51]. Inputs distributions are listed in Table 2- 4, with *MC* and *T* supposed to distribute uniformly in [4% 29%] and in [1℃ 30℃] respectively, and other factors consistent with the normal distribution.

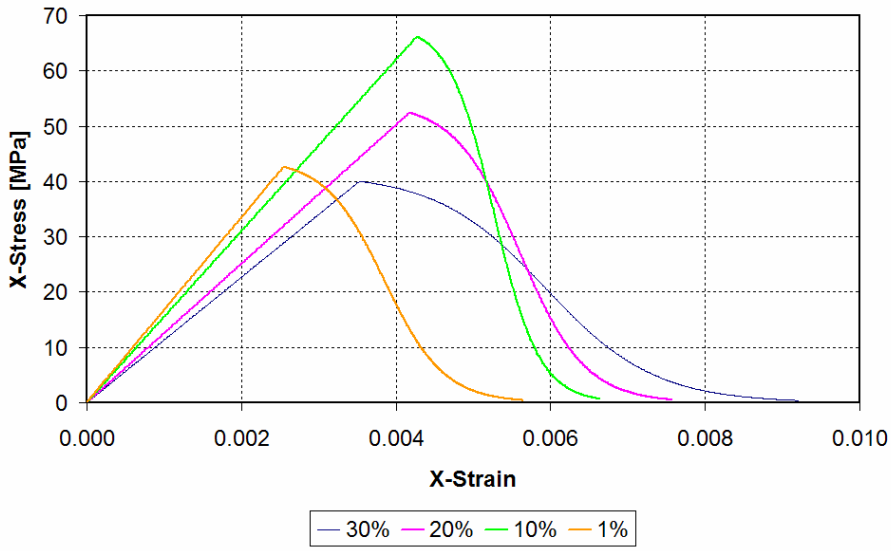

Figure 2- 10 Moisture Content effect – wood tensile test simulation results [49]

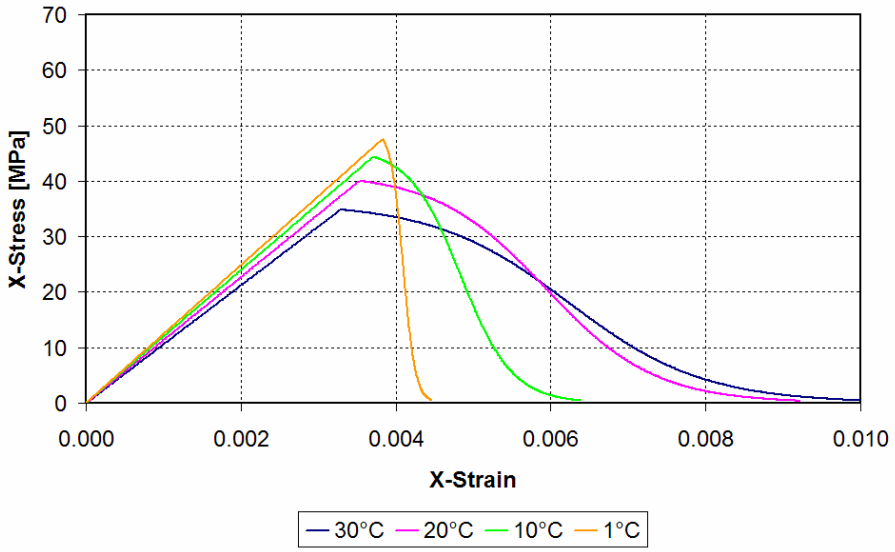

Figure 2- 11 Temperature effect – wood tensile test simulation results [49]

Type	Factors	Distribution	Unit	Mean	St D
Wood uncertain factors	Moisture Content (*MC*)	Uniform	%	16.5	4.9
	Temperature (*T*)	Uniform	℃	15.5	8.37
	Grade (*G*)	Gauss	1	0.635	0.135
Steel uncertain factors	Yield strength (*Y*)	Gauss	MPa	284.5	21.5
	Young's Modulus (*MY*)	Gauss	GPa	210	12.6
	Tangent Modulus (*MT*)	Gauss	GPa	0.86	0.08

Table 2- 4 Distribution of noisy factors for bending test

2.2.2.b Outputs criteria

Three experimental tests were realized in the same conditions and the deceleration of the impactor during the tests and in simulation analysis are illustrated in Figure 2- 12 and Figure 2- 13. Deceleration signals are with background noises, filtering process is required to removes some unwanted signal, and it is not possible to predict the deceleration of the impactor at a specified moment. Figure 2- 14 illustrates the velocity of impactor during bending test with uncertain factors defined at different levels: evidently, performances of the beam are highly influenced by the uncertain factors. During the beginning of the crash, the simulated beam shows its elastic properties, then the reinforced wood beam demonstrates complex nonlinear mechanical properties during the breaking process, Figure 2- 15 illustrates the crash process in the early state with impact time is 0.02s and the final state of the crash test. Velocity at impact time 0.02s $V_{0.02}$ and final velocity V_{∞} of impactor are chosen as the two output criteria of the model.

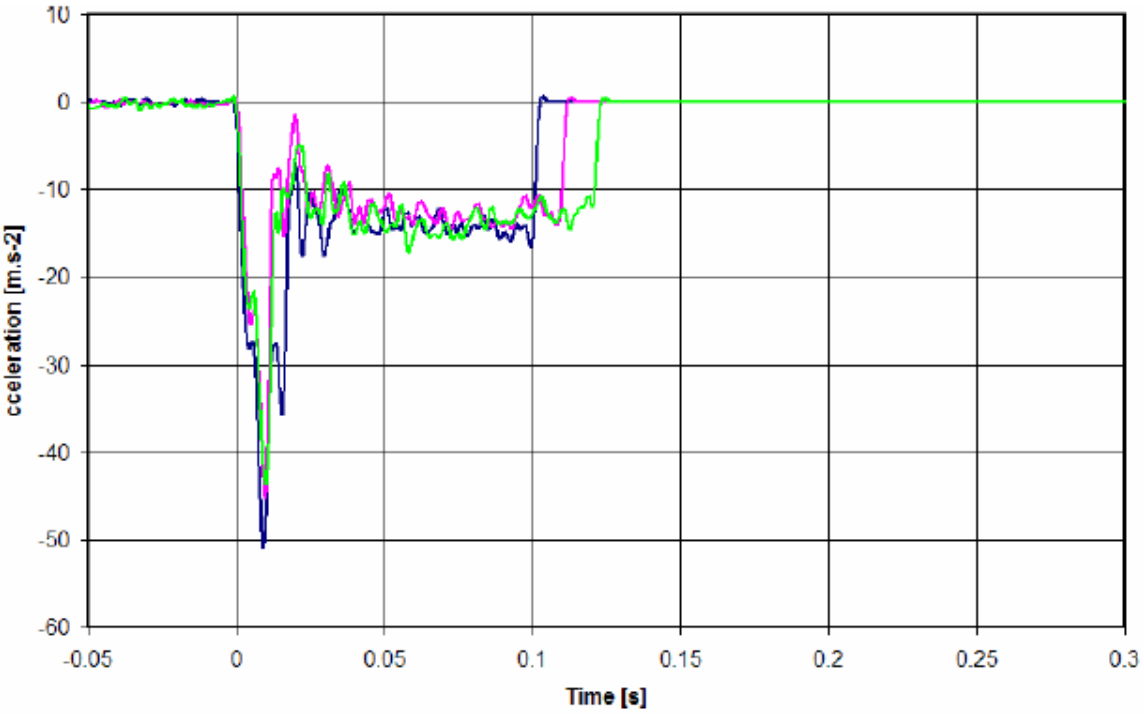

Figure 2- 12 Deceleration results experimental test [49]

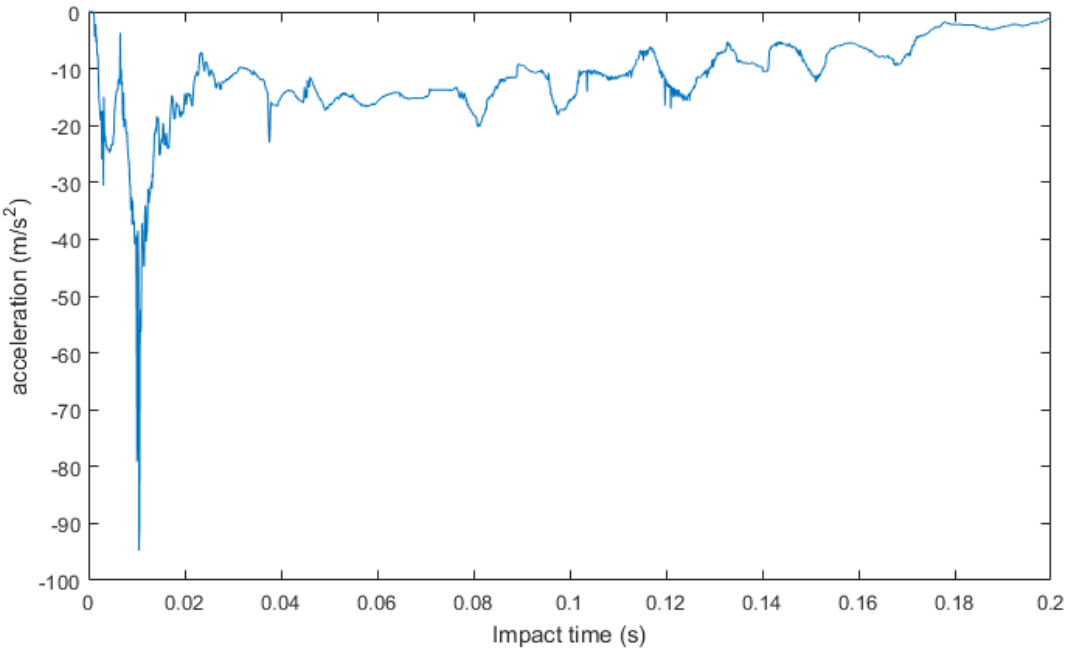

Figure 2- 13 Deceleration results simulation analysis

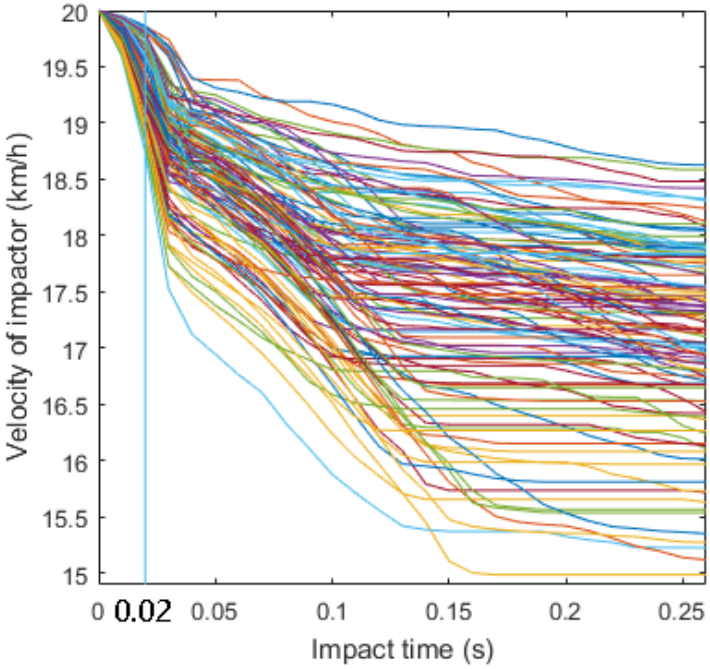

Figure 2- 14 Velocity of impactor during bending test

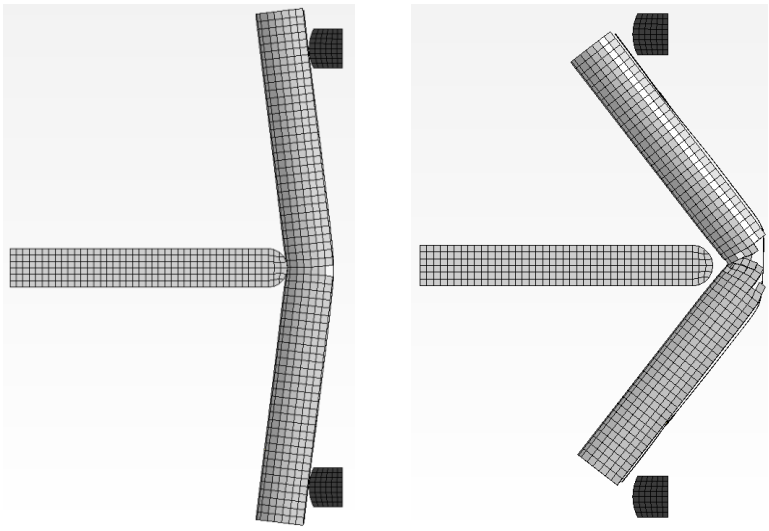

Figure 2- 15 Simulation of bending test with t=0.02s (left) and final breaking of beam (right)

2.2.2.c Results analysis

Different screening methods --- Marris Analysis (MA), Factorial Design (FD), Half-Fractional Factorial Design (HFFD), Orthogonal Array (OA), One-at-A-Time (OAT), Cotter Design (CD), Parameter Study (PS) --- are used for screening analyses of the system. Influential uncertain factors are identified and their influences are quantified with Sobol' indices, the detail of analyses is described in Appendix I Details for Sensitivity analysis of the three points bending test model. Table 2- 5 and Table 2- 6 list the normalized SA results with the two outputs as criteria separately, with accurate method indicated in bold and high

error SA results showed with red font. The normalized main effects of the uncertain factors on velocity of the impactor calculated with FD, HFFD and OA along the impact process are illustrated in Figure 2- 16, Figure 2- 17, Figure 2- 18 respectively.

The efficiency and accuracy of the screening methods are analyzed:

- The Cumulative Distribution Function (CDF) value of a factor is unitless and is uniformly distributed across the interval [0, 1] regardless of the factor distribution, rather than concentrated in one part of the interval. In MA, the CDF values of the parameters were treated as inputs variables and 6 levels (1/12, 3/12, 5/12, 7/12, 9/12, 11/12) were taken for each variables with Δ=0.5. The relative factor values were calculated through inverse transformations. r trajectories with each trajectory corresponds to (k+1) model executions based on once-at-a-time sampling strategy were selected and a total number of 63 model runs (i.e. r.(k+1) model runs with r=9, k=6) were realized. The value of μ_i* (see eq. 2-21) was calculated. The multi-level MA is one of the most accurate screening method and the analysis results could be treated as a reference for accuracy evaluation of two-level screening analyses;
- Suppose that the velocity of the impactor is inversely proportional to the stiffness of the beam. For two-level screening analyses, values of inputs *G*, *Y*, *MY*, *MT* are taken as the mean value plus/minus standard deviation. The mechanical properties of the wood have monotonous relationship with *MC* in interval [8% 29%] and with *T* in interval [1℃ 30℃]. Low *MC* may greatly degrade properties of the wood and its energy absorption capability goes down when wood freeze at T<0℃. Two levels of *MC* and *T* were taken as (10%, 26%) and (1℃, 30℃) separately. Considering all possible combinations, FD is the most accurate two-level screening method, with 64 number of model runs. HFFD take half of the full FD samples, i.e. 32 samples, and is of relatively high accuracy. Only 8 samples were required for fractional design with OA. OAT design is efficient for linear models and needs 12 model runs to estimate the effect of changing each parameter, but it's of low accuracy for screening analysis of the bending test model here. CD and PS take only one sample for each factor at each level, and the screening outputs are influence by single model simulation precision;
- Table 2- 5 and Table 2- 6 show that *MC*, *T*, *G*, *MT* are the most influential parameters. Their respective influences were then quantified with Sobol' indices. Though a single run of the bending test model requires only 10min, thousands of samples are needed for quantitative analysis. A surrogate model was created for calculation of Sobol' indices: 100 runs were realized with samples generated through Latin Hypercube Sampling (LHS); Kriging interpolation was used to create the metamodel; 20 additional model simulations were used to evaluate the accuracy of the surrogate model. Main effect S_i for each factor is calculated, the critical influential factors wood Temperature (*T*) and wood Grade (*G*) were identified and their influences are quantified; Wood moisture (*MC*) affect the early state of crash test (i.e. $V_{0.02}$), but of little influence compared to the two critical factors on the final velocity of the impactor.
- Comparing results in Figure 2- 16, Figure 2- 17, and Figure 2- 18: FFD such as HFFD and OA reduced the samples runs by choosing a fraction of the full FD, and is more efficient than FD; with the lowest calculation cost, two-level screening analysis with OA can still identify the influential factors.
- MA can be used for SA of nonlinear models; OAT, CD, PS are proposed for models of special assumptions, but of low accuracy for our dynamic model of unknown properties.

	MA	**FD**	HFFD	OA	OAT	CD	PS	**SOBOL**
MC	**0.21**	**0.22**	0.20	0.16	0.19	0.29	0.21	**0.17**
T	**0.24**	**0.40**	0.41	0.32	0.20	0.34	0.29	**0.35**
G	**0.42**	**0.38**	0.37	0.29	0.26	0.36	0.49	**0.48**
Y	**0.05**	**0**	0.01	0.02	0.22	0	0	-
MY	**0.06**	**0**	0.01	0.12	0.07	0.01	0.01	-
MT	**0.02**	**0**	0	0.09	0.06	0	0	**0**

Table 2- 5 SA of bending test model for $V_{0.02}$ as output criterion

	MA	**FD**	HFFD	OA	OAT	CD	PS	**SOBOL**
MC	**0.11**	**0.14**	0.17	0.12	0.16	0.19	0.20	**0.01**
T	**0.41**	**0.47**	0.48	0.30	0.26	0.29	0.09	**0.62**
G	**0.26**	**0.28**	0.30	0.28	0.20	0.07	0.49	**0.35**
Y	**0.06**	**0.03**	0	0.08	0.25	0.12	0.03	-
MY	**0.04**	**0.02**	0.02	0.02	0.10	0.13	0.04	-
MT	**0.12**	**0.06**	0.03	0.20	0.03	0.19	0.15	**0.01**

Table 2- 6 SA of bending test model for V_{∞} as output criterion

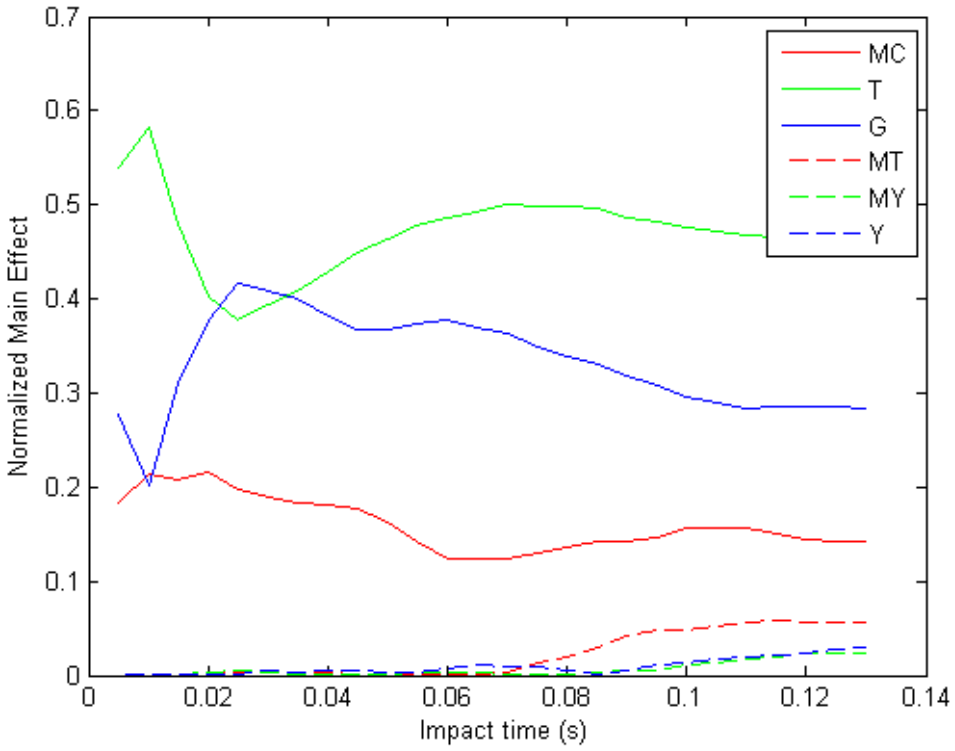

Figure 2- 16 Parameters screening with FD

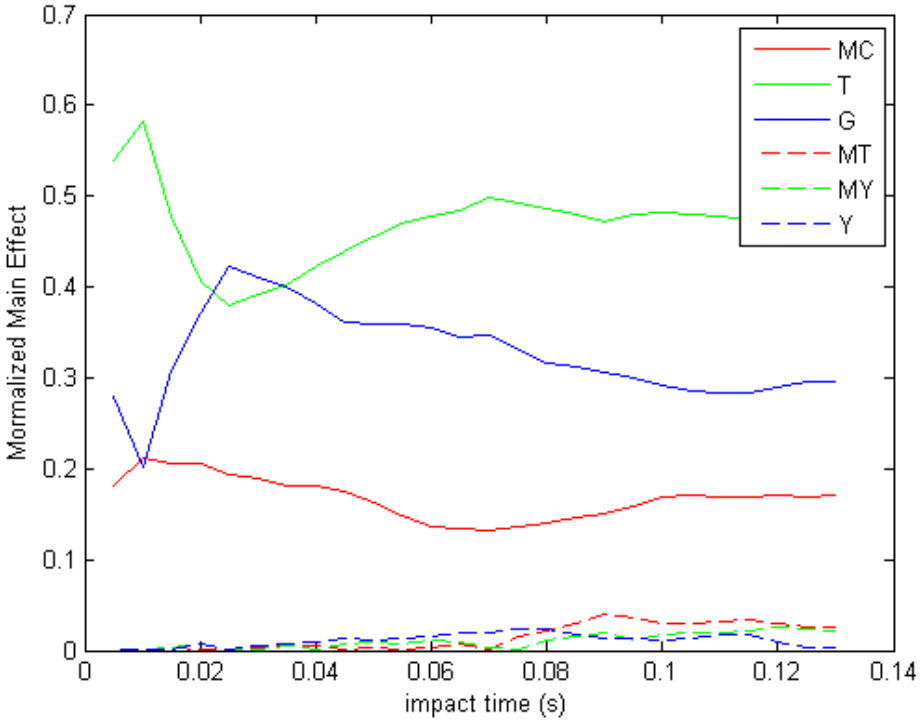

Figure 2- 17 Parameters screening with HFFD

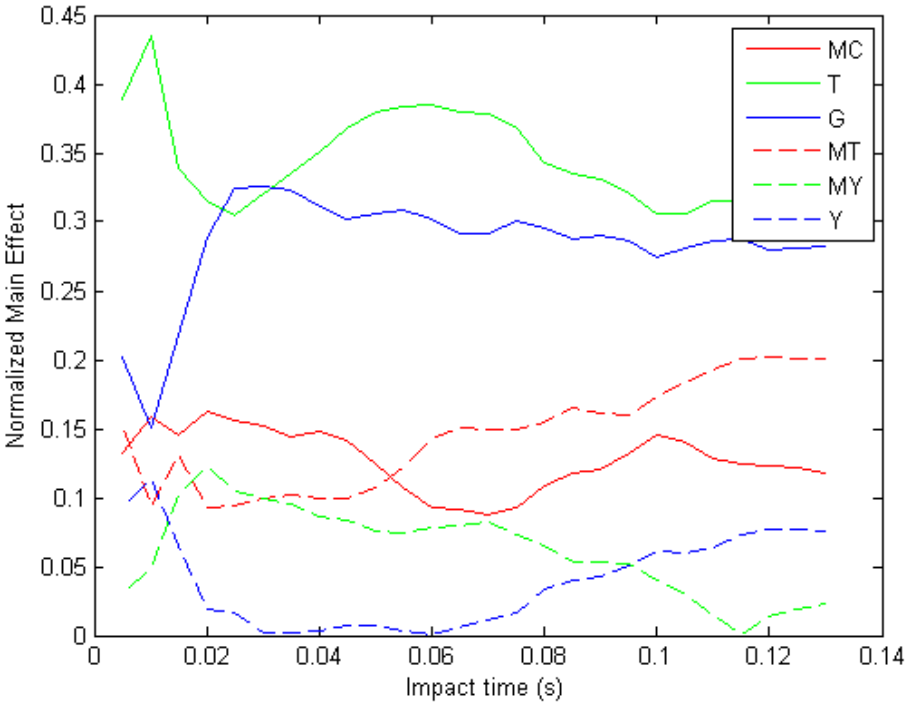

Figure 2- 18 Parameters screening with OA

2.3 Conclusions

Although all SA techniques have not been listed, this chapter has illustrated the great variety of the available methods, positioning in terms of assumptions and kind of results.

Methods such as regression/Correlation analysis and differential-based local method can be used for the SA of property assumption known systems; in the modeling of systems with unknown properties, screening analyses help to removal the noise and insignificant variables and terms, and to identity the interactions in problems [52]. They are proposed before quantitative analysis in the SA of complex models.

Both MA and Sobol' indices could be used in SA of black-boxes systems where no specific assumption is made. Lamoureux [53] proposed to quantify influences of the influential uncertain parameters with the sequential SA and realized the robustness analysis of an aircraft engine's pumping unit (see Figure 2- 19): MA was realized to identity the influential uncertain parameters; the Sobol' indices were calculated to quantify influences of the influential parameters with the help of kriging surrogate modeling; effects are needed to evaluate the real distribution of the most influent parameters, and it help to increase calculation accuracy of the numerical simulation; the model robustness can be evaluated considering only uncertainties of the influential parameters. Ge [54] discussed the sequential SA with MA and Sobol' indices of the test functions (*G* function, *G** function, *K* function, *Morris* function): his study shows that the sequential SA has a very high accuracy in both qualitative SA and quantitative SA of a high-dimensional model.

Oberkampf [55] discussed error and uncertainty in model simulations. Numerical solution errors are inevitable in the modeling & simulation of complex systems, especially in dynamic simulations where the instantaneous error can be integrated, and the field of numerical error estimation is separate from that of uncertainty analysis. MA has a high accuracy in identifying the most influential parameters. But numerical errors may dominate the EE_i calculation of non-influential parameters as show in equation (2-40), where e_{i1} e_{i2} represent the numerical errors and $Y(X_1, X_2, \cdots, X_i + \Delta, \cdots) \approx Y(X_1, X_2, \cdots)$.

$$EE_i = \frac{\left[Y\left(X_1, X_2, ..., X_i + \Delta, ...\right) + e_{i1}\right] - \left[Y\left(X_1, X_2, ...\right) + e_{i2}\right]}{\Delta} \approx \frac{e_{i1} - e_{i2}}{\Delta} \qquad (2\text{-}40)$$

Screening analyses with samples taken by FD or FFD run the model multiple times with every uncertain parameter at each level, which helps to offset the influence of numerical errors on uncertainty analysis of the complex systems. Screening methods such as OAT, CD and PS can be efficient for SA of models with special assumptions, but of low accuracy for complex model with unknown properties as they run the model only one/two times with every uncertain parameter at each level and the numerical error or the interaction effects of uncertain parameters could dominate the evaluation of main effects.

Restrained by the high number of uncertain parameters and time expensive cost in the simulation of VRS crash tests, current SA of the VRS remain qualitative[2][56][57] and assumptions are made to cut back the number of uncertain parameters. By taking samples through FD, Goubel [2] analyzed qualitatively the robustness of a steel-wood VRS. His analysis could illustrate the uncertainty of model outputs, but only 3 uncertain parameters are analyzed according to the failure modes of the VRS during crash test. Many other uncertain parameters exist and the number of model runs could be numerous if we take samples considering all the uncertain parameters (n^k samples for *n* level FD of *k* uncertain parameters).

Two-level screening with uncertain parameters taken through FFD (e.g. OA) could greatly reduce the number of samples required and well identity the non-influential uncertain parameters according to previous SA of the bending test. Comparing to MA, although could only be used in qualitative SA of monotonous models and interaction effects of uncertain parameters can't be estimated, two-level screening with FFD could eliminate the numerical error and identity the most non-influential uncertain parameters with much less samples and model runs.

Quantitative SA, such as with the Sobol' indices, requires a large number of model evaluations and often unacceptable for time expensive computer codes. Metamodel methods, especially Kriging interpolation has been integrated in mathematical software [58] and widely be used for parameters studies of complex systems to create a low calculation cost surrogate models[53]. Marrel[59] studied the application of Kriging in calculation of the Sobol' indices, and the use of Kriging instead of other metamodel is proven to be highly efficient.

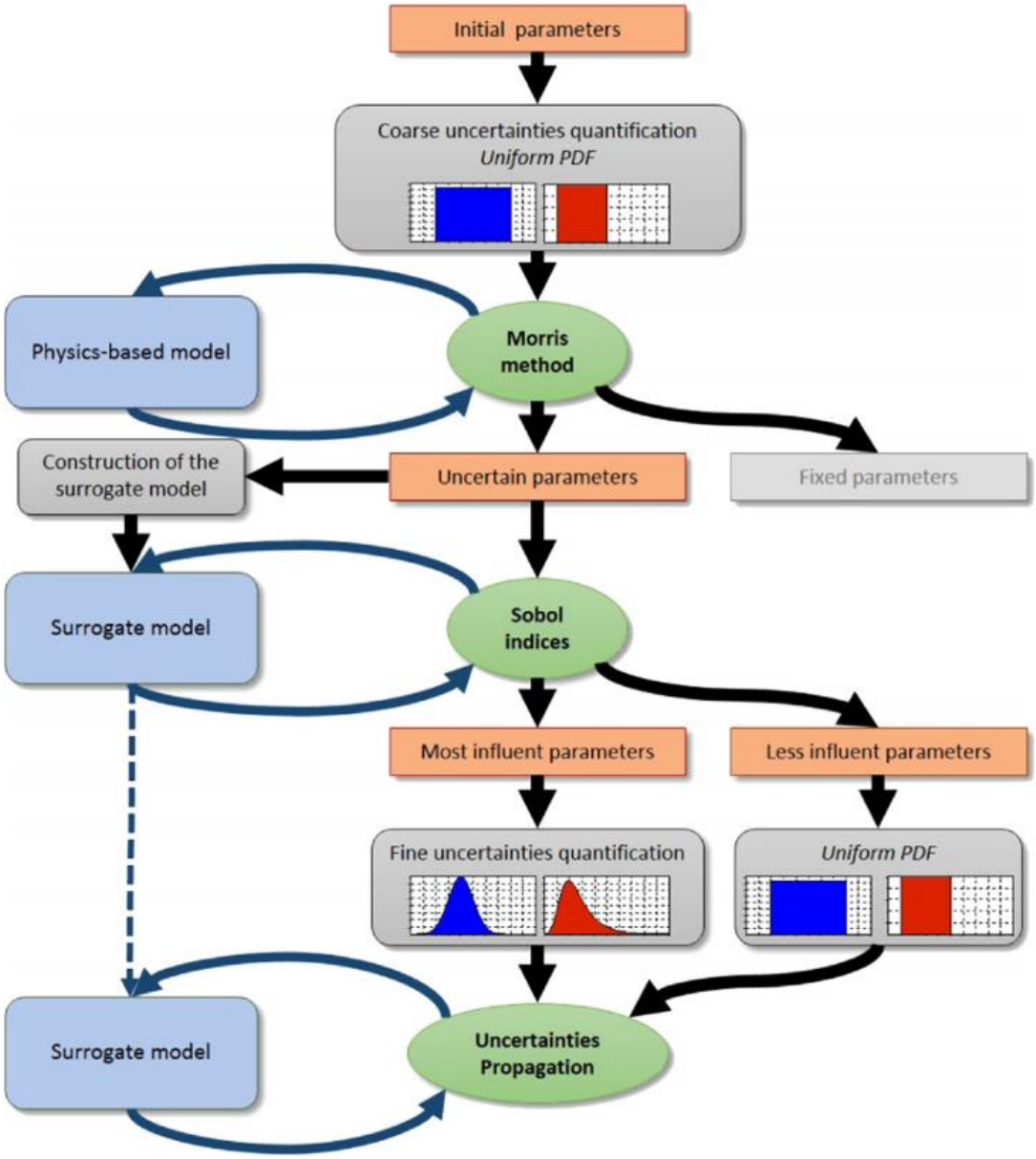

Figure 2- 19 Uncertainties management and SA[53]

As a consequence, the steps for quantitative SA of complex engineering models can be summarized as follows:

1) Two-level screening ---FFD (such as HFFD, OA)

2) Multi-level screening---MA

3) VBSA---Sobol' indices

A complex model may have tens or hundreds of input factors, but only a few of them may be influential. By carefully choosing the samples, although with low precision for SA, two-level screening methods are of lowest calculation cost for SA to find the influential factors. VRS performances generally have monotonous relationship with rigidity of the device and screening analysis studies the variation of outputs with inputs change only around their mean values. Two-level screening methods can be used for SA of such models. Considering the high simulation cost of VRS crash test, FFD with OA will firstly be used for parameters screening of high simulation cost systems.

Limited by calculation precision, two-level screening can only preliminarily select the influential variables. Non-influential variables will then be treated as constant, which can greatly facilitate Multi-level screening. MA will then be used to classify the influential variables with a multi-level screening.

The few variables of great influence on model performance will be identified after MA. VBSA---Sobol' indices---will then be used to quantity the influences of the influential variables. Even for a model with few factors, thousands of model runs might be needed for the quantitative SA, metamodeling can be used to generate surrogate models.

Chapter 3 Sensitivity Analysis of a W-beam steel VRS

3.1 Crash test

3.1.1 Device details

Crash test of a GS2 hard shoulder safety barrier, acceptance test TB32 in compliance with European standards EN 1317-1 and EN 1317-2 [12,13], was carried out by LIER-Transpolis [60, 61]. General view of the crash equipment is shown in Figure 3- 1. The VRS consisted of: C100×50×25 posts, 1500mm in length, driven into the asphalt every 2m; welded spacers fixed to the posts by means of one bolt connection; W-beam, 4315mm in length, fixed to the spacers by one bolt connection and a rectangular washer; the link between the W-beam was realized by 8 bolts-nuts (see Figure 3- 2). The profiles of the VRS components are shown in Figure 3- 3. The length of the device was 60m, at each extremity was a 12m long turned down rails. The installation height at the point of impact was 0.72m. A BMW 520i vehicle is used and the test conditions meet the needs of TB32. Test conditions are listed in Table 3- 1. The components of VRS rails, spacers & posts were numbered and the simplified top view of the test is shown in Figure 3- 4. The guided vehicle struck the barrier 1.46 m after the end of Rail no.3.

	TB32_under	Real test	TB32_upper
Impact speed (km/h)	110	113.6	117.7
Impact angle (°)	19	20	21.5
Vehicle mass (kg)	1425	1431	1575

Table 3- 1 Test conditions boundaries of TB32 and real test conditions

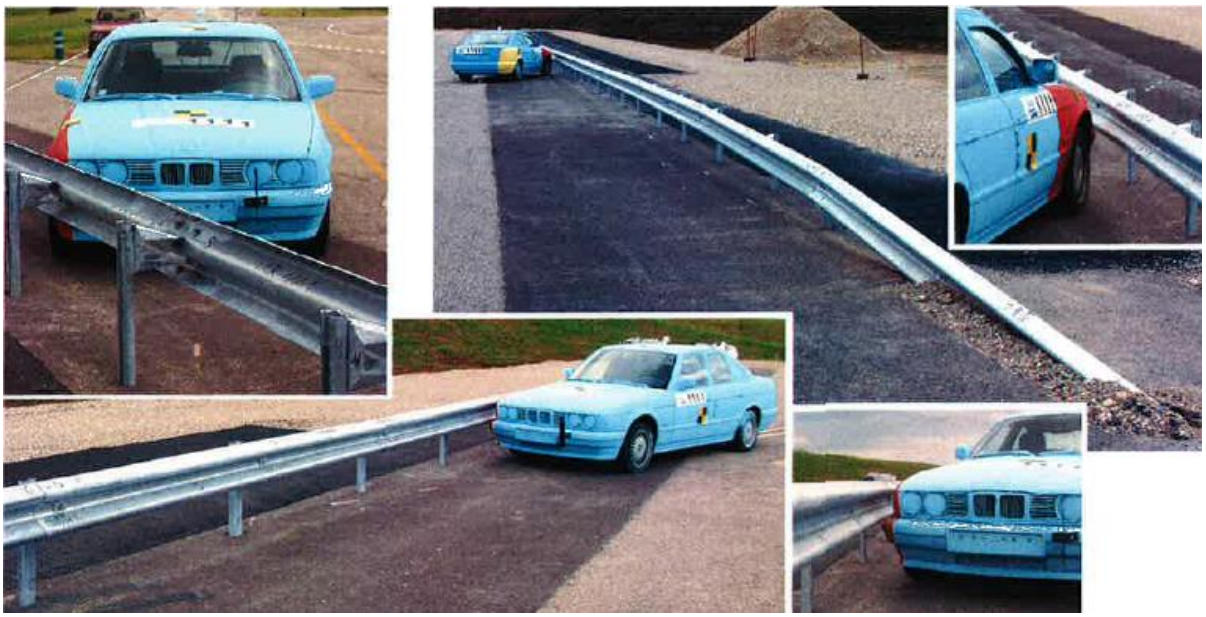

Figure 3- 1 General view of the VRS crash test [60]

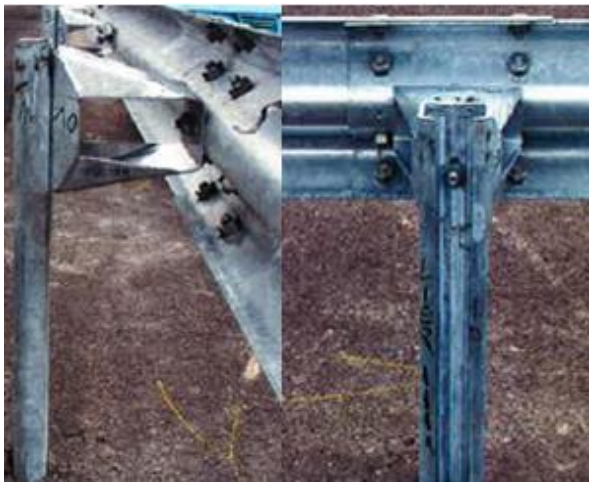

Figure 3- 2 Components connections of the VRS [60]

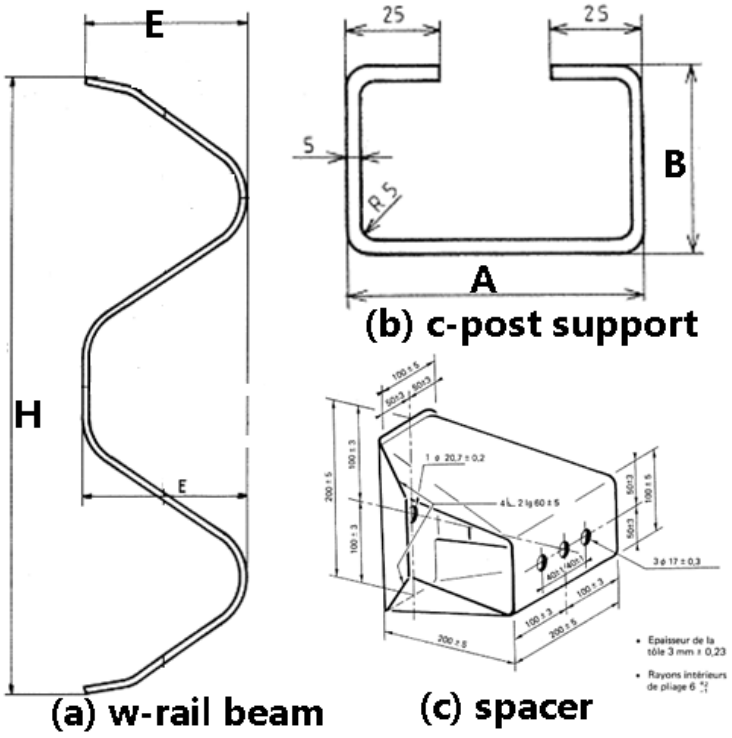

Figure 3- 3 Profiles of VRS components: *A*=100mm; *B*=50mm; *H*=310mm; *E*=81mm [60]

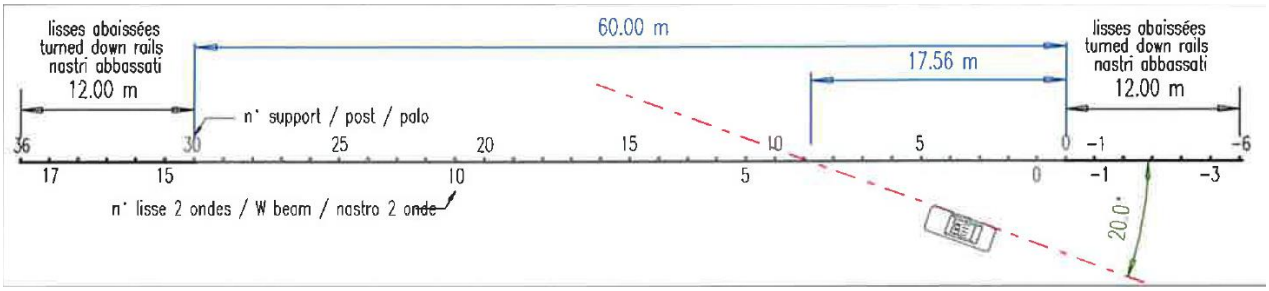

Figure 3- 4 Simplified view of the crash test [60]

3.1.2 Test results

The impact created a 28 m long bow with a permanent deflection of 0.98 m and the dynamic deflection of 1.2 m at post no.12; W-rail no.3 to 9 were deformed; Posts no.-3 to 22 were deformed; Spacers no.-3 to 33 were deformed; No part of the barrier penetrated the interior of the vehicle; The vehicle did not roll over within test area; The vehicle did not pass over the device; Vehicle did not breach the barrier; Right side of the vehicle was damaged; No part of the vehicle was totally detached; Vehicle ran along the barrier until 0.51 m before the end of W-rail no.8 and left the device at an angle of 3.6 °. Vehicle trajectory is shown in Figure 3- 5 and damage of the barrier and vehicle is shown in Figure 3- 6. Quantitative criteria of the device are listed in Table 3- 2, accident severity is of level A, deformation of the device is of level W5 (see Section 1.1.3). Table 3- 3 lists the permanent deflection of the devices after the impact, with parameters shown in Figure 3- 7.

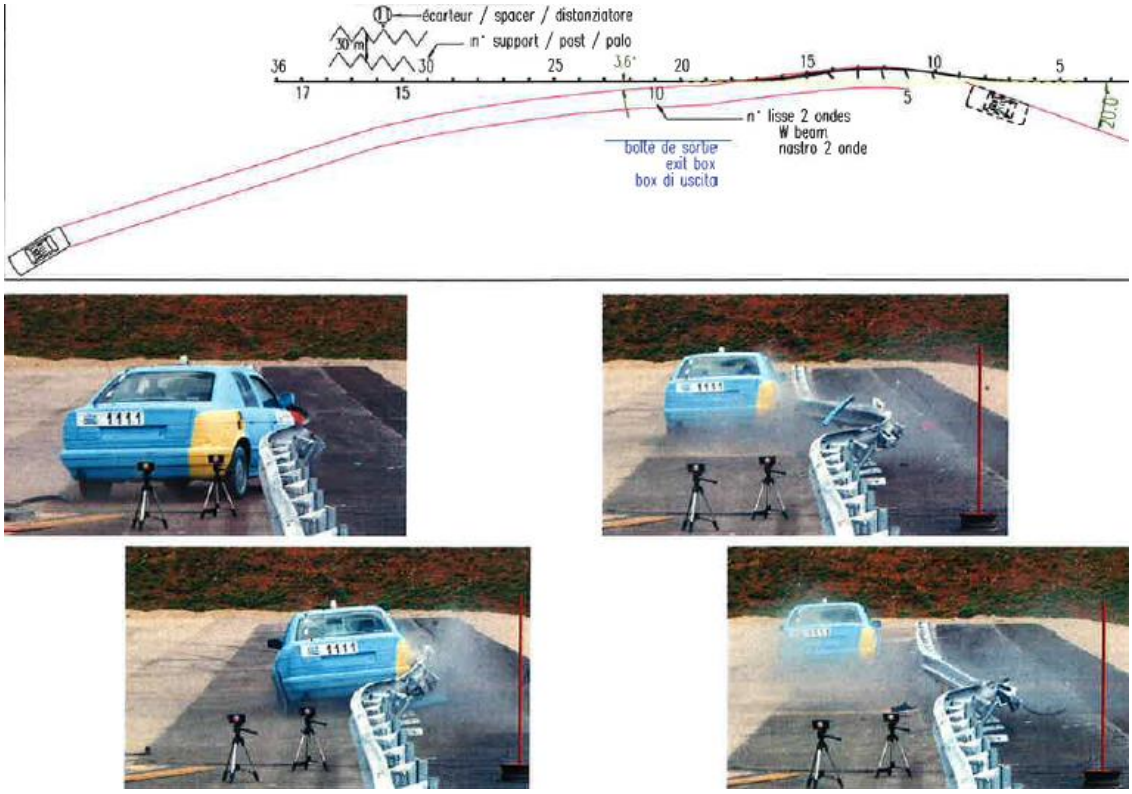

Figure 3- 5 Vehicle trajectory in crash test of the barrier [60]

Figure 3- 6 Damage of the barrier and vehicle [60]

Severity		Dynamic Deformation	
ASI	*THIV*(km/h)	W_m (m)	D_m (m)
0.8	24	1.5	1.2
Level A		W5	---

Table 3- 2 Quantitative criteria of VRS performances [60]

Post No.	*Da* (m)	*Db* (m)	*Wp* (m)
7	0.03	0.02	-
8	0.14	0.10	0.49
9	0.39	0.36	0.74
10	0.68	0.72	1.02
11	0.89	0.94	1.03
12	0.98	0.96	1.23
13	0.94	0.87	1.19
14	0.77	0.84	0.92
15	0.53	0.40	0.75
16	0.26	0.13	0.84
17	0.08	0.03	0.40

Table 3- 3 Permanent deformations of the safety barrier [60]

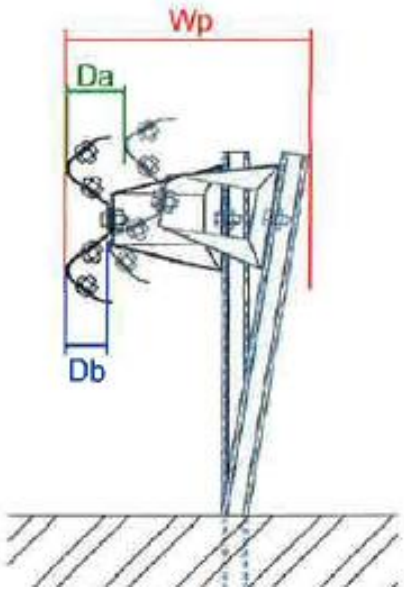

Figure 3- 7 Deformation parameters of the device [60]

3.2 Numerical model of the crash test

The modelling of the roadside barrier as well as of the vehicle demands for great accuracy and high skills (see Section 1.1.4). Although a tested roadside barrier may hundreds of meters in length and the vehicle used may contain thousands of components, only the parts which are exposed directly to impact loading are of remarkable deformations and should be modeled in detail. Considering the magnitude of the components' deformations, the crash test was modeled and simplified, and simulation was realized within LS-DYNA.

3.2.1 General settings of model

3.2.1.a Element type

In road equipment modeling, under-integrated elements (reduced one–point integration) are often used due to their low cost in tern of CPU time. The biggest disadvantage to one-point integration is the need to control the nonphysical modes of deformation, i.e. zero energy hourglass modes (see Figure 3- 8, Figure 3- 9) [62,63]. Hourglass can usually be controlled by applying internal forces to resist hourglass modes via one of several control algorithms. And hourglass energy, which is work done by the forces calculated to resist hourglass modes, takes away physical energy of the system. To increase simulation speed, one point integration elements (Belytschko-Tsay shell and constant stress solid) were used for element definition of the major parts of the VRS and the vehicle model, with hourglass control at the recommended levels [64]:

- Recommend stiffness hourglass control, IHQ=4, with hourglass coefficient QM=0.03 for metal and plastic parts;
- Recommend hourglass type 6 with hourglass coefficient between 0.5 and 1.0 for foams and rubbers.

Components of the steel barrier and the enclosure of the vehicle were modeled with shell elements, the parts which are exposed to the crash load were of large deformations and were modeled with full integrated shell elements to avoid the hourglass deformation and increase the accuracy of simulation.

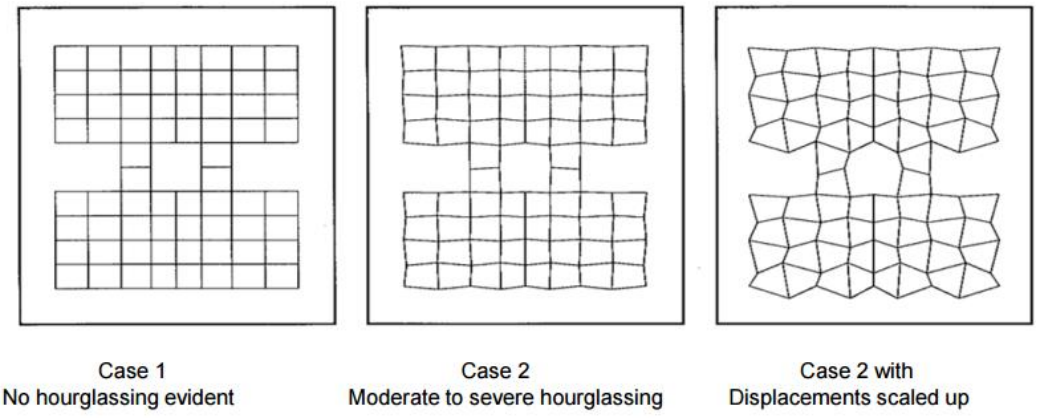

Figure 3- 8 Hourglass modes of shell elements [62]

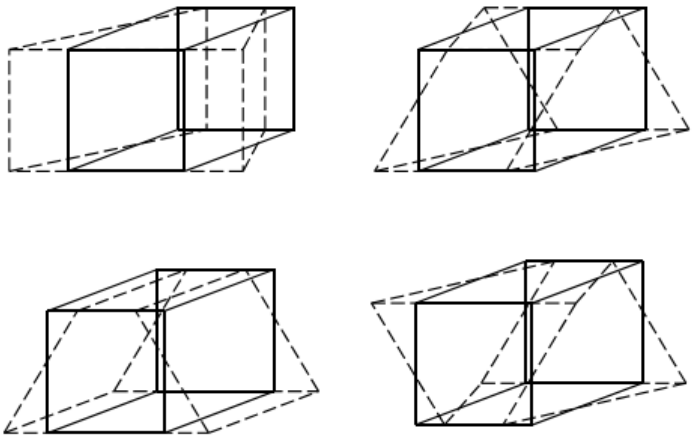

Figure 3- 9 Hourglass modes of solid elements [62]

3.2.1.b Material definition

For the S235 steel used for the fabrication of the VRS, the minimum value for the yield point is 235MPa. Nevertheless, the steel certificate analysis shows values higher than 330MPa, the tensile ultimate strength could be higher than 440MPa [65], and steel mechanical properties are influenced by the thickness of the plate being tested. J. Melcher [51] analyzed mechanical properties of the structural steels with statistical approaches. The statistical yield strengths of S235 are illustrated in Figure 3- 10 and the mean value of yield strength and tensile strength are 284.5MPa and 422MPa. Mechanical properties of steel are influenced by fabrication process and many other factors, stress & strain relationship of S235 steel defined in the crash simulation is shown in Figure 3- 11. Referent to the study of Bruce [66], the influence of steel deformation rate on its mechanical properties are considered and defined using the Cowper and Symonds model which scale the yield stress with the factor:

$$1+\left(\frac{\dot{\varepsilon}}{C}\right)^{1/p} \tag{3-1}$$

where C=6000, p=6. And the steel shell is defined in addition with MAT 24 (MAT_PIECEWISE_LINEAR_PLASTICITY).

Soil Material Model 147 [67] was developed for use in roadside safety applications. In addition to the plasticity model, the soil material model includes pre-peak hardening, post-peak strain softening (damage), strain-rate effects (strength enhancement), pore-water effects (moisture effects), and erosion capability. These enhancements to the standard soil material models were made to increase the accuracy, robustness, and ease of use for roadside safety applications. Material 147 was used for modeling of the soil.

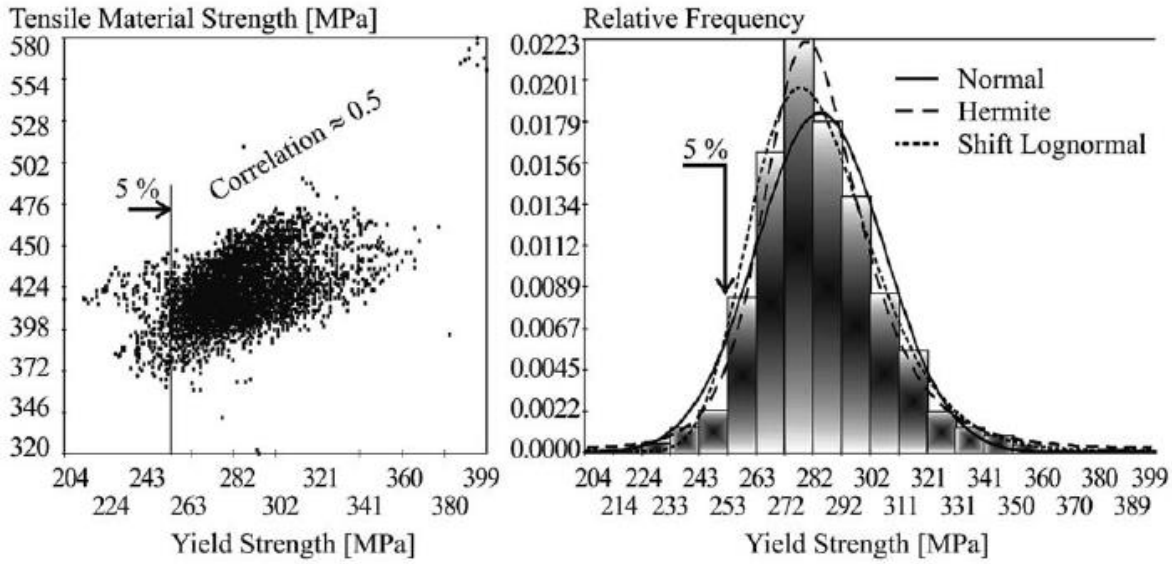

Figure 3- 10 Statistic characteristics of material S235 steel [51]

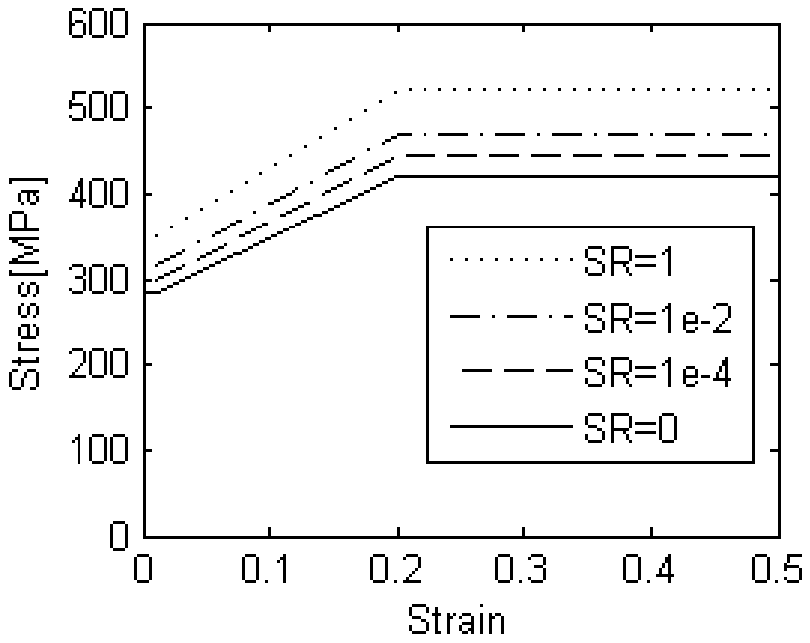

Figure 3- 11 S235 steel properties definition

3.2.1.c Contact definitions

The contact type *Contact_Automatic_Single_Surface* was used to define the contact conditions of vehicle or the VRS within itself and *Contact_Automatic_Surface_To_Surface* was used to define the contact between the vehicle and the VRS. One of the main factors contributing to road safety and need to be defined is the friction generated between vehicle tires and the road pavement surfaces, since the motion of a ground vehicle is primarily determined by the friction forces transferred from roads via tires. In fact, the tire/road friction force is affected by several different factors including tire/road surface conditions, tire

pressure, vehicle load, and steering angle, etc. Figure 3- 12 [68] shows the influence of the side slip and angle of slip on lateral tire/road friction coefficient and Figure 3- 13 [69] shows the longitudinal road friction profiles for the vehicle running on different road surface conditions and vehicles running on dry asphalt road with varied velocities.

In short, the friction coefficient of tire/road is influenced by many factors and is inversely proportional to the velocity of vehicle. Crash test was carried out on dry asphalt road. The longitudinal friction coefficient can be 0.8, but the side slips of the vehicle reduce the grip of the tires. In this study, the friction coefficient is defined to be 0.4 at the beginning with the vehicle velocity at 110km/h and to be 0.5 when the vehicle left the barrier with the velocity at about 60km/h.

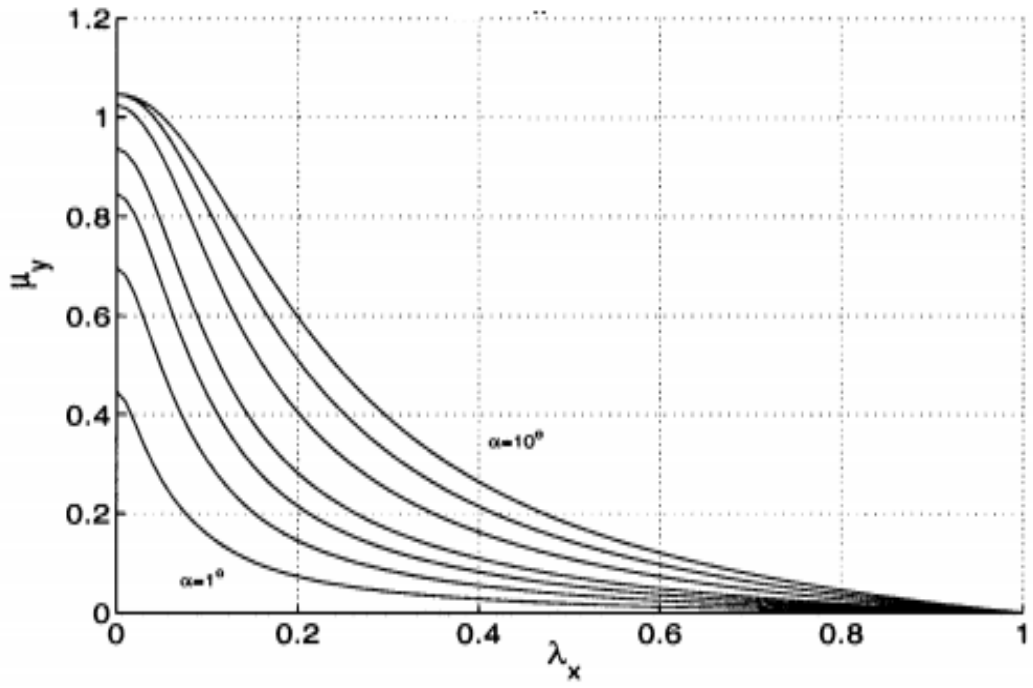

Figure 3- 12 Tire side slip/friction curves [68]

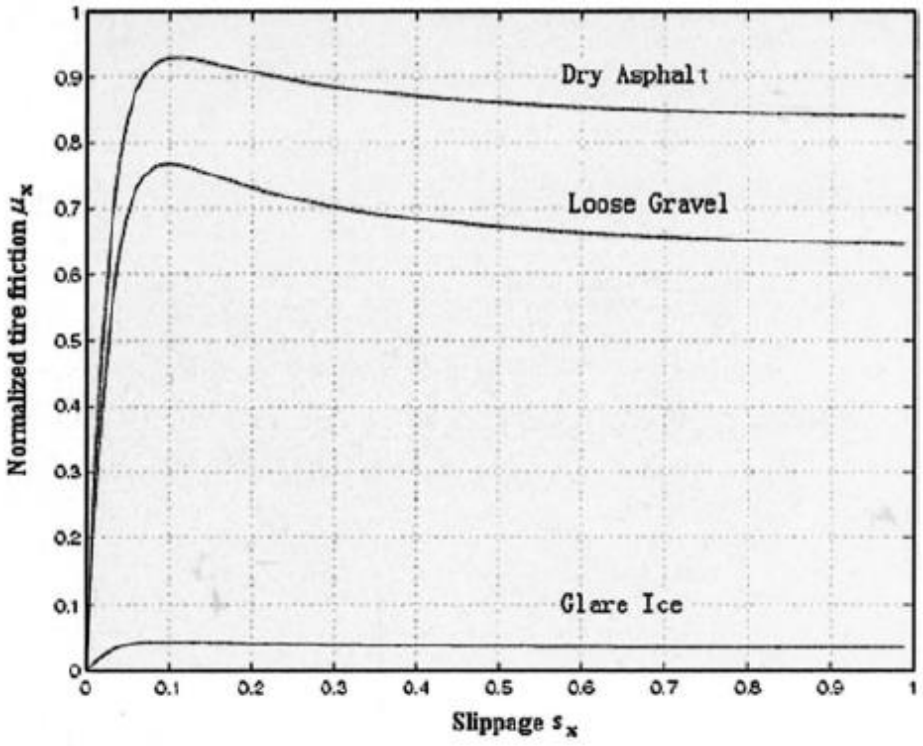

(a)

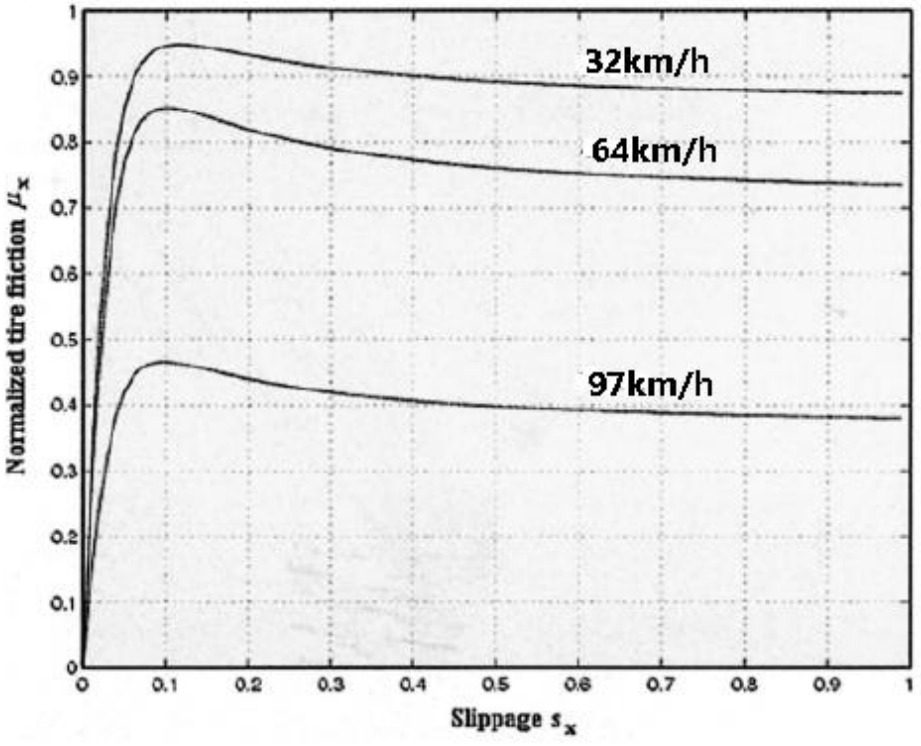

(b)

Figure 3- 13 Typical longitudinal tire/road friction profiles for : (a) vehicle running on different road surface conditions with velocity 32km/h, (b) vehicles running on dry asphalt road with varied velocities [69]

3.2.2 Vehicle model

The reduced FE model of the vehicle was provided by L.I.E.R., and used in the simulation for simplification of the crash test. The vehicle model was modified to insure the accuracy of simulations: Right side of the vehicle was in contact with the barrier in the collision and of large deformations. The mesh of right-front part of the vehicle model was refined to increase simulation accuracy (see Figure 3- 14); The multi-part model of Vehicle consist of different components and sharp corners exist, especially at the connection position of two components, the model was modified to eliminate sharp corners in order to avoid mesh penetrations of the vehicle with the barrier (see Figure 3- 15). Real damages of the vehicle and the simulation result are illustrated in Figure 3- 16. No elements penetrations are detected during the collision process and the numerical model has well simulated the damage of the vehicle.

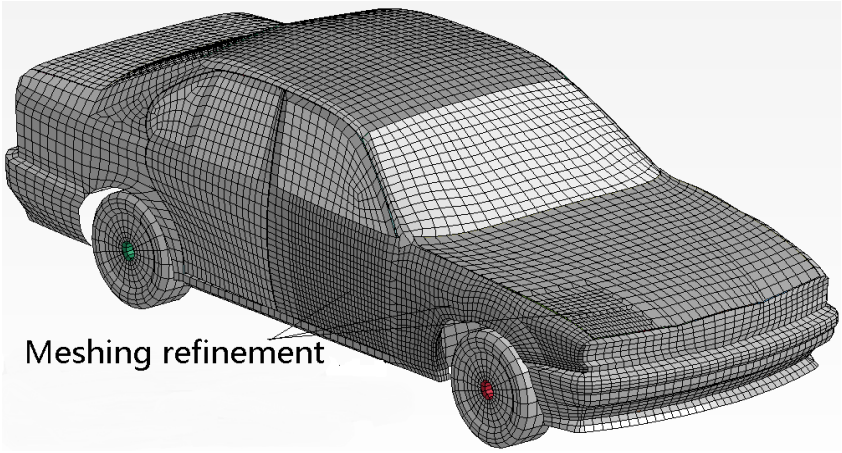

Figure 3- 14 Vehicle model of L.I.E.R. mesh refinement of the right-front part

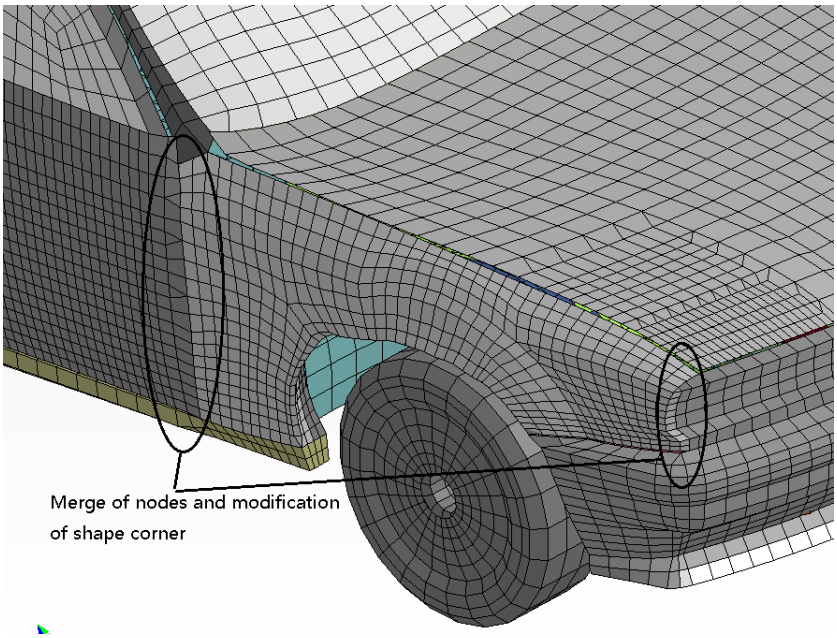

Figure 3- 15 Modification of sharp corner of vehicle model

Figure 3- 16 Vehicle damages after crash test

3.2.3 VRS model

3.2.3.a Meshing

The components of the safety barrier were modeled in accordance with the drawing provided in the test report (see Figure 3- 3). The mesh of VRS components are shown in Figure 3- 17. VRS components--- Rail, Spacer, Post --- were modeled by shell elements with coarse mesh. Mesh of the parts of the VRS in the middle of the device which are exposed to impact loading and of large deformations were refined and defined by full – integration shell elements, while the one-point integration shell were used for element define of other parts; The holes for bolted connections are modeled. Connection load lead to large deformations or even fracture of the holes, mesh were refined around the holes; bending of the post is mainly at the ground position, post mesh and the connected soil mesh are refined at the ground position.

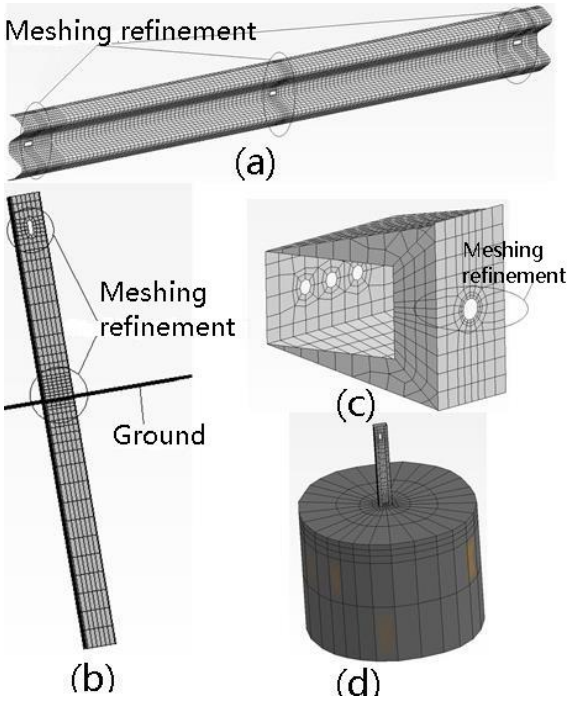

Figure 3- 17 Meshes of the VRS components: (a) Rail, (b) Post, (c) Spacer, (d) Soil

3.2.3.b Bolted joints

Rails, spacers and posts are connected by bolts, and the connection failures observed after the real crash-test are illustrated in Figure 3- 18. After the crash test, the Rail-Rail bolts connections were not damaged and the slippage between two rails was negligible, the Rail-Rail connections were simplified with high-strength spring elements in the numerical model. Both Post-Spacer and Spacer-Rail are connected with one single bolts, and the connection failure was the bolt pull-out from spacer slotted hole for the Post - Spacer connection (see Figure 3- 18), and the edges of the slotted holes of the Spacers were broken. To simulate the real connection conditions of Post-Spacer and Spacer-Rail, slotted holes were modeled (see Figure 3- 17); bolts-nuts were modeled with rigid shell elements and connected with spring elements for Post-Spacer and Spacer-Rail connections in numerical model.

The quality class of the bolts used for the connections is between level 5.6 and level 6.8. Yield strength of the bolts is between 300MPa and 480 MPa and connection break force is between 78500N and 94000N [70]. The spring elements to connect the bolts and nuts are characterized by the curve in Figure 3- 19, with the Modulus Young of bolt defined to be 400GPa and the connection break at deformation equals 1mm with the force at 82880N. The Pre-load of the spring elements are defined to be 12432N (15% of the break force).

The Rail-Rail connections were simplified and components displacement freedoms (rail, spacer rotations, slip of slotted hole between the post and spacer and the horizontal slip of the slotted hole between the rail and the spacer, bolt pull-out failure from the hole) were respected in the FE model (see Figure 3- 20). The bolts connection failure in numerical simulation is illustrated in Figure 3- 21: Broken of the slotted holes of the Spacers and bolt pull out failures were well simulated.

Figure 3- 18 Bolts pull out failure of post-spacer connection [60]

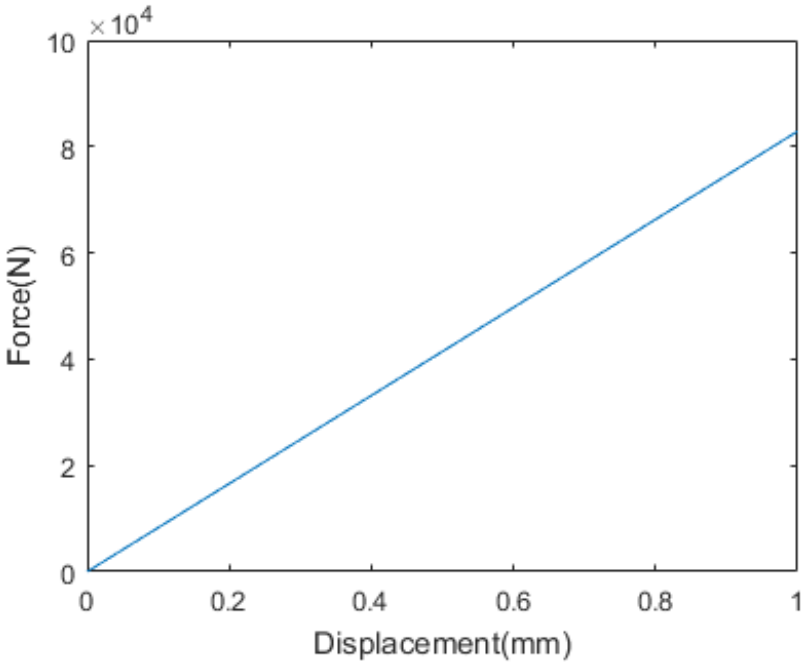

Figure 3- 19 Characterization of spring elements to connect the bolts and nuts

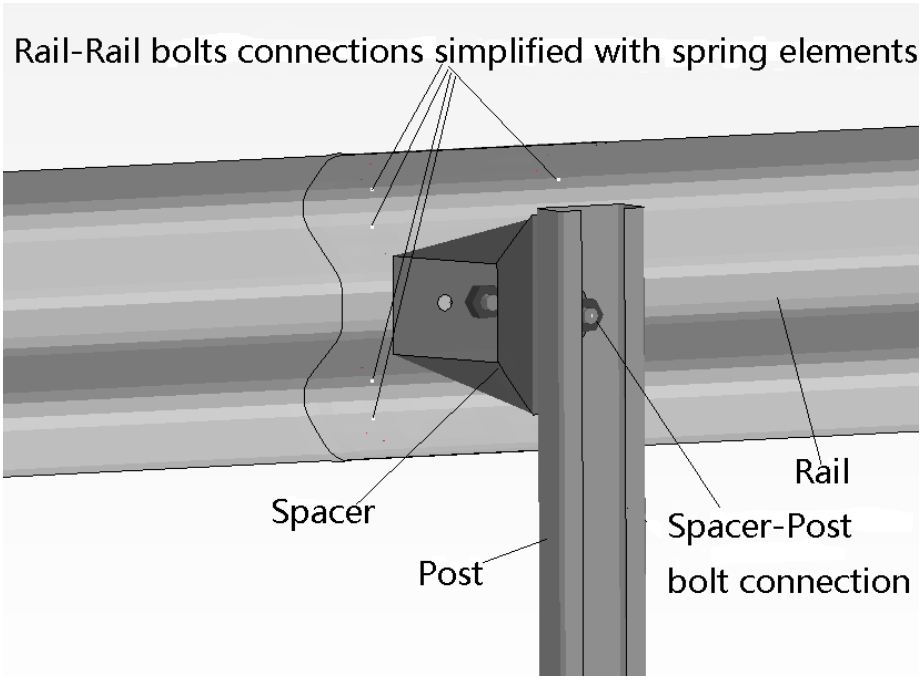

Figure 3- 20 VRS modeling

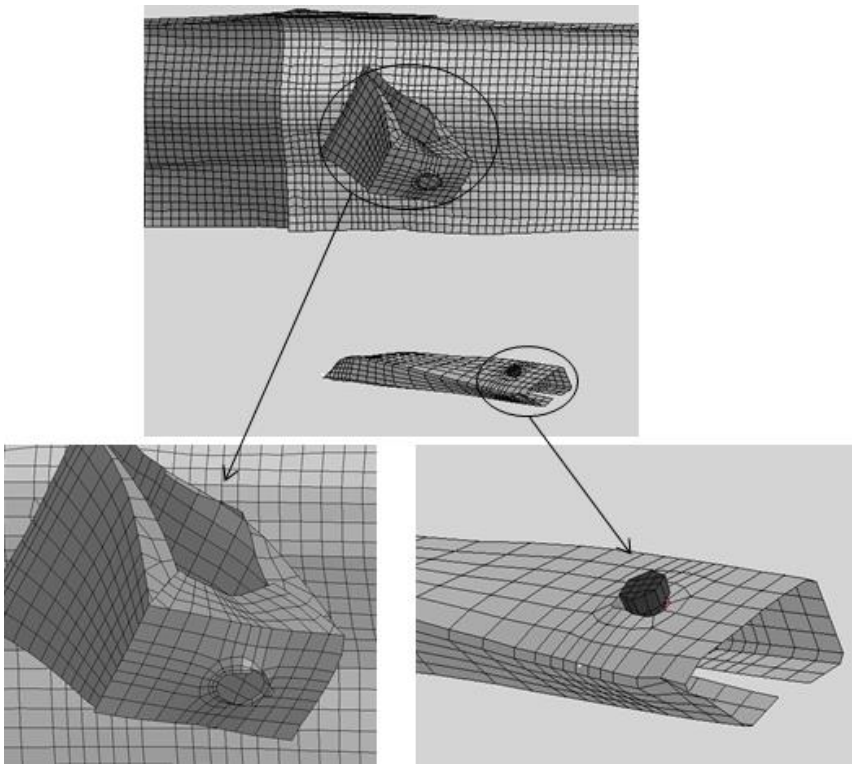

Figure 3- 21 Bolts pull out failure simulation

3.2.3.c Soil modeling

Posts in the middle parts of VRS were of large deformation and their corresponding soil were modelled with solid elements of cylindrical shape to simulate the interactions of Post and Ground in detail. Deformations of Post and Ground in real test and simulation are shown in Figure 3- 22. The other soil parts were simplified by spring elements (see Figure 3- 23 (a)). With elasto-viscoplastic characteristic varying with depth, appropriate material properties of spring elements were determined from performed parametric simulations. Comparing to previous studies [19,20,22,23] who simulate the soil with only solid elements or spring elements, the combination of the two forms modeling of soil ensure simulation accuracy and decrease calculation cost.

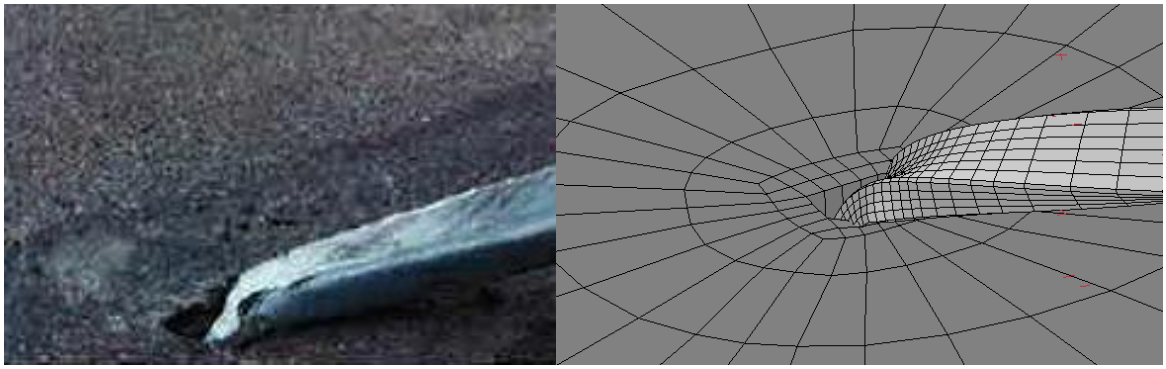

Figure 3- 22 Deformations of post and ground in real test and simulation

3.2.3.d Continuations

The tested safety barrier contains 21 beams and was 84m long with the two ends fixed to the ground, while only the 7 beams in the middle of the device were deformed after crash test according to report [60]. In the numerical simulation, 9 beams (7 beams with large deformations and the connected two beams) and the related posts, spacers were modelled. Continuations of the barrier at ends were modelled with springs (see Figure 3- 23(a)).

The omitted barrier parts were modelled to characterize mechanical properties of the spring elements (see Figure 3- 23(b) (c)): One end of the omitted barrier was fixed and the other end was loaded with a time dependent force, the relations between loaded force and the displacement at the loaded end were measured, which defines the spring stiffness in the continuation positions. 33 spring elements were used at each ends to define boundary constraints of barrier and spring stiffness is illustrated in Figure 3- 24. Spring elements we defined with nonlinear properties. Different from [15, 22] who define the spring constraints with linear elastic properties by analytical analyses, we defined accurately the boundary conditions at the continuation positions.

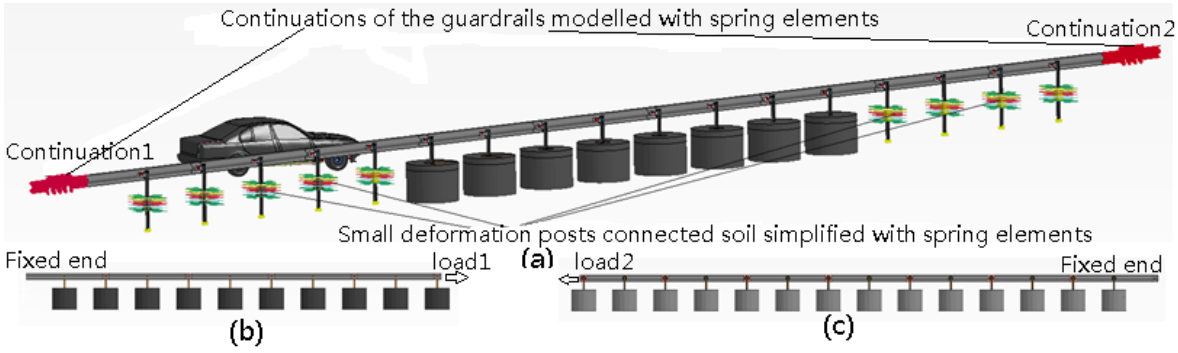

Figure 3- 23 Numerical barrier crash model: (a) simplified barrier crash model; (b) characterization of continuation 1; (c) characterization of continuation 2

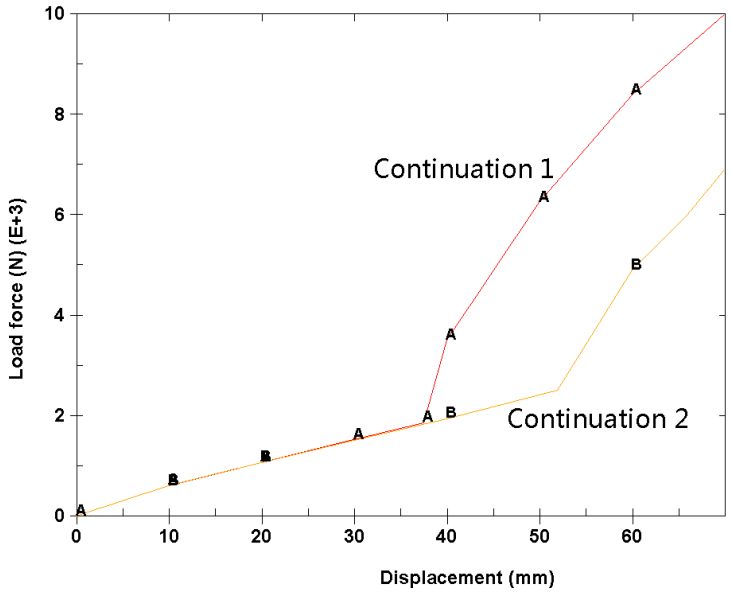

Figure 3- 24 Characterization of spring elements at two ends of barrier model

3.2.4 Model validations

The vehicle and VRS experimental crash test and simulation is illustrated in Figure 3-25. The crash begins at t=0s, with initial crash angle of 20 °; the vehicle was redirected by the barrier and it was parallel to the barrier at impact time t=0.25s, with about three-quarters of the vehicle invading into the barrier; the barrier restraints the vehicle on the road and about half the vehicle body invade into the barrier at t=0.45s; the numerical model has simulated precisely the major steps of the crash test, but from t=0.55s, the differences between experimental test and simulation analysis become more and more obvious. These differences were caused mainly by the defects of the vehicle model. Vehicle FE model was more rigid than the tested vehicle: after the impaction, the right front wheel was detached form the vehicle body and the tire was broken while in our numerical simulations, the right front wheel remained connected to the vehicle body and no damage was detected to the tire (see Figure 3- 16). Right front wheel of the vehicle was in direct contact with the barrier support post at t=0.55s (see Figure 3- 26), and the defects of the vehicle in rigidity affects barrier deformations and vehicle trajectory after t=0.55s.

However, the criteria of main interest - *ASI*, *THIV*, *W* and *D* - were measured before t=0.55s and they have a very good match with the measured values in the experimental test (see Table 3- 4). *THIV* was calculated at t=0.154s in the test and the impact moment of head and vehicle inner side is t=0.153s in the simulation. *W* and *D* were detected at position Post No.12 in both experimental test and the simulation. The failure modes of the VRS in the crash process are shown in Appendix II Failure modes of the VRS. The VRS deformations and the relative simulation results are shown in Appendix III Deformations of the VRS. Rails no.4-8 were in direct contact with the vehicle during impact process and of large deformations after the crash (see Appendix III Deformations of the VRS).

Time	Experiments	Simulations
0s		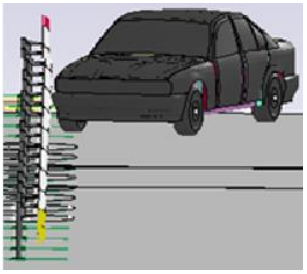
0.2s		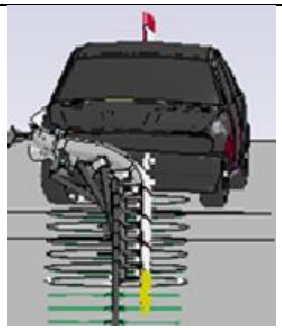

0.25s		
0.45s		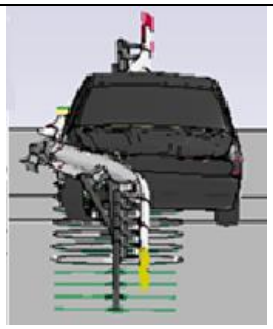
0.55s		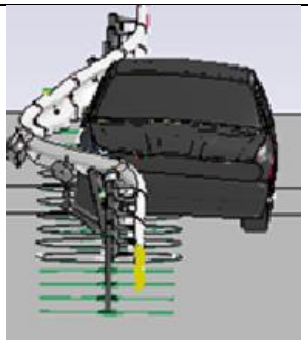
0.65s		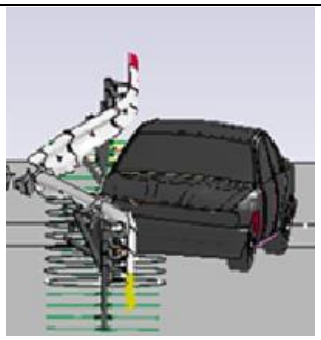
0.70s		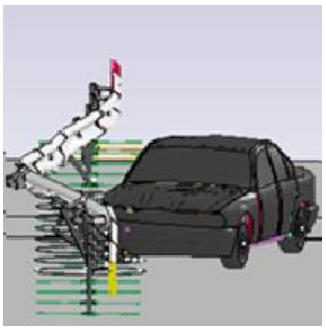

Figure 3- 25 VRS crash test & simulation visual comparison

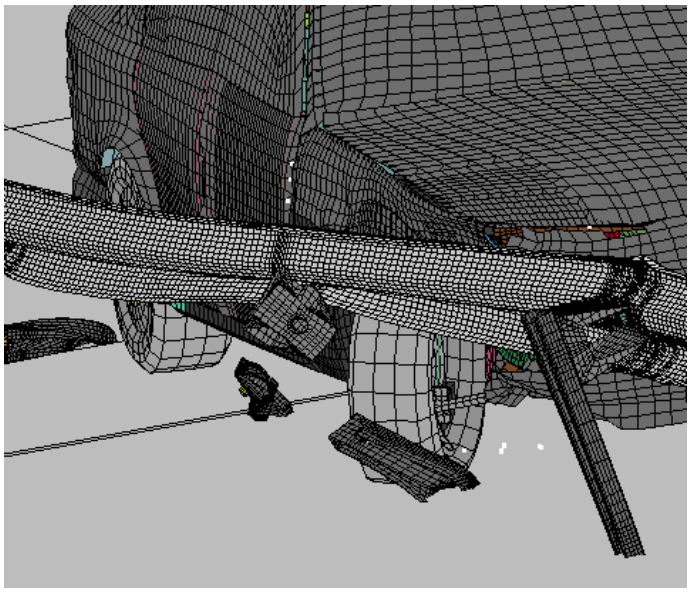

Figure 3- 26 Right front wheel contact with Post at t=0.55s

	ASI	*THIV*(km/h)	*W*(m)	*D*(m)
Test	0.8	24	1.5	1.2
Simulation	0.8	22	1.5	1.2

Table 3- 4 Comparison of results from the simulation and the test

Figure 3- 27 shows the velocity at the mass centre of the vehicle in fixed reference framework (X: barrier direction; Y: lateral direction perpendicular to barrier) during the crash simulation. The vehicle impacts the barrier with V_{X0}=104km/h and V_{Y0}=-38km/h and leave the barrier with V_{X1}=60km/h and V_{Y1}=10km/h. Velocity of the vehicle in the barrier direction was reduced. The velocity V_Y changed direction at impact time t=0.28s and the vehicle was contained on the road.

Energy distributions during crash simulation are illustrated in Figure 3- 28. Thanks to the roadside guardrail, about 66% of total energy was absorbed by vehicle & barrier deformation (curve C). By redirecting and restraining the vehicle on the road, more than 20% of vehicle kinetic energy remained after the crash event (curve B). 12% of total energy was dissipated in sliding contact (curve D), especially the friction between vehicle tires and the pavement. Spring elements were used to simplify the crash model, low value of spring & damper energy (curve E) demonstrates the rationality of our simplification. Model parts with remarkable deformations were simulated with full – integration elements and hourglass energy (curve G) added to small deformation parts is negligible comparing to internal energy. Almost all the kinetic energy will be converted into vehicle internal energy in a short time when vehicle collides with rigid fixed objects (trees or rocks on the roadside for example). The roadside barrier has well dissipated kinetic energy and extended the collision time, which largely reduced the impact severity.

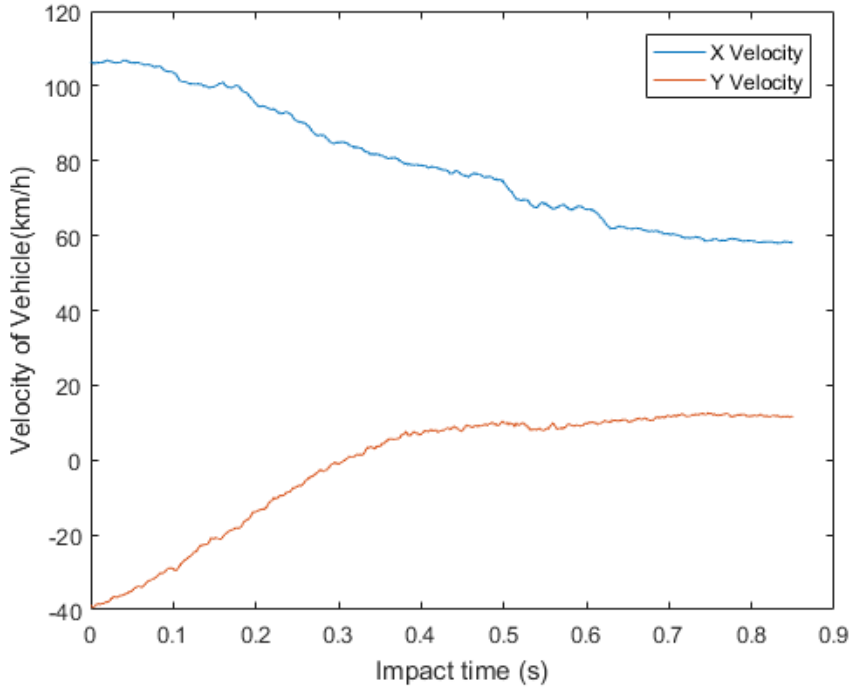

Figure 3- 27 Vehicle velocity during the crash test simulation

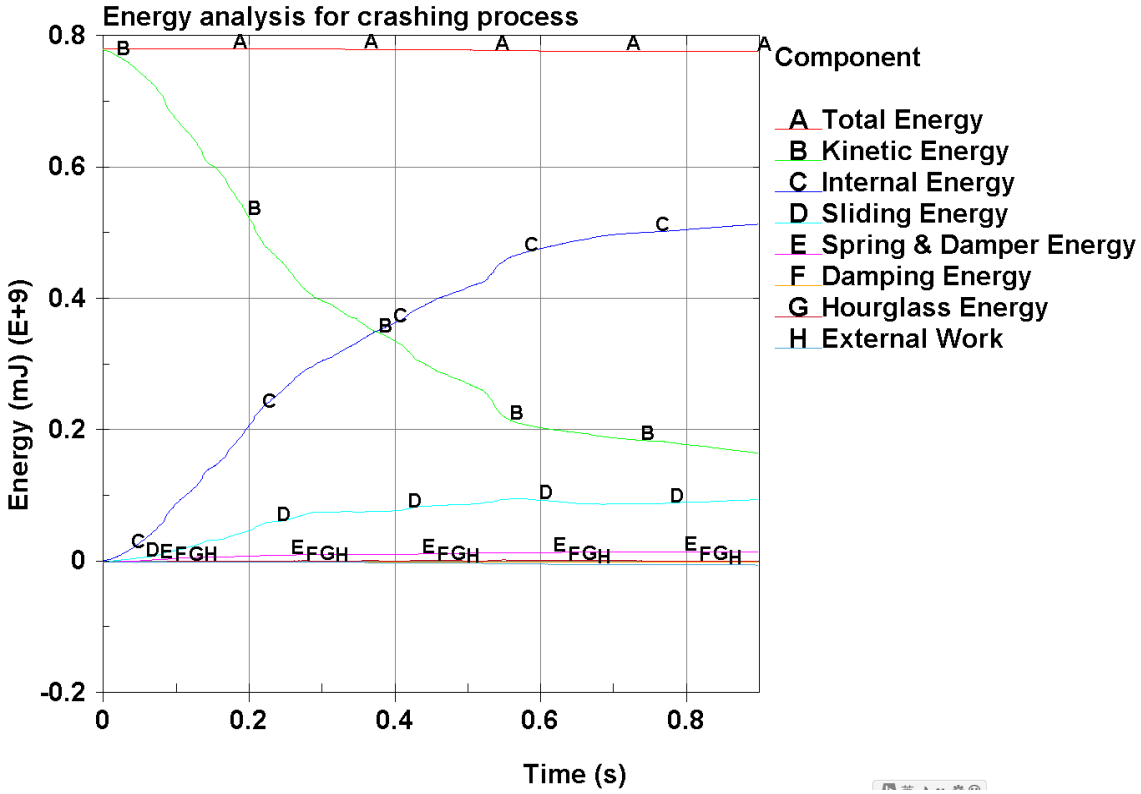

Figure 3- 28 Energy distribution during crash analysis

3.2.5 Discussions

Considering the magnitudes of component deformations in crash experiment, the numerical VRS crash test model was simplified in these major issues:

- Reduced model with mesh refinement for parts of remarkable deformation;
- Boundary constraint applications for barrier continuations at two ends with spring elements;
- Soil detailed modelling with solid elements for parts of evident deformation and its replacement with spring elements for others soil parts.
- Bolted joints simplification for Rail-Rail connections and detailed modelling for Post-Spacer and Spacer-Rail bolt connections considering magnitude of deformations and components degree of freedom.

Different from the full modelling of barrier crash test which may need a week for the crash simulation of the VRS, the simplified model simulate the VRS crash in 7 hours with a regular PC. Validated by comparison with the experimental test, the simplified model is of good accuracy. More efforts are needed for vehicle wheel and tire modelling to predict vehicle trajectory during crash test, but these defects have little influence on global performance evaluations of the VRS.

In fact, the real mechanical properties of the VRS can't be defined exactly in the simulation of the crash test. Experimental tests can be carried out to measure factors such as material mechanical properties of the VRS, but uncertain factors exist in the model and what we obtained after the experimental tests is a set of values of the measured parameters.

Mechanical properties of VRS model are defined by the mean values of the parameters obtained through literature studies. Varying the uncertain factors of the model input in their possible distribution interval, sampling based simulations help to characterize performance uncertainties of the VRS. Identifying of critical factors whose uncertainties have great influence on VRS performances and quantification of their influences are the main objects of next section---Sensitivity Analysis (SA) of the VRS.

3.3 SA of the VRS

According to the strategy proposed in section 2.3. Two-level screening method and Morris Analysis will firstly be used to identify the influential uncertain factors with relatively low number of samples and the Sobol' indices will be used to quantify their influences.

3.3.1 Uncertain factors & Outputs

Uncertain factors

Due to the variations of material mechanical properties and the tolerances in manufacturing, the uncertainties of the following parameters are considered:

- VRS components Rail, Spacer and Post are fabricated with S235 structural steel. S235 mechanical properties have been analysed statistically in literature study [51]. Supposing that the steel tensile strength is proportional to its yield strength, uncertainties in steel mechanical properties influence Rail Yield strength (*RY*), Rail Young Modulus (*RM*), Spacer Yield strength (*SY*), Spacer Young Modulus (*SM*), Post Yield strength (*PY*) and Post Young Modulus (*PM*);
- The designed Rail Thickness (*RT*), Spacer Thickness (*ST*), Post Thickness (*PT*) are 3mm, 3mm, 5mm respectively, and the standard deviations of the thickness parameters caused by the fabrication tolerances is defined to be 5% of their mean values;
- Fixed to the ground, the VRS performances are affected by Soil bulk Modulus (*SoilM*); The VRS components are connected by bolts and the Bolt Pre-load (*BP*) is defined.

Type	Variables	Unit	Mean	St. D
S235 steel mechanical properties	Rail Yield strength (*RY*)	MPa	284.5	21.5
	Rail Young Modulus (*RM*)	GPa	203	12.6
	Spacer Yield strength (*SY*)	MPa	284.5	21.5
	Spacer Young Modulus (*SM*)	GPa	203	12.6
	Post Yield strength (*PY*)	MPa	284.5	21.5
	Post Young Modulus (*PM*)	GPa	203	12.6
Tolerances of fabrication	Rail Thickness (*RT*)	mm	3	0.15
	Spacer Thickness (*ST*)	mm	3	0.15
	Post Thickness (*PT*)	mm	5	0.25
Soil & Bolts pre-load	Soil bulk Modulus (*SoilM*)	MPa	400	100
	Bolt Pre-load (*BP*)	N	12432	4144

Table 3- 5 Uncertainties on VRS input variables

Definition of the distributions that characterize uncertainties of these model input parameters could be the most important part of the SA study as these distributions determine

both the uncertainty in model performances and the sensitivity of the elements of outputs to the elements of inputs. The distributions are typically defined through an expert review process by statistics studies, and their development can constitute a major analysis cost. To simplify the characterization of uncertainty, the uncertain parameters are defined with the classic 'crude' method in this study by supposing they have normal distributions. Mean values and standard deviations of the uncertain factors are defined in Table 3- 5.

Outputs criteria

The impact severity criteria Acceleration Severity Index (*ASI*), Theoretical Head Impact Velocity (*THIV*) and the device deformation indices Working width (*W*), Dynamic deflection (*D*) are quantitative criteria for performance evaluations of the VRS.

ASI is an important index to evaluate maximum force load to the passenger during crash. Acceleration is supposed to be estimated by average value during 50ms (see eq. 1-1, 1-2). Figure 3- 29 shows the time series of *ASI*(*t*) in the impact simulation. The *ASI*(*t*) curve is noisy and the maximum values of *ASI*(*t*), i.e. *ASI*, is influenced by the unwanted signal. Figure 3- 30 shows the *ASI*(*t*), with the raw acceleration filtered with a four-pole phaseless Butterworth low-pass digital filter, having a cut-off frequency of 13 Hz. Instead of averaging acceleration values at 50ms, filter helps to remove some frequencies and smooth the *ASI*(*t*) signal, but the *ASI* value may be underestimated with the filtering method. It is not possible to calculate accurately *ASI*. *W* and *D* have similar temporal behavior and both represent the maximum deformation of the device. For SA of the VRS, only the two criteria *THIV*, *D* are considered.

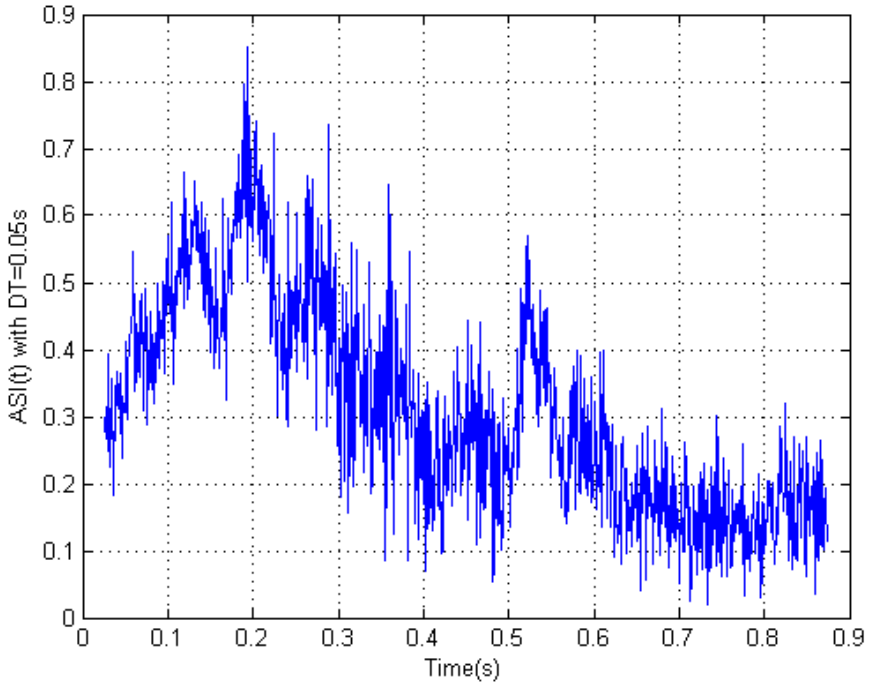

Figure 3- 29 ASI(t) with accelerations estimated by average value in 50ms

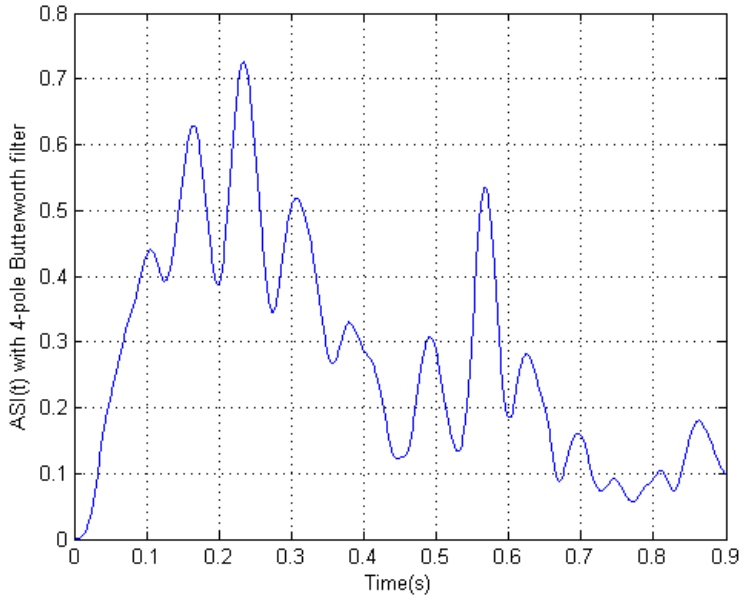

Figure 3- 30 ASI(t) with acceleration filtered by four-pole phaseless Butterworth filter

3.3.2 Two-level screening---Orthogonal Array (OA)

The influences of the 11 uncertain factors on the model performances were studied by a two-level screening analysis using OA. The OA and the outputs *THIV* and *D* are listed in Table 3- 6. Columns in OA represent the 11 variables listed in Table 3- 5. Each variable takes two values: 0, which corresponds to μ_k-σ_k and 1, which corresponds to μ_k+σ_k (μ_k: average value of factor *k*; σ_k: standard deviation of factor *k*).

No.	OA	*THIV*(km/h)	*D*(m)
1	1 1 1 1 1 1 1 1 1 1 1	22.4481	1.044
2	1 1 1 1 1 0 0 0 0 0 0	21.2421	1.182
3	1 1 0 0 0 1 1 1 0 0 0	20.3844	1.221
4	1 0 1 0 0 1 0 0 1 1 0	21.5142	1.160
5	1 0 0 1 0 0 1 0 1 0 1	21.4796	1.170
6	1 0 0 0 1 0 0 1 0 1 1	20.2277	1.159
7	0 1 1 0 0 0 1 0 0 1 1	21.5688	1.213
8	0 1 0 1 0 0 0 1 1 1 0	21.5030	1.186
9	0 1 0 0 1 1 0 0 1 0 1	22.9677	1.150
10	0 0 1 1 0 1 0 1 0 0 1	21.5258	1.246
11	0 0 1 0 1 0 1 1 1 0 0	22.1834	1.092
12	0 0 0 1 1 1 1 0 0 1 0	22.3825	1.167

Table 3- 6 OA sampling and simulation outputs of the crash model

Parameters	*THIV*		*D*	
	ME (km/h)	Rank	*ME* (mm)	Rank
RY	**-0.4029**	**1**	**-9.8**	**4**
RM	**0.1227**	**8**	**9.8**	**4**
SY	0.1281	7	-9.7	6
SM	0.1446	6	0	11
PY	**0.2896**	**3**	**-33.5**	**1**
PM	0.2315	5	-1.2	10
RT	**0.1222**	**9**	**-14.7**	**3**
ST	**-0.2402**	**4**	**-7.8**	**8**
PT	**0.3971**	**2**	**-32.2**	**2**
SoilM	-0.0116	11	-9.7	6
BP	0.0840	10	-2.2	9

Table 3- 7 Main effect of OA screening

A total number of 12 model runs were conducted. Half the values in each column were equal to 0 and the other half values were 1. The $ME_r(Y)$ of each variable on the two outputs *THIV* and *D* were calculated and their influences were ranked from the most influential (1) to the least influential (11) according to the absolute value of $ME_r(Y)$ in Table 3- 7.

Limited by analysis precision, the two-level screening with OA can only identity qualitatively the influential parameters. The first 4 influential factors for both *THIV* and *D* were selected separately and a total number of 6 variables (variables on bold in Table 3- 7) out of 11 are considered as influential after this analysis.

3.3.3 Multi-level Screening---Morris Analysis (MA)

The 6 selected variables are re-screened with MA. The Cumulative Distribution Function (CDF) value of a factor is unitless and is uniformly distributed across the interval [0, 1] regardless of the factor distribution, rather than concentrated in one part of the interval. The CDF values of the parameters were treated as inputs variables and 4 levels (1/8, 3/8, 5/8, 7/8) were taken for each variables with Δ=0.5 (see eq.2-20). 6 trajectories with each trajectory corresponding to 7 model executions based on a once-at-a-time sampling strategy were selected and a total number of 42 model runs were realized. Samples and simulation results are listed in Appendix IV Data for Morris Analysis of the VRS. And the analytical results of MA are plotted in Figure 3- 31, for both outputs *THIV* and *D*.

The value of μ^* (eq. 2-21) is used to calculate the main effect (ME) of the factor, and large value of the standard deviation σ implies significant interaction effects (Inter) of a parameter. Considering ME and Inter with both *THIV* and *D* as criteria, the three variables tolerance of the Post Thickness (*PT*), uncertainty of Post Yield strength (*PY*) and tolerance of the Rail Thickness (*RT*) are of significant influence on VRS performances (see Figure 3- 31).

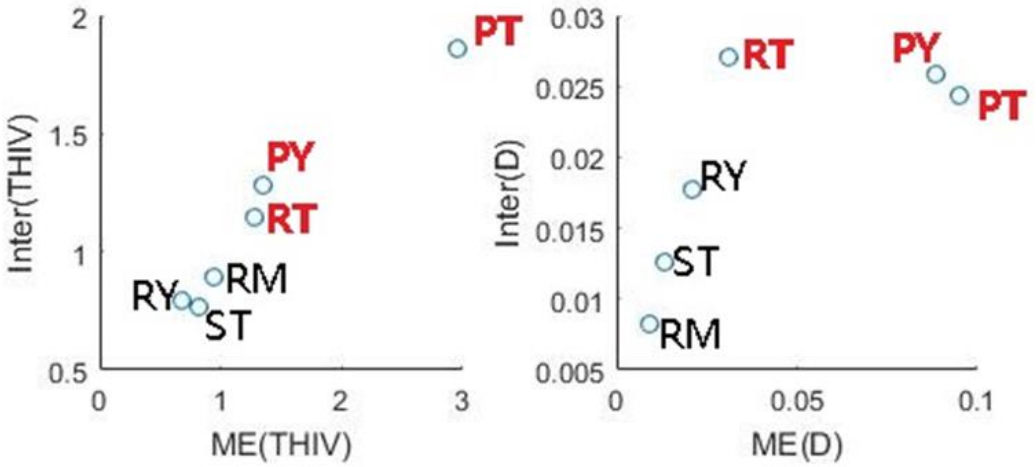

Figure 3- 31 ME & Interaction effect with both *THIV* and *D* as criteria for MA

3.3.4 VBSA---Sobol' indices

Three variables out of eleven were identified as of great influences on VRS performances after the screening analyses. VBSA---Sobol' indices---was used to quantity the influence of the three variables --- *PT*, *PY* and *RT*. 100 model runs were realized with Latin Hyper Cube sampling. Then the metamodel was created with the Matlab toolbox of Kriging interpolation --- DACE [58], and the surrogate model was validated with 20 additional samples. The scatterplot of the simulation results of the 120 model runs are given in Figure 3-32: *THIV* has positive correlation with *PT* and *PY* while deformation of the device *D* has negative correlation with the input values. The correlation of *RT* on the output values is not evident, especially for *THIV*.

The Sobol' indices were calculated with the metamodel and plotted in Figure 3- 33. The quantitative analysis results show that among the three influential factors, the variance of post thickness (*PT*) is the most influential factor for VRS performances (with S_{PT}=0.6069, ST_{PT}=0.6311 for *THIV* and S_{PT}=0.529, ST_{PT}=0.5583 for *D*). Uncertainties of post yield strength (*PY*) also play an important role for robustness of the VRS (with S_{PY}=0.3283, ST_{PY}=0.3534 for *THIV* and S_{PY}=0.3762, ST_{PY}=0.3903 for *D*). Relative to the other two factors, the influences of rail thickness (*RT*) are negligible (with S_{RT}=0.0648, ST_{RT}=0.0695 for *THIV* and S_{RT}=0.0948, ST_{RT}=0.0890 for *D*). For all the three variables, their main effects are approximately equal to their total effects, which indicate that there are nearly no interactions effects.

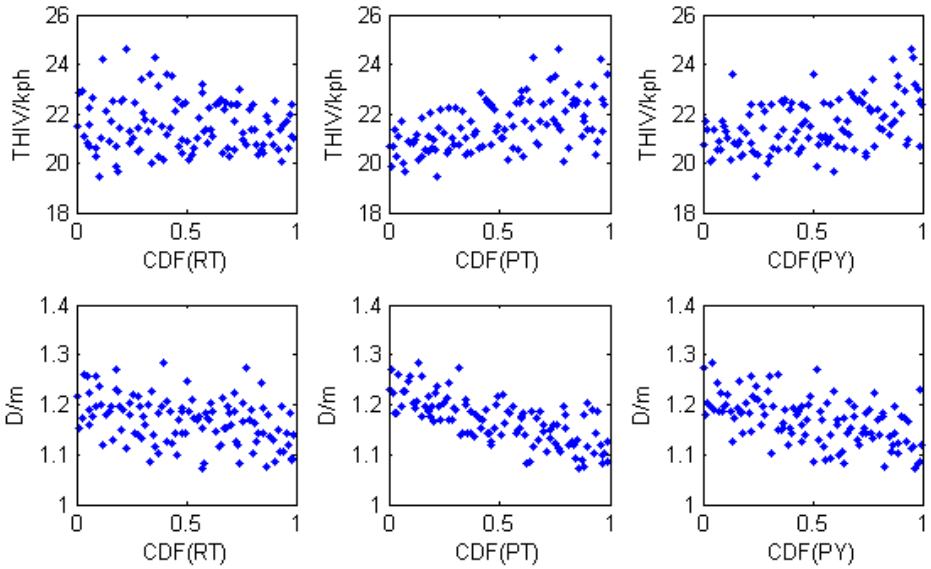

Figure 3- 32 Scatterplots of CDF values of inputs *RT*, *PT*, *PY* and the outputs *THIV*, *D*

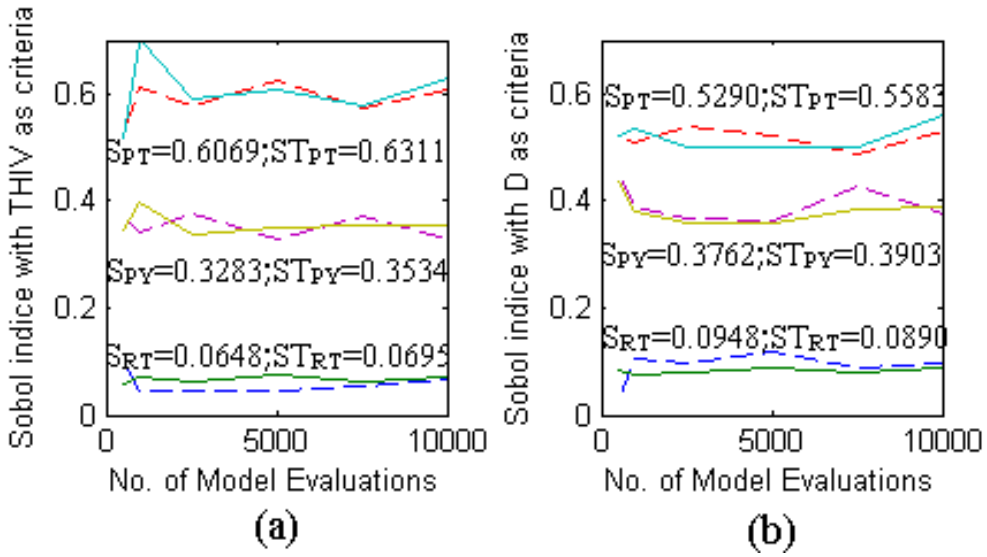

Figure 3- 33 Evolution of Sobol' indices against sample data size: (a) *THIV* as criteria (b) *D* as criteria (Solid line: total effects of *PT* (ST_{PT}), *PY*(ST_{PY}) and *RT*(ST_{RT}); Dotted line: main effects of *PT*(S_{PT}), *PY*(S_{PY}), *RT*(S_{RT}))

3.4 Conclusions

A VRS must succeed the crash test before being installed on the roadside: crash test of a VRS---GS2 hard shoulder safety barrier was realized by LIER laboratory; the tested device has well restraint the severity level at level A with the device deformation at level W5 [12,13].

Considering the magnitudes of components deformations in crash test, the numerical VRS crash test model was created and simplified. Different from full modeling for the VRS crash test which may need days of simulation time, the simplified model simulate VRS crash in 7 hours with a regular PC; Validated by experimental test, the simplified model is of good accuracy. Still more efforts are needed for the modeling of vehicle wheel and tire to predict vehicle trajectory during crash test, but these defects have little influence on barrier performance evaluations.

Uncertain factors exist in the VRS. The influences of the model inputs' uncertainties on model robustness were analyzed with numerical simulations through SA with three steps (see Table 3- 8): Eleven noisy factors were selected for uncertainty analysis of the VRS. Three variables were identified as influential after screening analyses of OA and MA with 12 and 42 model runs respectively. 120 model runs were used to create the Kriging metamodel, and sensitivities of the selected three variables were quantified with Sobol' indices by using the surrogate model. Two of the three influential variables have been classified as of critical influence on the VRS performances---tolerance of the Post Thickness (*PT*) and uncertainties of the Post material Yield strength (*PY*). The most efficient way to increase model robustness is to decrease the fabrication tolerance of the Post Thickness. Another way to increase the model robustness is to construct the Post with the structural steel fabricated by the same manufacturer under the same fabrication conditions (i.e. decrease Post Yield strength uncertainty).

Numerous uncertain parameters exist in the VRS model and it is expensive to measure the distributions of all the parameters. Assumptions help to define the distributions of the 11 uncertain parameters in the SA of the VRS and the two most influential parameters are identified after the analysis. More efforts are needed to measure the real distribution of the two influential uncertain parameters, and it helps to increase the accuracy of the numerical model.

SA can also provide useful information for system structural design. Due to their great influence on model performances, the uncertainties of the two variables *PT* and *PY* must be considered in the VRS structural design.

Eleven uncertain factors	***RY, RM, SY, SM, PY, PM, RT, ST, PT, SoilM, BP***
Step1: Two-level OA screening Factors chosen after OA	with 12 model runs ***RY, RM, PY, RT, ST, PT***
Step2: Multi-level MA screening Factors chosen after MA	with 42 model runs ***PY, RT, PT***
Step3: Sobol' indices Critical factors	with 120 model runs to create the surrogate model ***PY, PT***

Table 3- 8 Sensitivity analysis of the VRS model in three steps

Chapter 4 Optimization of VRS

4.1 Multi-Objective Non-deterministic Optimization (MONO)

4.1.1 Multi-Objective Optimization

Multi-objective optimization, also known as Pareto optimization, is "an area of multiple criteria decision making that is concerned with mathematical optimization problems involving more than one objective function to be optimized simultaneously [71]". Pareto efficiency is "a state of allocation of resources in which it is impossible to make any one individual better off without making at least one individual worse off [72]". The set of Pareto efficient designs is called "Pareto frontier", from which the optimal solution could be chosen according to the demands of the designer. Optimization problems trends to minimize objects **F**, since maximizing of the objects **F** is equivalent to minimizing **–F**. The general formulation of a multi-objective optimization problem can be written as follows:

$$\begin{aligned} &\min_{\mathbf{x}} \mathbf{F}\left(\mathbf{x},\mathbf{p}\right)=\left[F_1\left(\mathbf{x},\mathbf{p}\right),...,F_m\left(\mathbf{x},\mathbf{p}\right)\right] \\ &s.t:\begin{cases} g_i\left(\mathbf{x},\mathbf{p}\right)\le 0, i=1,2,...,k \\ h_j\left(\mathbf{x},\mathbf{p}\right)=0,\ j=1,2,...,l \end{cases} \\ &with:\mathbf{x}^{under}\le\mathbf{x}\le\mathbf{x}^{upper} \end{aligned} \tag{4-1}$$

where:

x is the deterministic design variable vector to be optimized, with under boundary $\mathbf{x}^{under}$ and upper boundary $\mathbf{x}^{upper}$;

p is the vector of random variables (noisy factors) encompassing all uncertainties;

F(x,p) is a vector of *m* objective functions;

g(x,p)=[g_1, g_2,…, g_k] is a vector of *k* inequality constraints;

h(x,p)=[h_1, h_2,…, h_l] is a vector of *l* equality constraints.

Uncertain factors are fixed to their mean values $\mathbf{p_0}$ in the deterministic optimization. Influenced by uncertainties of **p**, the objects and constraints need to be redefined in "Multi-Objective Non-deterministic Optimization (MONO)". Considering model feasibility [73], the constraints are defined:

$$s.t:\begin{cases} \max\limits_{\mathbf{p}} g_i\left(\mathbf{x},\mathbf{p}\right)\le 0 \\ \max\limits_{\mathbf{p}}\left|h_j\left(\mathbf{x},\mathbf{p}\right)\right|\le\xi_j \end{cases} \tag{4-2}$$

or

$$\begin{cases} \Pr\left(g_i\left(\mathbf{x},\mathbf{p}\right)\le 0\right)\ge C_i, i=1,2,...,k \\ \Pr\left(\left|h_j\left(\mathbf{x},\mathbf{p}\right)\right|\le\xi_j\right)\ge D_j,\ j=1,2,...,l \end{cases} \tag{4-3}$$

Eq. (4-2) ensures the feasibility of inequality constraints g_j and restrains the deviation of the equality constraints h_j under the limits ξ_j. Eq. (4-3) defines the model feasibility with probability and statistics approach, and restrains that the feasible probabilities of the constraints exceed C_i and D_j.

The outputs can be redefined as follows for the purpose of objective robustness in non-deterministic design:

$$\min_{\mathbf{x}}\left(\max_{\mathbf{p}}\mathbf{F}\left(\mathbf{x},\mathbf{p}\right)\right) \tag{4-4}$$

or

$$\min_{\mathbf{x}}\left(\mathbf{F}\left(\mathbf{x},\mathbf{p}_0\right)+c\,\boldsymbol{\sigma}_{\mathbf{p}}\left(\mathbf{F}\right)\right) \tag{4-5}$$

or

$$\min_{\mathbf{x}}\mathbf{F}\left(\mathbf{x},\mathbf{p}_0\right) s.t \max\mathbf{F}\left(\mathbf{x},\mathbf{p}\right)-\mathbf{F}\left(\mathbf{x},\mathbf{p}_0\right)\le\boldsymbol{\Delta}_{\mathbf{F}} \tag{4-6}$$

Eq. (4-4) minimizes the possible maximum output values of the designs. Eq. (4-5), with statistics method, calculates the outputs distributions for each inputs combination, and minimizes the sum of normal value and deviation value with the scale factor c. Eq. (4-6), with robust optimization, selects the optimized solutions with the outputs deviations under the defined limit $\boldsymbol{\Delta}_{\mathbf{F}}$ [74].

4.1.2 Approaches for MONO

The challenges for MONO of a complex engineering system include: the high calculation cost of model simulations; numerous uncertain factors in the models; lack of information about the design variables and model uncertainties. The procedure for MONO of engineering systems is discussed thereafter.

4.1.2.a System modeling & simplification

Thousands of model runs are needed in computer aided engineering system optimization problems. Numerical simulations are usually of high calculation cost. A model of high accuracy and relatively low calculation cost is needed, and the system modeling & simplification are of great importance in optimization problems.

4.1.2.b Sensitivity Analysis

Although many noisy factors may exist in an engineering model, only a few of them might be influential on model performance. Optimizations considering all the noisy factors may increase greatly the number of simulations. SA can be used to identify the influential ones. The number of noisy factors can be reduced by fixing the non-influential factors and consider only the uncertainties of critical ones in MONO. SA is a natural previous & next

step of robust optimization, especially for the applications where it is critical to identify the noisy parameters whose uncertainties have great influence on system's performances.

4.1.2.c Pre-study of inputs-outputs

The design variables, constraints, and objectives need to be defined (section 4.1.1). And before the optimization process, the intervals of design variables [$\mathbf{x}^{under}$ $\mathbf{x}^{upper}$] need to be selected. Initially, we have no information about inputs space and we define artificially the intervals. The predefined inputs intervals may not cover the whole combinations of inputs which are Pareto efficient or cover the regions away from the optimal solutions which will cause unnecessary simulations for optimization. Design of Experiment (DOE) takes samples and runs the simulations across the whole inputs space. The rationality of the predefined inputs space can be checked through DOE, and then the inputs space will be redefined to cover the all possible Pareto efficient inputs combinations and to take samples around the optimal points.

4.1.2.d Creation of surrogate model

Engineering simulation generally of high calculation cost and metamodeling technologies are widely used to create the surrogate model. DOE and model runs across the whole inputs space are needed to clarify the relationship between outputs and inputs in order to generate the surrogate model. For a model of n_x design variables and n_p noisy factors, the model inputs dimension is n_x+n_p and large number of samples is required in order to ensure accuracy of the surrogate model through the whole inputs space. Latin Hypercube Sampling (LHS) is a widely used DOE technique for model performance study [75,76]. Stochastic interpolation with Kriging method gives unbiased prediction of the intermediate values and is used in the domain of simulation experiment [77,78]. LHS will be used to generate samples and Kriging interpolation method will be used to create the surrogate model in the optimization of VRS.

Generally, surrogate models need to be validated before being used to replace the engineering models. The precision of a surrogate model can be tested by comparing the outputs of model simulation and outputs calculated by surrogate model for new samples. It's hard to define the acceptable error of a surrogate model in MONO problems: MONO models are of high dimension, and the surrogate model needs to be validated across the whole inputs space; precision of surrogate model may influence Pareto efficiency of a design [74]. In Figure 4- 1 left, both *i* and *j* are Pareto efficient predicted with the surrogate model, but in fact design *i* is more preferable for both outputs criteria. In Figure 4- 1 right, design *i* is preferable to *j* in the surrogate model, in fact it is exactly the opposite. Li [74] created the criteria to examine if Pareto efficiency of a design could be influenced by the error of the surrogate model: the efficiency influenced designs will be calculated with simulations and non-influenced designs will be predicted with surrogate model during optimization process. Li's method is efficient, but efforts are needed to integrate this approach into an existing optimization algorithm.

Here a practical way is proposed to ensure the accuracy of surrogate model in MONO problems and the validation of the surrogate model is shown in Figure 4- 2:

- The surrogate model will firstly be created with reasonable number of samples and be used for system optimization;

- The Pareto efficient designs $\mathbf{X}_{0i}=\left(x_{0i}^{1},x_{0i}^{2},\cdots,x_{0i}^{k}\right)$ are then selected, where k is the number of design variables, i=1,2,…,n_0, for the optimization design with n_0 solutions;
- The input intervals of the optimal designs are studied and defined: $\left[\mathbf{X}_0^{j\min}\ \mathbf{X}_0^{j\max}\right]$, where $\mathbf{X}_0^{j\min}=\min\left(x_{01}^{j},x_{02}^{j},\cdots,x_{0n_0}^{j}\right),\mathbf{X}_0^{j\max}=\max\left(x_{01}^{j},x_{02}^{j},\cdots,x_{0n_0}^{j}\right)$, with j=1,2,…,k.
- Additional samples will be taken and simulated in the new defined input intervals $\left[\mathbf{X}_0^{j\min}\ \mathbf{X}_0^{j\max}\right],j=1,2,\cdots,k$. The surrogate model is then updated with the new samples and the model will be optimized with the new surrogate model; new optimal designs $\mathbf{X}_{1i}=\left(x_{1i}^{1},x_{1i}^{2},\cdots,x_{1i}^{k}\right)$ and updated intervals $\left[\mathbf{X}_1^{j\min}\ \mathbf{X}_1^{j\max}\right]$ are obtained;
- The samples refinement for accuracy improvement of surrogate model and the system re-optimization are repeated, and final optimal designs are obtained when they are no longer influenced by the refinement of samples.

Instead of taking additional samples cross the whole inputs space, refinement of samples around the potential optimal solutions which will greatly reduce additional samples required to create an accurate surrogate model.

More efforts are needed to normalize this metamodeling & optimization process: generally, the number of samples initially taken should be proportional to the number of design variables, and their relationship could be created; the conditions when the optimal solutions are no longer influenced by the refinement of samples need to be standardized. As these researches are not the main tasks of our study, the number of the initial samples and the criterion for accuracy evaluation of the surrogate model are artificially defined in the optimization of the VRS.

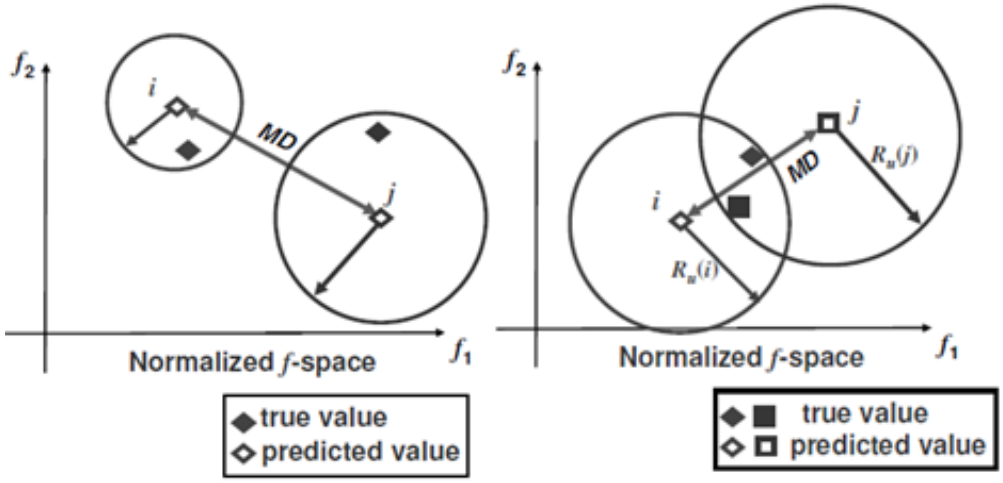

Figure 4- 1 Failure of Pareto efficient design selection with surrogate model---true value: outputs calculated with model simulation; predicted value: outputs predicted with surrogate model; *Ru*: error region of surrogate model [74]

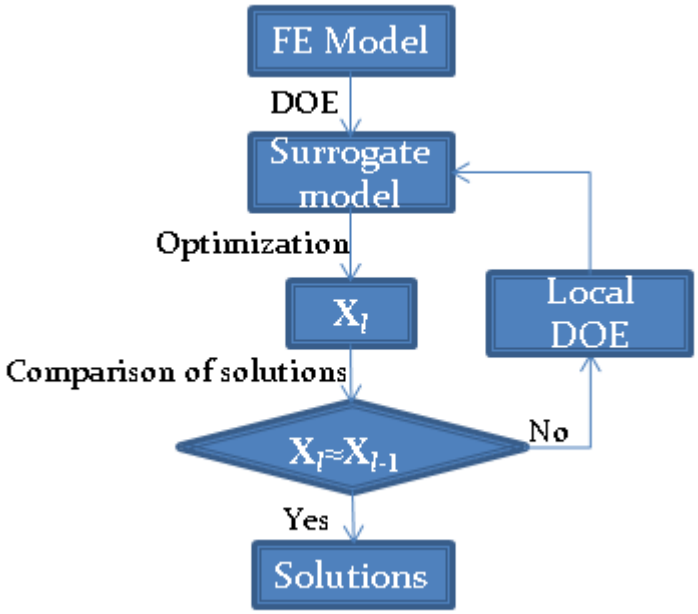

Figure 4- 2 Validation of the surrogate model for multi-objective optimization

4.1.2.e Algorithm selection

The dimension reduction of noisy factors with SA simplified the engineering model and decreased the number of samples needed to create the surrogate model. Robust optimization objects, constraints, design intervals are defined and the surrogate model is created after the previous steps. Optimization algorithms can be used for multi-objective designs:

- Gradient based methods have been developed for optimization of mathematical problems [79];
- Engineering systems are generally evaluated through experimental test or numerical simulations and the relationship between the model inputs and outputs is unknown. Some of the non-gradient based methods for optimization of "black box" problems (such as Particle Swarm [80,81], Genetic Algorithms [82, 83], etc.) can be used for multi-objective designs.

Optimization algorithms have been integrated in many mathematical software such as Optimization Toolbox of Matlab [84] and Optimization Component in automate design software Isight [85], which greatly facilitate the design process.

4.2 Optimization of VRS

The studied VRS was modeled (see section 3.2); uncertain factors *PT* and *PY* are identified of critical influence on model performance uncertainties and their influences were quantified through SA in chapter 3. For the optimization of VRS, uncertainties of the two factors will be considered.

4.2.1 Parameters of the optimization process

The objects of optimization are to minimize *THIV* and *D*, with barrier *Mass* (i.e. price of installation) as constraint. Both formula (4-4), (4-6) will be used for objectives definition in MONO and the deterministic optimization results will also be calculated as comparison. Model *Mass* uncertainties are caused by tolerances of *RT*, *ST* and *PT*. The maximum deviation of *Mass* remains nearly the same, and the influence of uncertain factors on *Mass* is neglected.

The VRS components are illustrated in Figure 3- 3. The 4 dimensions parameters *H*, *E*, *A*, *B* are used as design variables. The under boundary and upper boundary of each design variable is pre-defined as initial value decrease and increase by 20%. 50 samples were taken through LHS and the performances of VRS were analyzed in the pre-defined design space: The decrease of rail beam dimensions, especially the value of *E*, degrades the redirection capability of the VRS (see Figure 4- 3); Decrease of post dimensions increases greatly the deflection of VRS. The design intervals are updated and listed in Table 4- 1.

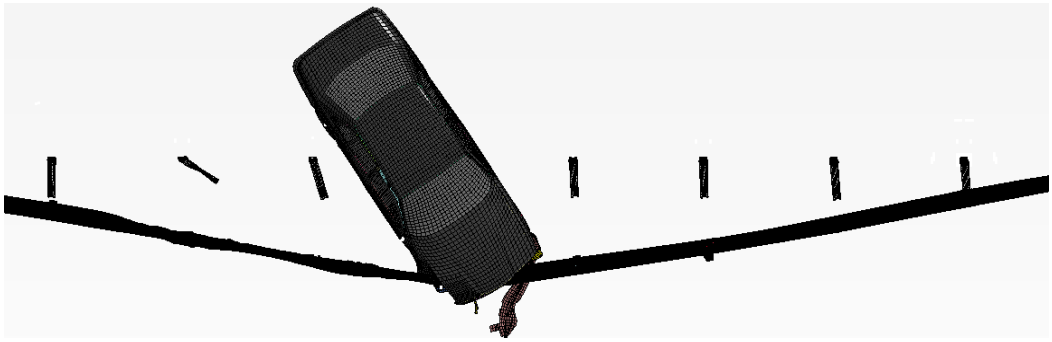

Figure 4- 3 Failure of vehicle redirection when H and E decrease greatly

Variables	Under	Initial/mm	Upper
H	-15%	310	+25%
E	-10%	81	+25%
A	-20%	100	+25%
B	-15%	50	+25%

Table 4- 1 Intervals of design variables

4.2.2 Creation of surrogate model

Optimization processes of the VRS with automate design software Isight is shown in Appendix V Automation of design for VRS. 240 samples are taken with LHS in the inputs space of 6 dimensions (4 design variables and 2 uncertain factors). The scatter plots of uncertain factors *PT*, *PY* and model outputs *THIV*, *D* are illustrated in Figure 4- 4. Kriging interpolation was used to create the surrogate mode, with *H, E, A, B, PT, PY* as inputs and *THIV, D, Mass* as outputs.

It is evident that *THIV* has positive correlation with the rigidity of the support Post (i.e. *PT*, *PY*), and *D* has negative correlation with the rigidity of the support Post (see Figure 4- 4). The objects of the optimization problem is to minimize *THIV* and *D*, and we are interest in their maximum values of a design considering uncertainties of the uncertain factors (i.e. $\max_{\mathbf{p}} \mathbf{F}(\mathbf{x},\mathbf{p})$ in eq. 4-4 & 4-6. $\max_{PT,PY} THIV$ is obtained when the uncertain factors *PT*, *PY* take their maximum values and $\max_{PT,PY} D$ is obtained when *PT*, *PY* take their minimum values. Assuming *PT, PY* have normal distributions, the maximum and minimum values of *PT, PY* were taken with their Cumulative Distribution Function (CDF):

$$\begin{cases} \min PT = 4.68mm \\ \max PT = 5.32mm \end{cases} \& \begin{cases} \min PY = 256.95MPa \\ \max PY = 312.05MPa \end{cases}$$

where

$$\begin{cases} CDF\left(\min PT\right) = 0.1 \\ CDF\left(\max PT\right) = 0.9 \end{cases} \& \begin{cases} CDF\left(\min PY\right) = 0.1 \\ CDF\left(\max PY\right) = 0.9 \end{cases} \tag{4-7}$$

with

$$PT\left(MPa\right) \sim N\left(284.5, 21.5\right)$$

$$PY\left(mm\right) \sim N\left(5, 0.25\right)$$

Monte Carlo designs were used to test the rationality of eq. (4-7): For different designs $\mathbf{x}_i$, LHS is used to test the relationship between uncertain factors and outputs with the surrogate model. With min*PT*, max*PT*, min*PY*, max*PY* defined in eq. (4-7), we have:

$$\begin{aligned} &\Pr\left(THIV\left(\mathbf{x}_i\right) \le THIV\left(\mathbf{x}_i, \left[\max PT, \max PY\right]\right)\right) > 97.5\% \\ &\Pr\left(Dd\left(\mathbf{x}_i\right) \le Dd\left(\mathbf{x}_i, \left[\min PT, \min PY\right]\right)\right) > 97.5\% \end{aligned} \tag{4-8}$$

The Outer-Inner optimization problem defined in eq. 4-4 & 4-6 requires $n_{out} \times n_{in}$ model runs (n_{out}: number of model runs for outer minimization; n_{in}: number of model runs for inner maximization), the inner maximization process is simplified, which greatly reduced model runs of the optimization problem. In addition, the surrogate model only needs to be validated in the design variables space, with the uncertain factors *PT, PY* fixed on the specified values. With the 'surrogate model verification' method proposed in section 4.1.2. 90 additional model runs are realized to refine the samples around the potential optimal designs and the precision of the surrogate model is validated.

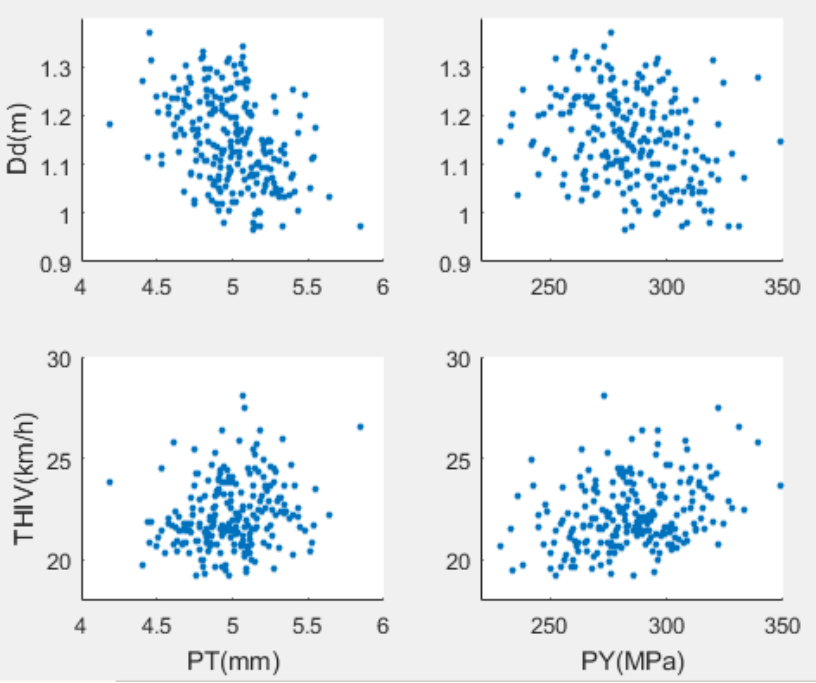

Figure 4- 4 Scatter plot of uncertain factors *PT*, *PY* and outputs *THIV*, *D*

4.2.3 Optimization calculation

4.2.3.a Define of constraints

In order to define the *Mass* constraint and the limits of outputs deviations $\mathbf{\Delta_F}$ (see eq. 4-6), 1000 samples was generated with LHS for uncertainty study of the model outputs: model *Mass* varies in the interval [610 810]*kg*; deviation of *THIV* (i.e. max*THIV*($\mathbf{x}_i$,$\mathbf{p}$)-*THIV*($\mathbf{x}_i$,$\mathbf{p}_0$)) varies in the interval [0.17 1.84]*km/h*; deviation of *D* (i.e. max*Dd*($\mathbf{x}_i$,$\mathbf{p}$)-*Dd*($\mathbf{x}_i$,$\mathbf{p}_0$)) varies in the interval [37 102]*mm*. The limits of constraints were determined artificially according to the uncertainties of the outputs and the optimization constraints are defined as:

$$\begin{aligned} &Mass \le 730kg \\ &\max THIV\left(\mathbf{x}_i,\mathbf{p}\right) - THIV\left(\mathbf{x}_i,\mathbf{p}_0\right) \le 1km/h \\ &\max Dd\left(\mathbf{x}_i,\mathbf{p}\right) - Dd\left(\mathbf{x}_i,\mathbf{p}_0\right) \le 70mm \end{aligned} \tag{4-9}$$

4.2.3.b Results analysis of Robust Optimization solutions

Mathematical software Matlab was used to create the surrogate model and the automate design and optimization platform ISIGHT was used for multi-objective optimization with Genetic Algorithm. With eq. (4-9) as constraint (i.e. eq. 4-6 as objects), the Pareto efficient solutions are illustrated in Figure 4- 5. The designs in Region 1 reduced both *D* and *THIV*,

and the designs in Region 2 are preferred when the main objects of the optimization is to increase rigidity of the VRS and decrease its deformations during the crash process. Scatterplots in Figure 4- 6---Figure 4- 9 illustrate the relationship between scaled factors of the design variables and the outputs for the Pareto efficient designs. Optimal solution is chosen depending on the requirements of designer and the 5 design options *a, b, c, d, e* (see Figure 4- 5) were studied:

- For all optimized solutions, the value of inputs *E, B* are proposed to be increased with their scaling values change in interval [1.16 1.24] and interval [1.16 1.25] respectively;
- The value of input *A* is proposed to be decreased (design *b, c, d, e*) when the minimization of *D* isn't of critical importance; *A* is proposed to be increased and *H* is proposed to be decreased in situations where the main object of the optimization design is to minimize deformation and to increase restraint level of the device.
- From solutions *a* to *e*, the dimensions of the VRS support Post (i.e. inputs *A*, *B*) tend to decrease, and the scaling factor of input *H* need to increase properly in order to maintain the optimal state.
- The under design limit for the scaling factor of input *A* is 0.8 and the upper design limit for the scaling factor of input *B* is 1.25 in the study. Unfortunately, these two limits restrained the selection of Pareto efficient designs (see Figure 4- 8, Figure 4- 9). Better solutions might be found beyond these two limits.

In short, the dimensions of the *w*-beam Rail component, especially for input *E*, need to be increased in order to increase the energy absorption capability of the VRS; The Post component is of rectangular shape (see Figure 3- 3) with *A*=100*mm*, *B*=50*mm*.The input *A* is proposed to be decreased and input *B* is proposed to be increased in the optimization process; In addition, more material is needed in order to increase the rigidity of VRS and decrease the output *D*, the *Mass* constraint defined in the optimization problem mainly restraint the minimization of *D.*

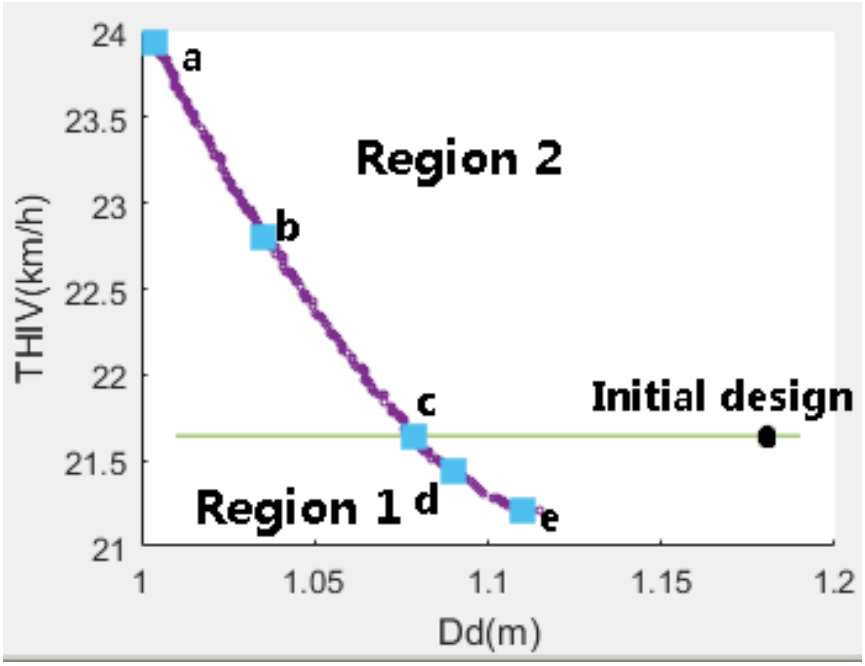

Figure 4- 5 Pareto efficient solution of VRS MONO

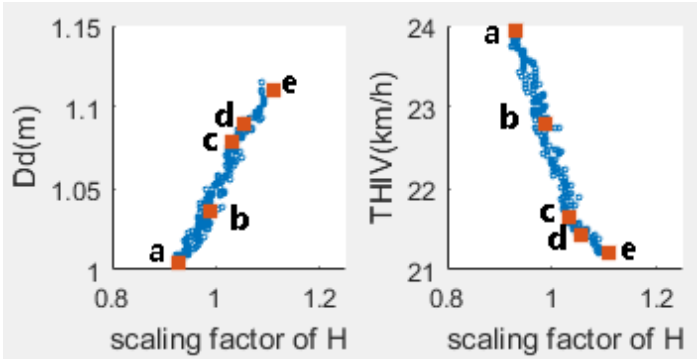

Figure 4- 6 Scatter plot of input *H* and outputs of Pareto efficient solutions

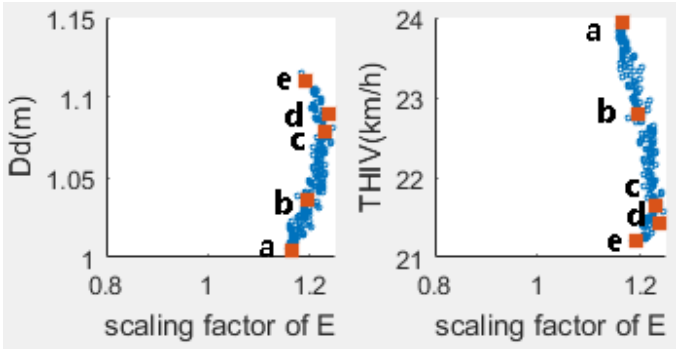

Figure 4- 7 Scatter plot of input *E* and outputs of Pareto efficient solutions

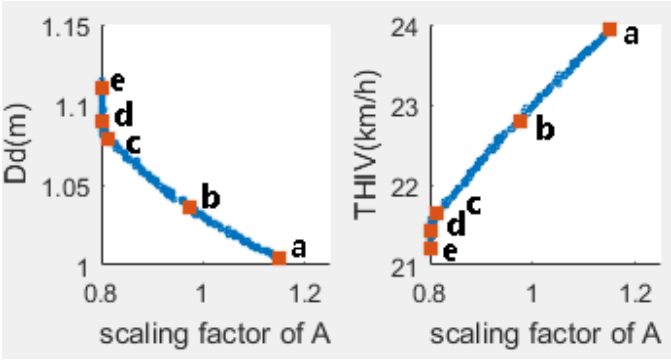

Figure 4- 8 Scatter plot of input *A* and outputs of Pareto efficient solutions

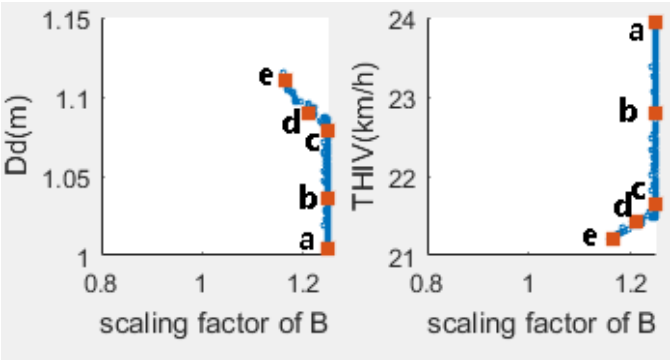

Figure 4- 9 Scatter plot of input *B* and outputs of Pareto efficient solutions

4.2.3.c Comparison of different MONO methods

Figure 4- 10 compared the optimal solutions of Non-deterministic (MON) method (eq. 4-4 as objectives) with deterministic optimization (MOD). Figure 4- 11 compared the optimal solutions of MONO (eq. 4-6 as objectives) with deterministic optimization minimization. For the optimization of VRS, we have:

- In Figure 4- 10: Outputs values and their possible maximum values obtained with MONO coincide with those of deterministic solutions. And this MONO method hasn't increase evidently the model robustness relative to deterministic designs.
- In Figure 4- 11: The influences of noisy factors on VRS performances decrease with the increase of model rigidity. The optimal solutions with low model deformation *Dd* and relatively high rigidity were selected with the robust method. Robust Optimization with eq. (4-6) select the optimal designs with outputs uncertainties within the limit $\mathbf{\Delta_F}$. The value of $\mathbf{\Delta_F}$ influenced the robustness of the model and the selection of optimization designs.

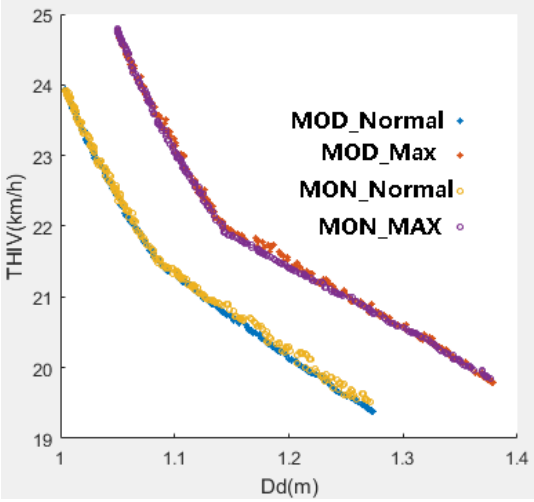

Figure 4- 10 Optimal designs obtained with MOD and with MON

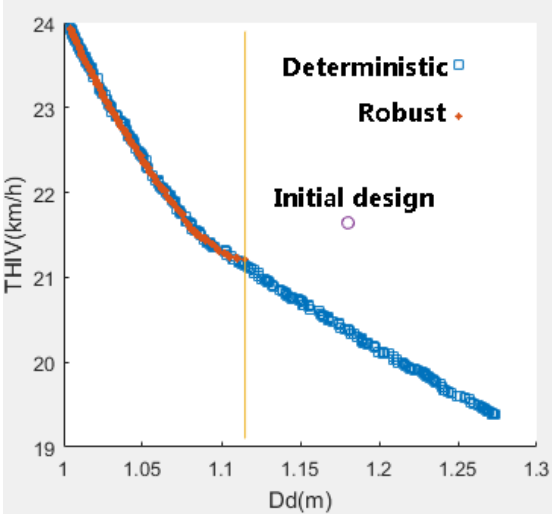

Figure 4- 11 Optimal designs of VRS obtained with different methods

4.3 Generalization of impact conditions

According to EN1317, the crash test of the VRS was realized under TB32 test conditions; sensitivity of model performances on the uncertainties of material, tolerance of fabrications, assemble loads of bolt-nut connections and soil rigidity were analyzed through Sensitivity Analysis; The safety barrier was optimized with dimension parameters of the barrier as design variables. In fact, the real crash accidents are more complex:

- The real life conditions of installation of road equipment is innumerable: straight longitudinal barriers are tested although curved installations exist; flat ground is recommended even though installations are sometimes situated on sloped shoulders or behind curbs;
- Test conditions are normalized but it may not represent the entire real life of crash: The errant vehicle may of various types (bus, truck, car, even motorcycle) with different dimensions and mass; crash velocity and angle, impact point, friction coefficient of road surface and the tire, etc. are not fixed factors.

Performances of the optimized safety barrier were evaluated under generalized test conditions. Restrained by numerical model, only the crash velocity and angle were considered. To optimize both the *THIV* and *D*, the optimized design *e* (see Figure 4- 5) was chosen. Simulations of the optimized design with crash velocity and angle at different levels were realized and relationship between impact angle (*a*) and velocity (*v*) with severity index *THIV* and deformation of the barrier *W* at different levels are calculated:

- The barrier fails to contain and redirect the vehicle only at the extreme crash conditions with large value of *a* and high value of *v*, e.g. *v*=130km/h, *a*>32 ° or *v*>100km/h, *a*=32 °. The threshold (fail line) under which the device has well redirect the vehicle is shown with dotted line in Figure 4- 12 and Figure 4- 13. And the device can well redirect the vehicle;
- In all possible crash conditions, the accident severity is of level A (see section 1.1.3) with ASI<1 and THIV<33km/h. Severity indices are restrained at acceptable levels.
- With polynomial regression analysis, relationships between *a* and *v* with output *THIV* at values [18 21 24 27 30]km/h are created and shown in Figure 4- 12. The relationship functions are listed in eq. (4-10); Relationships between *a* and *v* with deformation W_m at level [*W2 W3 W4 W5 W6*] are created and shown in Figure 4- 13. The relationship functions are listed in eq. (4-11);

$$\begin{aligned} v_{THIV18} &= 0.0525a^2 - 6.2697a + 196.4188 \\ v_{THIV21} &= 0.0379a^2 - 5.9393a + 215.1071 \\ v_{THIV24} &= 0.0158a^2 - 5.0282a + 226.7711 \\ v_{THIV27} &= 0.0052a^2 - 4.0126a + 233.6191 \\ v_{THIV30} &= -3.4a + 227 \end{aligned} \tag{4-10}$$

$$
\begin{aligned}
v_{W2} &= 0.0576a^2 - 5.4024a + 160.0000 \\
v_{W3} &= 0.0598a^2 - 5.7790a + 181.9330 \\
v_{W4} &= 0.0429a^2 - 5.2486a + 196.8000 \\
v_{W5} &= 0.0400a^2 - 5.2000a + 217.4000 \\
v_{W6} &= 0.0700a^2 - 7.0100a + 260.4500
\end{aligned}
\tag{4-11}
$$

- Derivative function measures the sensitivity to change of a quantity which is determined by another quantity. $v'(a)$ are listed in eq. (4-12), (4-13). The performance criteria are sensitive to the impact angle. For example, crash under *v*=110km/h, *a*=25 ° nearly have the same severity & deformation criteria values with crash under *v*=130km/h, *a*=20 °.

$$
\begin{aligned}
v'_{THIV18}(a) &= 0.1050a - 6.2697 \\
v'_{THIV21}(a) &= 0.0758a - 5.9393 \\
v'_{THIV24}(a) &= 0.0316a - 5.0282 \\
v'_{THIV27}(a) &= 0.0104a - 4.0126 \\
v'_{THIV30}(a) &= -3.4
\end{aligned}
\tag{4-12}
$$

$$
\begin{aligned}
v'_{W2}(a) &= 0.1152a - 5.4024 \\
v'_{W3}(a) &= 0.1196a - 5.7790 \\
v'_{W4}(a) &= 0.0858a - 5.2486 \\
v'_{W5}(a) &= 0.0800a - 5.2000 \\
v'_{W6}(a) &= 0.1400a - 7.0100
\end{aligned}
\tag{4-13}
$$

- The device works well for small value of impact angle: we have *THIV*<18km/h and W_m<*W3* when *a*=10 °, even for v=130km/h, which is the high speed limit in most of highways.
- Increases of the impact angle can greatly increase the severity of impact and the deformations of the barrier.

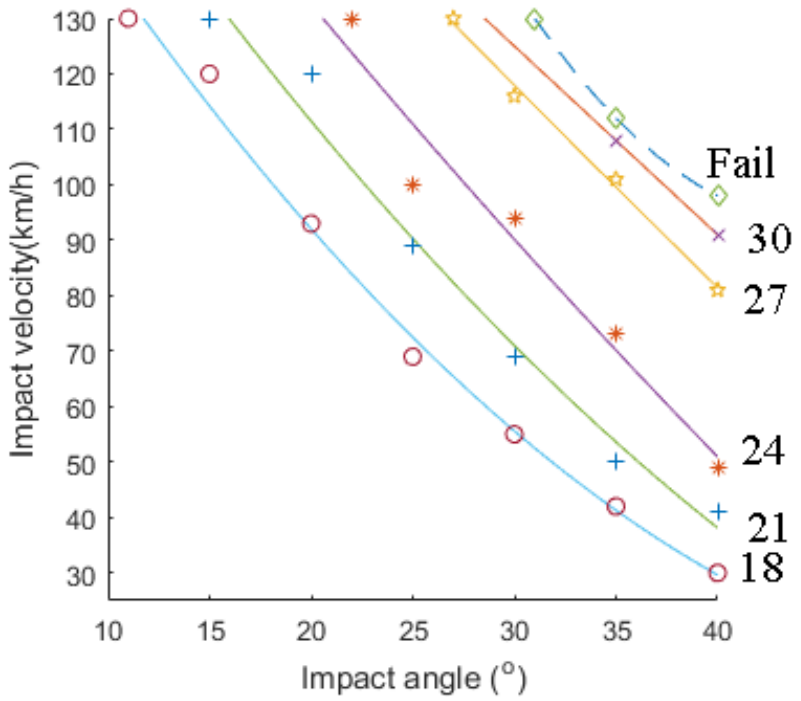

Figure 4- 12 Relationship between impact angle and velocity with *THIV* at different levels

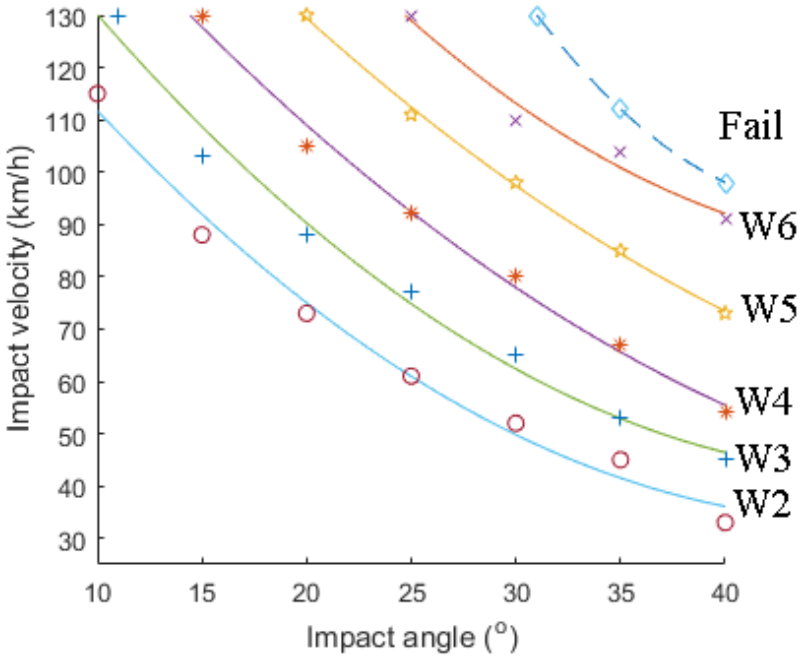

Figure 4- 13 Relationship between impact angle and velocity with W_m at different levels

4.4 Conclusions

The procedures for MONO of complex engineering systems are studied and the tested VRS is optimized with the proposed process; Performances of the optimized device were evaluated under different crash conditions:

- Before the optimization process, system model need to be simplified to reduce single model run cost and influential uncertain factors of which the uncertainties should be considered in optimization process need to be identified with SA;
- MONO minimize the outputs with their deviations constrained in limited intervals, the design intervals of input, outputs uncertainties need to be evaluated before the MONO design;
- Surrogate models are used to substitute the high calculation cost simulation models in optimization problems, accuracy of surrogate models need to be ensured in order to secure the precision of optimization. Instead of evaluating the surrogate model across the whole inputs space, we proposed a new approach to refine the samples around the potential optimal solutions which greatly reduces additional samples required to create an accurate surrogate model;
- Constraints and objects can be of difference forms depending on the demands of designers. The VRS was optimized with robust method, and strategies were proposed for VRS optimization. Optimal solutions obtained with different optimization methods are compared. The robust method with eq. 4-6 as objects is preferred for the MONO of VRS.
- The optimized design *e* shown in Figure 4- 5 was chosen, the performance criteria of the device before the optimization and after the optimization are compared in Table 4- 2. The initial design could well redirect the vehicle and constrain the crash severity at level **A** (lowest severity level defined in EN1317, see section 1.1.3); After the optimization, both the performance criteria *THIV* and *D* of the safety barrier are minimized, and the robustness of the device is increased (i.e. robust criteria in Table 4- 2 are minimized, where $\Delta THIV$, ΔD are the robust constraints defined in eq.(4-9)).

	Severity	Deformation	Robust criteria	
	THIV (km/h)	*D* (m)	$\Delta THIV$	ΔD
Initial design	21.66	1.180	1.09	0.072
Design *e*	21.19	1.111	0.46	0.070

Table 4- 2 Performance criteria and robust criteria of initial and the optimized design *e*

- Performances of the optimized design were evaluated under different crash conditions and the relationships between the impact speed and the impact angle were created with the performance criteria defined at different levels. The optimized device is capable of redirecting the errant vehicles at almost all the crash conditions and to restrain the accident severity at level **A**. And efforts are made to find above which impact conditions more injuries could be caused to the passengers or the VRS fail to restrain the vehicle.

General Conclusions

Context

Before being installed on the roadside, the performance of a VRS must be evaluated according to specific standards (EN 1317 in Europe for example) through crash test. Influenced by system uncertainties (such as uncertainty of material mechanical properties, tolerances of manufacture, installation conditions), the crash test results can be different for two crash test even with the same controlled test conditions. One cannot know how robust the design is because the repetition of crash test is economically infeasible and the system uncertainties can't be controlled. Dynamic simulations with Finite Element Analysis (FEA) programs such as LS-DYNA are widely used for structure design and performances evaluations of new devices. And the computational mechanics allow the evaluation of the robustness of a design taking into account all these variations.

Parameters' study of the VRS

Numerous variables exist in a VRS model that may influence its performances. Parameter studies of such models require large number of model runs:

- Sensitivity Analysis (SA) of VRS helps to have a deep understanding of model uncertainty and to identity the influential uncertain factors that should be taken into considerations during VRS performance studies and robust designs;
- Considering uncertainties of the influential factors, the performances of the VRS can be optimized with the design factors as variables; the VRS can only be optimized under the standardized crash conditions, and the optimized VRS need to be evaluated under different crash accident conditions.

Challenges for sampling based parameters' study of the VRS and many other complex engineering models include: a high simulation cost of single model run; the numerous model runs required for parameters analysis, especially for models of many variables; Properties unknown of the input parameters.

- FE simulation is used for parameters study and the numerical model was simplified;
- Efforts are paid for approaches study of SA in order to reduce the samples required for parameters study;
- Surrogate models are used for quantitative SA and optimization of the VRS;
- Distributions of uncertain factors determine both the uncertainty in model performances and the sensitivity of the model outputs to the uncertain factors. Uncertainties in the model inputs of the VRS are studied. Instead of characterizing the uncertain factors through costly statistics experts studies, normal distributions are used to define 'crudely' their uncertainties;
- Monte Carlo approach is used to define inputs intervals of the design variables.

Crash simulation of the VRS

Crash test of a VRS---GS2 hard shoulder safety barrier was realized; the tested device has well restraint the severity level at level A with the device deformation at level *W5*. Parameters' studies of the tested barrier were realized. Firstly, the numerical crash test model was created: Thousands of model runs are needed in computer aided engineering system

optimization problems. Numerical simulations are usually of high calculation cost. A model of high accuracy and relatively low calculation cost are needed, and the system modeling & simplification are of great importance in optimization problems.

The parameters of the numerical model of the tested device are defined with reference to literature studies. Considering the magnitude of component' deformations, the model is simplified in the four following aspects:

- Coarse mesh with refinement for the parts with large deformations;
- Simplification of VRS continuations at both ends of the barrier with spring elements to apply the boundary constraints;
- Detailed modeling of the soil for the parts with large deformation and its replacement by springs for the others soil parts;
- Bolted joints simplification with spring elements for rigid connections.

Different from full modeling for safety barrier crash simulation which may need days of CPU time, the simplified model simulate the crash process in 7 hours with a regular PC; compared to the experimental test, the simplified model is of good accuracy; the deformations of the barrier and the bolt joints connection failures have been simulated; more efforts are needed for vehicle wheel and tire modeling to predict vehicle trajectory during crash test, but these defects have little influence on performance evaluations of the device.

Sensitivity analysis of the VRS

Many sampling-based SA methods have been developed in the literature and they all have their advantages and disadvantages. As for the engineering applications, usually we don't have much information about the model. Screening analysis could firstly be used for qualitative analysis; influential certain factors could be identified after the qualitative analysis and then we could only focus on the quantitative SA of the influential factors.

The SA of a simple dynamic three points bending test model is realized: the efficiency and accuracy of different screening methods are compared. Morris Analysis (MA) and Fractional Factorial Design (FFD) are proposed for factor screening of the complex models such as the VRS; the influential factors are identified after screening analysis and their influences are quantified with Sobol' indices. Procedure for SA of the VRS is proposed with three steps: factors screening with FFD; factors re-screening with MA; quantitative SA of the influential factors with Sobol' indices.

SA of the tested VRS was realized: 11 uncertain factors were chosen considering uncertainties of material mechanical properties, the tolerance in fabrication of the components and uncertainties in the installation of the device. The three influential certain factors were identified after FFD and MA screening analyses. Reduction of the inputs dimensions greatly reduced the number of samples required to create the surrogate model of the VRS crash test. 120 samples were taken with LHS and surrogate model was created with Kriging interpolation. Influences of the three influential factors were quantified by Sobol' indices calculated with the surrogate model. Finally, two out of the eleven uncertain factors were identified as of critical influences on the model performances, i.e. yield strength uncertainty of the Post (*PY*), tolerance in the thickness of the Post (*PT*), and their influences were quantified. More efforts are needed to measure the real distribution of the two influential parameters, and it helps to increase the accuracy of the numerical model.

Optimization of the VRS

Optimization procedure helps to construct VRS of higher performances and of acceptable economic cost. Multi-objective Non-deterministic optimization of the VRS is realized to minimize the two performances criteria *THIV* and *D*:

- The geometrical dimensions of the VRS components are treated as the design variables. Robustness of the VRS which is influenced by the two influential uncertain factors and the installation cost of the device are the constraints of the design. The design space and reliability of the device are studied through Monte Carlo approach to define inputs intervals and the threshold of the constraints;
- Surrogate models are used to substitute the high calculation cost simulation models in optimization problems, accuracy of surrogate models need to be ensured in order to secure the precision of optimization. Instead of evaluating the surrogate model across the whole inputs space, we proposed a new approach to refine the samples around the potential optimal solutions which greatly reduce additional samples required to create an accurate surrogate model;
- The VRS was optimized with Genetic Algorithm. Performances of the optimal design were evaluated under different crash conditions and the relationships between the impact speed and the impact angle were created with the performance criteria defined at different levels. The optimized device is capable to redirect the errant vehicles at almost all the crash conditions and to restrain the accident severity at level A.

Synthesis

The framework of this thesis is sensitivity and robustness analysis of the VRS. A huge number of parameters drive the failure modes of the structures and it’s impossible to master all of them. The variables of the VRS are classified on three categories in this study:

- Uncertain input factors: the design strength of a structure is based on nominal values of basic strength variables, both material and geometric, such as yield strength and modulus of elasticity of the material, plate thickness. The actual values of these variables are often different from the nominal values and their random variability can cause the strength of VRS to vary beyond acceptable levels. Due to aging and human factors, the installation conditions of a VRS are also factors with uncertainties.
- Design variables: the dimensions of VRS components.
- Working conditions: the goal of a VRS is to redirect an errant vehicle and the impact conditions of a vehicle with the VRS (such as vehicle dimension, impact velocity & angle, friction before road and tires) are uncountable.

The design variables of the device characterize the main properties of a VRS. The VRS need to restraint the errant vehicles at any crash accident conditions and uncertainties in the VRS model many degrade its performances. It is not possible to realize the optimization of a VRS under all possible crash conditions considering inputs uncertainties in a single parameters study. The three categories of variables are studied respectively and successively by sensitivity analysis, robust optimization, generalization of impact conditions with numerical simulations in this study.

Perspective

Uncertainties exist in the VRS. And a crash test of the VRS can't be repeated even under the same impact conditions. As for the numerical simulations, in fact a model cannot be validated to 'have simulated the crash test accurately'. An optimal design obtained through deterministic design may not robustly reliable.

In the robust design of the VRS:

- Numerical simulation is used for the structure study of the VRS, and the model must be simplified as the parameters studies of the VRS require hundreds of model runs.
- Sensitivity Analysis helps to identity the influential uncertain factors. Simulations considering the variations of the influential uncertain factors helps to evaluate the robustness of a design and gives a cloud of results in which a real experiment test result is contained with a given probability. Efforts paid to reduce uncertainties of the identified influential factors helps to increase robustness of the design.
- The optimal but also robustly reliable designs can be obtained with robust optimizations considering variations of the influential uncertain factors.

The Europe Norm for VRS, EN1317, normalized the crash test conditions for the VRS of different containment levels, and defined the qualitative and quantitative performance criteria of the device. It provides a guideline for the design of VRS, but still could be revised:

- Statistics studies of the traffic accident data help to clarify under which impact conditions the crash between vehicle and the VRS happens. Sensitivities of the VRS performances to the impact conditions could be studied through numerical simulations. The normalized impact conditions in EN1317 should be defined depending on the purpose of the crash tests: e.g. For performance evaluation of the safety barrier of N2 containment level which has been discussed in this study, supposing the impact conditions TB32 defined in EN1317 represent the most common vehicle-barrier crash accidents after the statistics studies, TB32 crash test of the barrier evaluates its performances at most 'common' accidents; the barrier could undergo more fatal crash conditions and its performances are sensitive to the impact angle according to numerical study, crash test of the barrier with a larger impact angle could evaluate its performances at serious accidents and the relative crash conditions could be added to the EN1317 standard.
- The EN1317 don't take into account the uncertain factors of the VRS. Uncertainty & Sensitivity analyses help not only to evaluate the possible performance outputs intervals of a design, but also to the robust design of the device.
- Even a well evaluated design could fail to save lives in the real crash accidents of vehicle with the VRS. Though the severity level of crash test of a VRS with normalized test conditions could be **A**. It is important to find above which impact conditions more injuries could be caused to the passengers and the severity level is of **B**, and above which impact conditions fatal accident happens or the VRS fail to restrain the vehicle (e.g. section 4.3).

Though can't be evaluated directly with crash tests, the robustness of the VRS and influence of impact conditions on VRS performances could be studied through simulation approach, and the relative criteria could be added to the standards of VRS.

The main constraints for this research are:

- Although the influential uncertain factors are identified through screening analyses to reduce the number of samples required for quantitative SA. Still thousands of model runs are required and surrogate model was created for quantitative SA and robust optimization of the VRS. About 500 model runs in all were realized for screening SA, the creation of surrogate model for quantitative SA and the creation of surrogate model for robust optimization. Efforts are required for model simplification of the crash simulation to reduce CPU time of single model run.
- The VRS was analyzed under standardized test conditions and all the parameters are not considered: Apart from the crash speed & angle, many other factors such as vehicle dimension & mass, crash position, the friction force between tire & pavement, etc. may influence the redirection of the vehicle; only the dimension factors of the Rail and Post are considered and there are many other design factors. Parameters studies of these factors could be the objects of further studies of the VRS.

Reference

[1] OECD/ITF (2016), "Road Safety Annual Report 2016", OECD Publishing, Paris

[2] C. Goubel, "Vehicle restraint system crash test modeling – Application to steel-wood structures", Ph.D. dissertation, Dept. Mech. Eng., Univ. Claude Bernard Lyon1, France, 2012

[3] H.E. Ross, D. Sicking, and R.A. Zimmer, "Recommended Procedures for the Safety Performance Evaluation of Highway Features", NCHRP Report 350, Transportation Researsh Board, Washington D.C., 1993

[4] Livermore Software Technology Corporation <http://www.lstc.com/products/ls-dyna>

[5] "Road safety in France; 2012 annual report", Observatoire National Interministériel de la Sécurité Routière

[6] "SafetyNet (2009) Vehicle Safety", web text retrieved <16/10/2009>

[7] "Road Safety and Road Restraint Systems, A flexible and Cost-Effective Solution", European Union Road Federation, RRS-2015-02-V4

[8] Thomson et al, 2006. "D06 European best practice for roadside design: guidelines for roadside infrastructure on new and existing roads", Project Roadside infrastructure for safer European roads, European Community

[9] "Requirement for Road Restraint Systems, Design Manual for Roads and Bridges", 2(2006) Section 2, Part 8 TD 19/06

[10] "Road safety in France; 2009 annual report", Observatoire National Interministériel de la Sécurité Routière

[11] "La sécurité routière en France, 2014 bilan de l'accidentalité", Observatoire National Interministériel de la Sécurité Routière. ISBN : 978-2-11-010062-7

[12] EN1317-1:2010, "Road restraint systems - part 1: Terminology and general criteria for test methods", CEN, July 2010

[13] EN1317-2:2010, "Road restraint systems - part 2: Performance classed, impact test acceptance criteria and test methods for safety barriers including vehicle parapets", CEN, July 2010

[14] D.F. Neuenhaus, U.J. Geßler, M. Feldmann, "Using multibody-system modelling to make accurate predictions of vehicle impacts on road restraint systems", International Journal of Non-Linear Mechanics 53 (2013) 24–31

[15] A. Tabiei, J. Wu, "Roadmap for crashworthiness finite element simulation of roadside safety structures", Finite Elements in Analysis and Design 34 (2000) 145-57

[16] M. Mongiardini, “WP5 - Computational Mechanics: Modelling of bolt connections for the ESP-N2 barrier”, Department of Aerospace engineering Politecnico di Milano, Robust project report Doc. No.: ROBUST-05-016c - Rev. 0

[17] D.Neuenhaus, “Simple Multi-body System Models of Bolted Connections to Consider all Relevant Nonlinearities of Failure mechanisms”, TRB AFB (20)2 Meeting on Road Side Safety Design (2014)

[18] J. D. Reid, N. R. Hiser, “Detailed modeling of bolted joints with slippage”, Finite Elements in Analysis and Design 41 (2005) 547–62

[19] FHWA/NHTSA, “Development of a Finite Element Model for W-Beam Guardrails”, NCAC 2007-T-004

[20] D. Marzougui, U. Mahadevaiah, K.S. Opiela, “Development of a Modified MGS Design for Test Level 2 Impact Conditions Using Crash Simulation”, NCAC 2010-W-005

[21] M. R. Ferdous, et al., “Performance limit analysis for common roadside and median barriers using LS-DYNA”, International Journal of Crashworthiness, 16 (2011) 691–706

[22] M. Borovinsek, al., “Simulation of crash tests for high containment levels of road safety barriers”, Engineering Failure Analysis 14 (2007) 1711–18

[23] Z. Ren, M. Vesenjak, “Computational and experimental crash analysis of the road safety barrier”, Engineering Failure Analysis 12 (2005) 963–73

[24] S.O. Funtowicz, J. R. Ravetz (1990), “Uncertainty and Quality in Science for Policy”, Dordrecht: Kluwer Academic Publishers

[25] A. Saltelli, “What is Sensitivity Analysis”, in: Saltelli A, Chan K, Scott EM, editors. “Sensitivity analysis”, New York, NY: Wiley (2008) 3–14

[26] Web source Wikipedia: <https://en.wikipedia.org/wiki/Sensitivity_analysis>

[27] T. Turangyi, H. Rabitz, “Local Methods”, in: Saltelli A, Chan K, Scott EM, editors. “Sensitivity analysis”, Wiley (2008) 81–100

[28] A. Saltelli, et al., “Global Sensitivity Analysis: The Primer”, John Wiley (2008)

[29] J.C. Heltona, al., “Survey of sampling-based methods for uncertainty and sensitivity analysis”, Reliability Engineering and System Safety 91 (2006) 1175–209

[30] F. Campolongo, J. Kleijnen, T. Andres, “Screening Methods”, in: A. Saltelli, K. Chan, E.M. Scott editors, “Sensitivity analysis”, New York: Wiley (2008) 65–80

[31] A. Parkinson, C. Sorensen, and N. Pourhassan, “A General Approach to Robust Optimal Design”, Journal of Mechanical Design, 115(1993) 74-80

[32] G. SAPORTA, “Probabilités, analyse de données et statistique”, 2ed edition (2006)

[33] A. Saltelli, “Evaluation of Sensitivity and Uncertainty Analysis Methods in a Quality

Assessment Framework with Application to Environmental and Business Statistics", Lot 14 of EUROSTAT SUP COM 1997

[34] F. Campolongo, A. Saltelli, "Design of Experiments," in: A. Saltelli, K. Chan, E.M. Scott editors, "Sensitivity Analysis", New York: Wiley (2008) 51-64

[35] A.S. Hedayat, N.J.A. Sloane, J. Stufken, "Orthogonal Arrays: Theory and Applications", Springer (1999)

[36] M.D. Morris, "Factorial sampling plans for preliminary computational experiments", Technometrics 33 (1991), 161-74

[37] F. Campolongo, J. Cariboni, A. Saltelli, "An effective screening design for sensitivity analysis of large models", Environ Model Softw, 22(2007), 1509-18

[38] K. Chan, et al., "Variane-Based Mehtods", in: A. Saltelli, K. Chan, E.M. Scott editors, "Sensitivity Analysis", New York: Wiley (2008) 167-98

[39] A. Saltelli, al., "Variance based sensitivity analysis of model output. Design and estimator for the total sensitivity index", Computer Physics Communications 181 (2010) 259–70

[40] Q. Zhai, J. Yang , Y. Zhao, "Space-partition method for the variance-based sensitivity analysis: Optimal partition scheme and comparative study", Reliability Engineering and System Safety 131 (2014) 66–82

[41] E. Plischke, E. Borgonovo, C.L. Smith, "Global sensitivity measures from given data", European Journal of Operational Research 226(2012) 536–50

[42] X. Zhang, M. Pandey, "An effective approximation for variance-based global sensitivity analysis", Reliability Engineering and System Safety 121 (2014) 164–74

[43] M.C. Roger, M.N. Jan, "Graphical Methods", In: A. Saltelli, K. Chan, E.M. Scott editors, "Sensitivity analysis", New York: Wiley (2000) 245–66

[44] F. Pianosi, T. Wagener, "A simple and efficient method for global sensitivity analysis based on cumulative distribution functions", Environmental Modelling & Software 67 (2015) 1-11

[45] C. Xu, G. Gertner, "Understanding and comparisons of different sampling approaches for the Fourier Amplitudes Sensitivity Test (FAST)", Computational Statistics and Data Analysis 55 (2011) 184-98

[46] B. Iooss, "Revue sur l'analyse de sensibilité globale de modèles numériques", Journal de la Société Française de Statistique, Société Française de Statistique et Société Mathématique de France, 152 (2011) 1-23

[47] T. Simpson, al., "Metamodels for Computer-based Engineering Design: Survey and Recommendations", Engineering with Computers, 17(2001) 129-50

[48] E.D. Rocquigny, N. Devictor, S. Tarantola, "Uncertainty in industrial practice", Wiley

(2008)

[49] C. Goubel, M. Massenzio, S. Ronel, “Wood-steel structure for roadside safety barriers”, International Journal of Crashworthiness, 17(2012) 63-73

[50] Y.D. Murray, “Manual for LS-DYNA Wood Material Model 143”, Report No. FHWAHRT-04-097, Federal Highway Administration (2007)

[51] J. Melcher, al., “Design characteristics of structural steels based on statistical analysis of metallurgical products”, Journal of Constructional Steel Research 60(2004) 795-808

[52] S. Shan, G.G. Wang, “Survey of modeling and optimization strategies to solve high-dimensional design problems with computationally-expensive black-box functions”, Struct Multidisc Optim, 41(2010) 219-41

[53] B. Lamoureux, N. Mechbal, J: Massé, “A combined sensitivity analysis and kriging surrogate modeling for early validation of health indicators”, Reliab Eng Syst Safe, 130(2014) 12-26

[54] Q. Ge, B. Ciuffo, M. Menendez, “Combining screening and metamodel-based methods: An efficient sequential approach for the sensitivity analysis of model outputs”, Reliab Eng Syst Safe, 134(2015) 334-44

[55] W.L. Oberkampf, et al., “Error and uncertainty in modeling and simulation”, Reliab Eng Syst Safe, 75(2002) 333-57

[56] V. Kodjo, “Evaluation et modélisation des dispositifs de retenue pour motards”, Dissertation University Claude Bernard Lyon 1, France (2016)

[57] S. Yan, et al., “Sensitivity Analysis of Guardrail Impact Parameters Based on Deflection Index”, Modern Transportation, 3(2014) 1-7

[58] J.Ryu, et al., “Kriging interpolation methods in geostatistics and DACE model”, KSME International Journal, 16(2002) 619-32

[59] A. Marrel, et al., “Calculations of Sobol indices for the Gaussian process metamodel”, Reliab Eng Syst Safe, 94(2009) 742-51

[60] TRANSPOLIS <http://www.transpolis.fr>

[61] LIER-TRANSPOLIS, “GS2 hard shoulder W-beam guardrail TB32 experimental test report” (2007)

[62] J. O. Hallquist, “LS-Dyna Theoretical Manual”, Livermore Software Technology Corporation, Livermore (2006)

[63] “LS-DYNA Keyword user’s Manual”, Livermore Software Technology Corporation, Livermore (2007)

[64] S. Bala, J. Day, “General Guidelines for Crash Analysis in LS-DYNA”, Livermore Software Technology Corporation

[65] B. Silva, J. Meireles, “Study of the Connections Behaviour in Road Safety Barriers”, Conference ICEM15, July 2012, Porto

[66] D.M. Bruce, “Dynamic Tensile Testing of Sheet Steels & Influence of Strain Rate on Strengthening Mechanisms in Sheet Steels”, Dissertation, Colorado School of Mines, 2003

[67] Federal Highway Administration, “Manual for LS-DYNA Soil Material Model 147”, report FHWA-HRT-04-095 (2004)

[68] T.A. Johansen, et al., “Gain-scheduled wheel slip control in automotive brake systems”, IEEE Transactions on Control System Technology, 11(2003) 799-811

[69] J. Harned, L. Johnston, G. Scharpf, “Measurement of tire brake force characteristics as related to wheel slip (anti-block) control system design”, SAE Transactions, 78(1969), SAE 690214, 909-25

[70] Informations techniques de la technique d’assemblage, report of bossard, © bossard F-fr-2017.01

[71] Web source Wikipedia: <https://en.wikipedia.org/wiki/Multi-objective_optimization>

[72] Web source Wikipedia: <https://en.wikipedia.org/wiki/Pareto_efficiency>

[73] A. Parkinson, C. Sorensen, N. Pourhassan, “A general approach for robust optimal design”, ASME Trans. J Mech Des, 115(1993), 74–80

[74] L. Mian, “Robut Optimization and Sensitivity Analysis with Multi-objective Genetic Algorithms: Singe and Multidisciplinary applications,” Ph.D. dissertation, Dept. Mech. Eng., Univ. of Maryland, USA (2007)

[75] F.Viana, “Things you wanted to know about the Latin hypercube design and were afraid to ask,” 10th world congree on structural and multidisciplinary optimization, Orlando, USA, May 19-24, 2013

[76] J.C. Helton, F.J. Davis, “Latin hypercube sampling and the propagation of uncertainty in analysis of complex systems”, Reliability Engineering and System Safety, 81(2003), 23–69

[77] G. Zhang, et al., “Global optimization of reliability design for large ball mill gear transmission based on the Kriging model and genetic algorithm”, Mechanism and Machine Theory, 69(2013) 321-66

[78] K. Elsayed, C. Lacor, “Robust parameter design optimization using Kriging, RBF and RBFNN with gradient-based and evolutionary optimization techniques,” Applied Mathematics and Computation, 236(2014) 325-44

[79] J. Nocedal, S.J. Wright, “Numerical Optimization”, Springer Series in Operations Research (2006)

[80] J. Kennedy, R. C. Eberhart, “Particle swarm optimization”, In Proceedings of the IEEE International Conference on Neural Networks, 4(1995) 1942–8

[81] R.C. Eberhart, J. Kennedy, “A new optimizer using particle swarm theory”, Proceedings of the 6th International Symposium on Micro Machine and Human Science, 39–43 (1995)

[82] J. Holland, “Adaptation in Natural and Artificial Systems”, the University of Michigan Press, Michigan, USA (1975)

[83] K. Deb, “Multiobjective Optimization Using Evolutionary Algorithms”, John Wiley & Sons, New York, NY, USA (2001)

[84] “Global Optimization Toolbox User's Guide”, The MathWorks, Inc.(2016)

[85] “Isight Design Optimiaztion Methodologies”, SIMULIA (2010)

Appendix I Details for Sensitivity analysis of the three points bending test model

Automation for the Design of Experiment (DOE)

Large number of samples and model runs are required for the DOE of sensitivity analysis and the automate design software Isight [85] is used for auto-design. Figure A- 1 shows the DOE with Isight. The process component DOE generates samples of the inputs automatically or manually; the command component modifies the input file according to the inputs values obtained with DOE and run the Ls-Dyna for propagation of the model; after all the propagations, samples of the inputs and the relative outputs are stored in a data file. Matlab is used for sensitivity analysis with the data file.

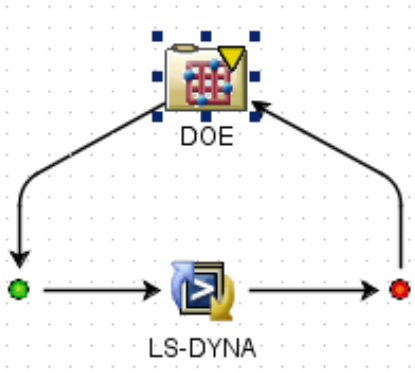

Figure A- 1 DOE with Isight for sensitivity analysis of the beam

Data for DOE

For two-level screening analysis, to take into consideration of all the possible combinations, 64 samples are taken for the DOE of the six uncertain factors; 9 trajectories are used with 7 samples in each trajectories are taken for multi-level screening with Morris analysis; 120 samples are taken with LHS to take samples cross the input space, and the surrogate model is created for quantitative SA with Sobol' indices. The samples and simulation results for two level screening are shown below.

- **Two level screening**

Array of FD: 0 & 1 are the two level taken according to section 2.2.2.c, with de columns represent the six factors *MC, MT, MY, T, Y, G* in order.

Main Effect of each factor can be evaluated with data listed in Table A- 1 for full FD screening analysis. The relative samples can be chosen from the full design for screening analysis with HFFD, OA, OAT, CD, PS.

DOE with FD	$V_{0.02}$ (m/s)	V_{∞} (m/s)
0 0 0 0 0 0	5.4622	4.9589
0 0 0 0 0 1	5.0975	4.9262
0 0 0 0 1 0	5.4626	5.0999
0 0 0 0 1 1	5.2016	4.9930
0 0 0 1 0 0	5.2497	4.9008
0 0 0 1 0 1	4.8221	4.2574
0 0 0 1 1 0	5.2635	4.6424
0 0 0 1 1 1	4.8034	4.1164
0 0 1 0 0 0	5.4537	5.0651
0 0 1 0 0 1	5.2081	4.9064
0 0 1 0 1 0	5.4565	4.9844
0 0 1 0 1 1	5.2112	4.9157
0 0 1 1 0 0	5.2599	4.9439
0 0 1 1 0 1	4.8309	4.3937
0 0 1 1 1 0	5.2610	4.9985
0 0 1 1 1 1	4.8133	4.2488
0 1 0 0 0 0	5.4592	4.8414
0 1 0 0 0 1	5.2232	4.6587
0 1 0 0 1 0	5.4578	4.8633
0 1 0 0 1 1	5.1587	4.8432
0 1 0 1 0 0	5.2638	4.9836
0 1 0 1 0 1	4.8227	4.3227
0 1 0 1 1 0	5.2647	4.9693
0 1 0 1 1 1	4.8292	4.4494
0 1 1 0 0 0	5.4584	4.9808
0 1 1 0 0 1	5.1975	4.8886
0 1 1 0 1 0	5.4605	5.0060
0 1 1 0 1 1	5.1580	4.9413
0 1 1 1 0 0	5.2606	4.5786
0 1 1 1 0 1	4.8237	4.4043
0 1 1 1 1 0	5.2588	4.4768
0 1 1 1 1 1	4.7951	4.3170
1 0 0 0 0 0	5.4994	5.2390
1 0 0 0 0 1	5.4101	5.0628
1 0 0 0 1 0	5.4944	5.2663
1 0 0 0 1 1	5.4214	5.0341
1 0 0 1 0 0	5.3053	4.9565
1 0 0 1 0 1	5.0902	4.5420
1 0 0 1 1 0	5.3070	4.8540
1 0 0 1 1 1	5.0835	4.5256

1 0 1 0 0 0	5.4945	5.1529
1 0 1 0 0 1	5.4239	5.0260
1 0 1 0 1 0	5.4930	5.2513
1 0 1 0 1 1	5.4146	5.0514
1 0 1 1 0 0	5.3047	4.7260
1 0 1 1 0 1	5.0840	4.4596
1 0 1 1 1 0	5.3050	4.6963
1 0 1 1 1 1	5.0843	4.4741
1 1 0 0 0 0	5.4943	5.1815
1 1 0 0 0 1	5.4146	4.9961
1 1 0 0 1 0	5.4934	5.1786
1 1 0 0 1 1	5.4178	5.0239
1 1 0 1 0 0	5.3086	4.7391
1 1 0 1 0 1	5.0735	4.0956
1 1 0 1 1 0	5.3078	4.8368
1 1 0 1 1 1	5.0814	4.5485
1 1 1 0 0 0	5.4929	5.2106
1 1 1 0 0 1	5.4210	5.0769
1 1 1 0 1 0	5.4929	5.2296
1 1 1 0 1 1	5.4237	5.0570
1 1 1 1 0 0	5.3042	4.8648
1 1 1 1 0 1	5.0803	4.4910
1 1 1 1 1 0	5.3010	4.7378
1 1 1 1 1 1	5.0829	4.5154

Table A- 1 Two-level DOE of the bending test

Appendix II Failure modes of the VRS

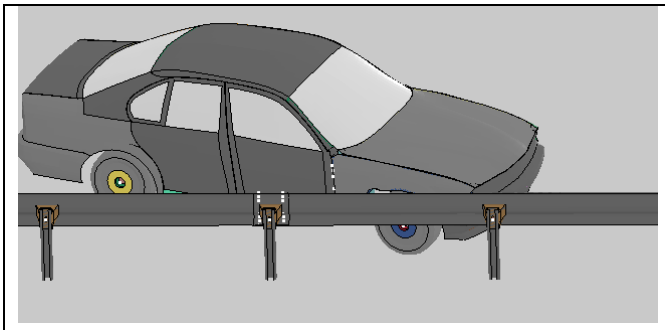	Initial state
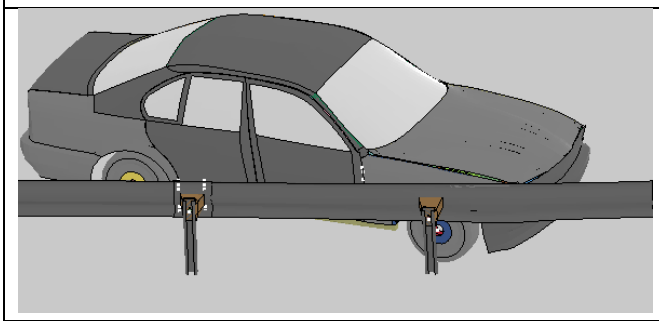	Plastic deformation of the VRS
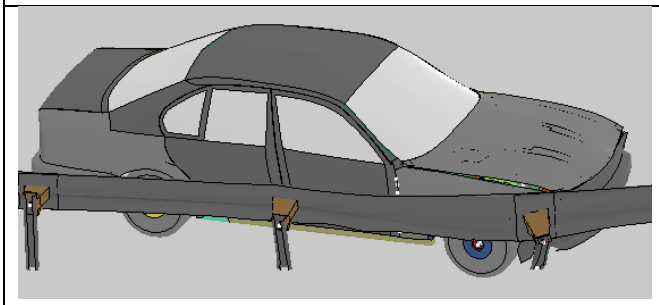	Hinge deformations for the rails and posts
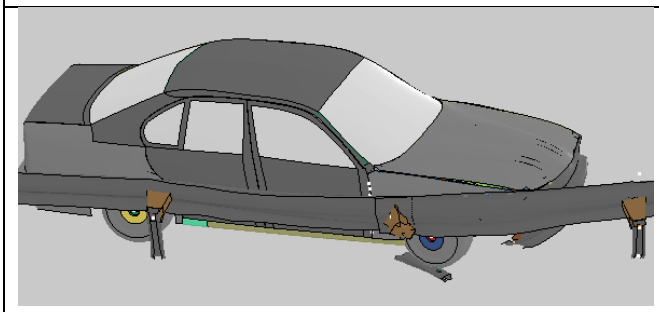	Bolt-nut connection failure between post and spacer
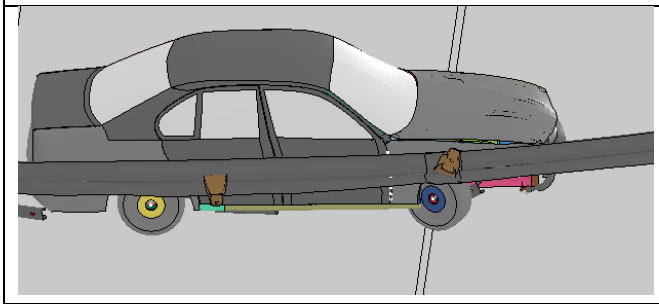	Permanent deformations of the device and redirection of the errant vehicle

Table A- 2 Failure modes analysis of the VRS

Appendix III Deformations of the VRS

The components of the VRS are numbered (see Figure 3- 4). The rails from no.4 to no.8 at the middle of the device are in direct contact with the vehicle during crash process. Deformations of these rails and the connected spacers and posts are shown below.

Rail 4	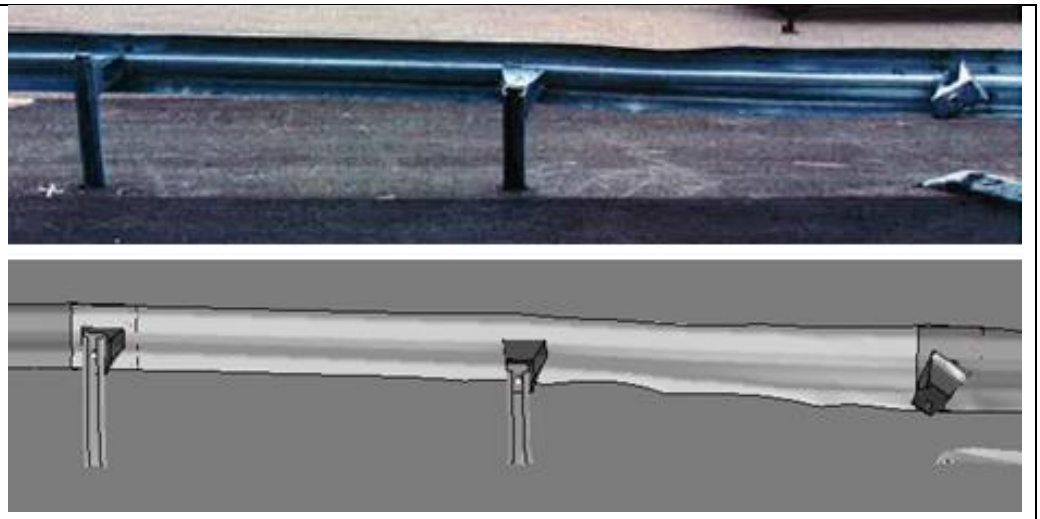
Rail 5	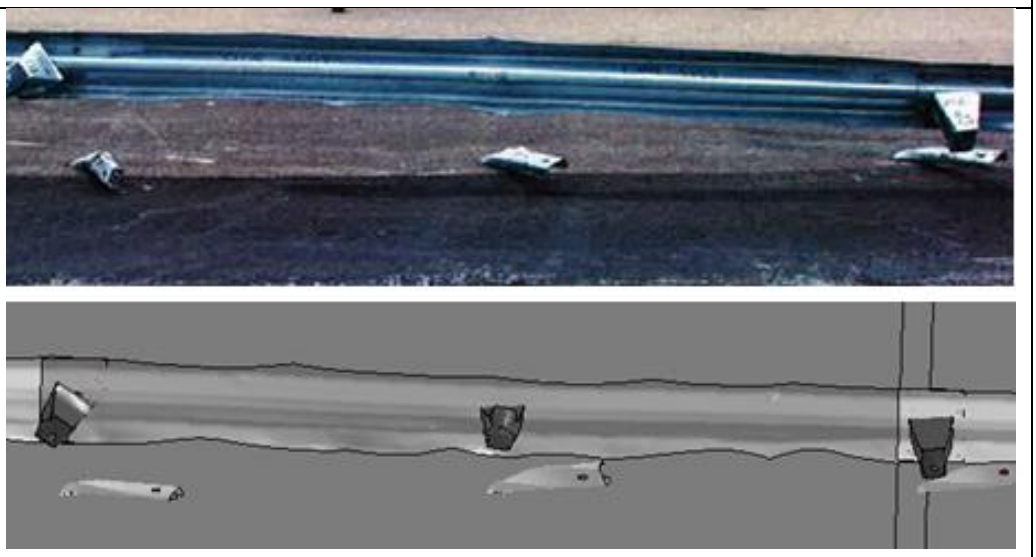

Rail 6	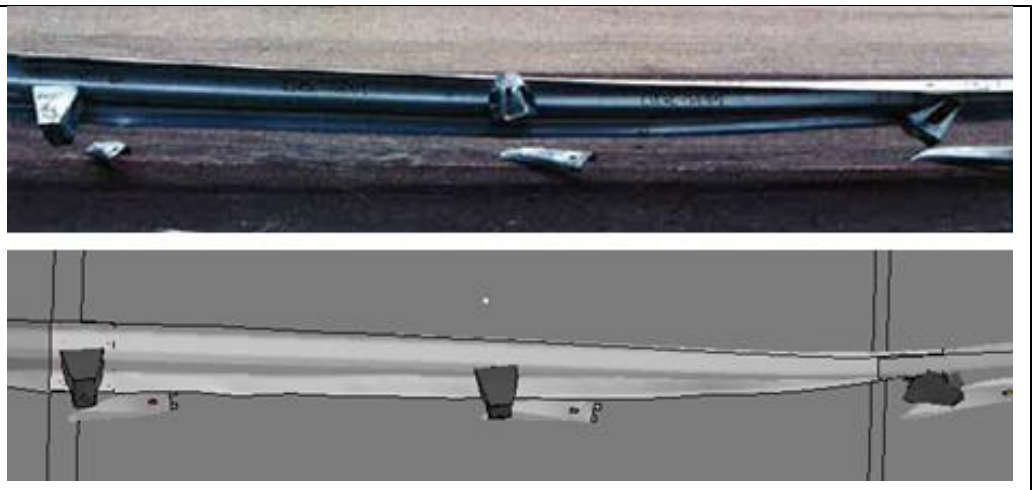
Rail 7	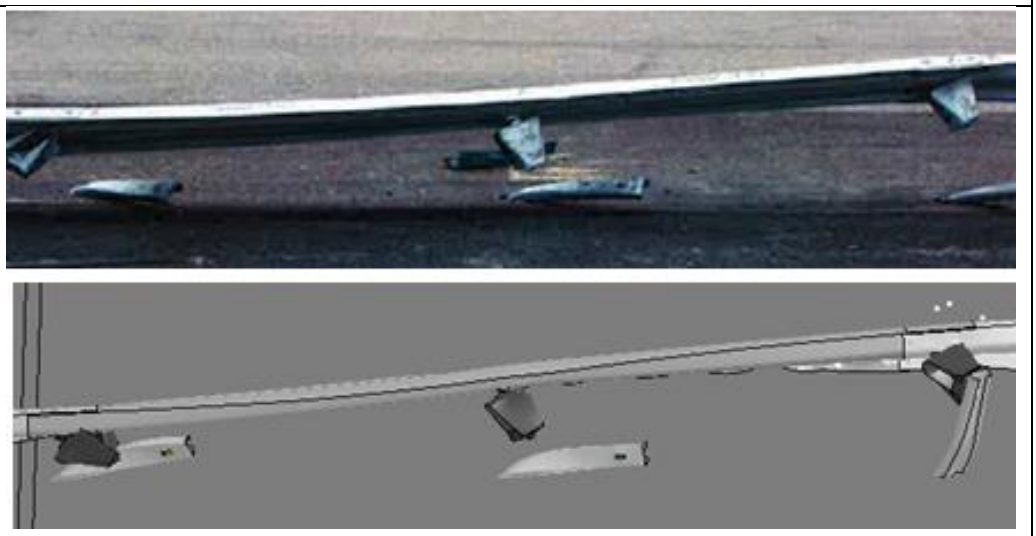
Rail 8	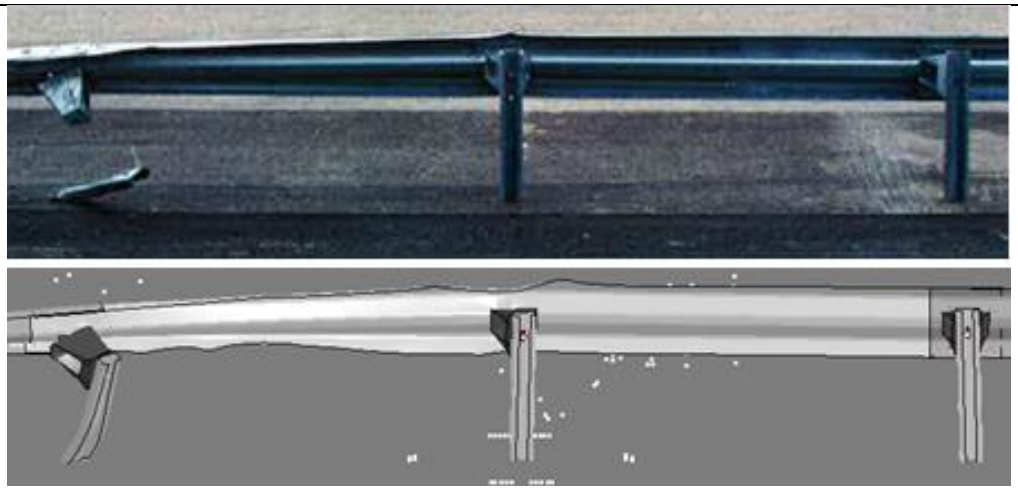

Figure A- 2 Rail no.4(a)-8(e) after impact

Appendix IV Data for Morris Analysis of the VRS

Vars	Inputs (Cumulative Distribution value)						Outputs	
	RT	ST	PT	RY	RM	PY	THIV	D
t1	1/8	5/8	7/8	7/8	1/8	3/8	22.3336	1.166
	1/8	5/8	3/8	7/8	1/8	3/8	21.1244	1.221
	1/8	5/8	3/8	7/8	1/8	7/8	22.6302	1.168
	5/8	5/8	3/8	7/8	1/8	7/8	21.9269	1.159
	5/8	5/8	3/8	3/8	1/8	7/8	22.9889	1.161
	5/8	1/8	3/8	3/8	1/8	7/8	22.0351	1.163
	5/8	1/8	3/8	3/8	5/8	7/8	22.9793	1.262
t2	1/8	3/8	3/8	5/8	7/8	5/8	20.3353	1.169
	1/8	3/8	7/8	5/8	7/8	5/8	23.0984	1.120
	1/8	7/8	7/8	5/8	7/8	5/8	23.1023	1.101
	5/8	7/8	7/8	5/8	7/8	5/8	21.3880	1.104
	5/8	7/8	7/8	1/8	7/8	5/8	21.8678	1.103
	5/8	7/8	7/8	1/8	7/8	1/8	21.8184	1.157
	5/8	7/8	7/8	1/8	3/8	1/8	21.9178	1.166
t3	7/8	5/8	1/8	1/8	7/8	1/8	21.1301	1.274
	7/8	5/8	1/8	1/8	3/8	1/8	20.3190	1.265
	7/8	1/8	1/8	1/8	3/8	1/8	20.7406	1.259
	7/8	1/8	5/8	1/8	3/8	1/8	21.9514	1.228
	7/8	1/8	5/8	5/8	3/8	1/8	22.0127	1.212
	3/8	1/8	5/8	5/8	3/8	1/8	21.4938	1.223
	3/8	1/8	5/8	5/8	3/8	5/8	21.3892	1.181
t4	3/8	3/8	5/8	7/8	5/8	3/8	22.2157	1.173
	3/8	3/8	5/8	3/8	5/8	3/8	21.8918	1.178
	3/8	3/8	1/8	3/8	5/8	3/8	21.0347	1.214
	3/8	3/8	1/8	3/8	5/8	7/8	22.4583	1.192
	3/8	3/8	1/8	3/8	1/8	7/8	21.6185	1.193
	3/8	7/8	1/8	3/8	1/8	7/8	21.3234	1.191
	7/8	7/8	1/8	3/8	1/8	7/8	21.3025	1.160
t5	5/8	1/8	5/8	3/8	3/8	7/8	21.7854	1.154
	5/8	1/8	5/8	3/8	3/8	3/8	21.3702	1.210
	5/8	1/8	5/8	7/8	3/8	3/8	21.3576	1.192
	1/8	1/8	5/8	7/8	3/8	3/8	21.7729	1.197
	1/8	5/8	5/8	7/8	3/8	3/8	22.5322	1.192
	1/8	5/8	5/8	7/8	7/8	3/8	23.5069	1.193
	1/8	5/8	1/8	7/8	7/8	3/8	21.0546	1.243
t6	7/8	7/8	3/8	1/8	1/8	5/8	21.1664	1.154
	7/8	7/8	3/8	1/8	5/8	5/8	21.0625	1.161

	7/8	7/8	3/8	5/8	5/8	5/8	20.9641	1.140
	3/8	7/8	3/8	5/8	5/8	5/8	21.4186	1.174
	3/8	7/8	7/8	5/8	5/8	5/8	21.7983	1.110
	3/8	3/8	7/8	5/8	5/8	5/8	21.8452	1.116
	3/8	3/8	7/8	5/8	5/8	1/8	21.2951	1.155

Table A- 3 Sampling of MA and outputs of results

Appendix V Automation of design for VRS

The automate design software Isight is used for DOE of sensitivity analysis & optimization of the VRS. Figure A- 1 shows the DOE with Isight, and can also be used for sensitivity analysis of the VRS.

The process for auto optimization of the VRS is shown in Figure A- 3:

- The 'Optimization' component generate samples of the inputs factors with DOE;
- Dimension values of the VRS are the design factors of the device. It is not possible to change the dimension parameters by directly modifying the model file. The component 'Ls-PrePost' reads the initial file, modify the VRS model according to parameters generated with DOE by calling Ls-PrePost, and create the new VRS model file.
- Component 'Ls-Dyna' run the crash model by calling the FE Ls-Dyna program.
- With the data files obtained after the model run, 'Matlab' could be used to calculate the performance criteria of the VRS.
- The surrogate model will be created after the model runs, and the component 'optimization' will then find the optimal solutions with the surrogate model.

The main constraint for the auto-optimization process is the CPU time. A single model run requires about 6h and hundreds of model runs might be needed for the creation of the surrogate model. The auto-optimization may take two months and it might be interrupted by some unknown reasons. In addition, although the numerical model is of good accuracy, with the dimension factors of the VRS changed, unreasonable simulation results such as mesh penetration of the vehicle and the VRS might be obtained, which greatly influence the accuracy of the surrogate model.

In this optimization study, Isight was used only for DOE to generate samples of inputs and to create the new model files of the VRS by calling 'Ls-PrePost'; the batch file was used for the running of the simulations; Matlab was used to create the surrogate model and to realize the multi-objective optimization of the device.

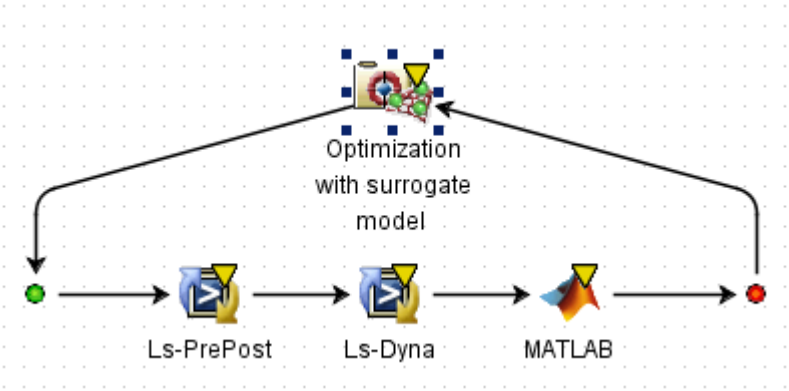

Figure A- 3 Auto-optimization of the VRS

Appendix VI French summary

Introduction

Chaque année, environ 1,2 million de personnes meurent dans des accidents sur les routes et beaucoup plus sont gravement blessés. En France, un tiers des personnes tuées sur la route le sont lors d'un accident sur un obstacle fixe. Les dispositifs de retenue de véhicule (DDR) sont des infrastructures passives de sécurité routière pour but est de maintenir les véhicules en perdition sur la chaussée en limitant la sévérité de l'impact. Le développement des DDR est une mesure efficace pour sauver des vies.

Les DDR doivent subir des essais de chocs avant d'être installés sur le bord des routes afin de pouvoir évaluer leurs performances en termes de sévérité d'impact et de déflexion de dispositif. Des règles (comme la norme EN1317 en Europe et NCHRP aux Etats-Unis) ont été créées pour l'évaluations des performances des DDR : Les conditions d'impact des essais de chocs de DDR sont normalisés ; les critères de performance de DDR sont définies. Avec le développement de l'ingénierie assistée par ordinateur (IAO), les simulations numériques permettent de réduire les coût de développement des DDR et aident à analyser les facteurs qui n'ont pas pu être étudiés avec les crash tests.

Différentes catégories de DDR sont développées pour différents types d'objectifs. La barrière de sécurité est un DDR continu installé à côté ou sur le terre-plein central d'une route pour empêcher les véhicules «hors de contrôle» de quitter la route et de frapper des obstacles fixes dangereux ou de traverser la trajectoire des véhicules arrivant à contresens.

Les performances des dispositifs peuvent être dégradées par des facteurs incertains ; la conception du DDR est un processus d'optimisation robuste de type multi-objectifs ; un DDR peut subir des collisions sous des conditions d'impact différentes. Cette thèse vise à définir une approche qui comporte deux objectifs:

- Méthodologie pour l'analyse de l'incertitude et la conception robuste des DDR;
- Enrichissement des normes existantes pour la conception des DDR.

Le cas d'une barrière de sécurité est spécifié dans l'étude: l'analyse d'incertitude et l'optimisation robuste de la barrière sélectionnée sont réalisées avec IAO. Bien que tous les facteurs qui peuvent influencer les performances de la barrière ne puissent pas être analysés, les approches présentées peuvent être utilisées pour la conception d'autres DDR ou plus largement pour des systèmes d'ingénierie complexes.

La norme EN1317 définit les conditions d'impact pour l'évaluation des performances des DDR, en réalité les conditions de travail des DDR sont nombreuses. Pour le cas de la barrière, seulement un ou deux essais de chocs sous les conditions d'impact spécifiées dans les normes sont utilisés pour l'évaluation de ses performances. On peut espérer que l'analyse de robuste et l'analyse de généralisation (i.e. l'évaluation des performances des DDR sous des conditions d'impact différentes) du DDR pourraient enrichir les normes.

Chapitre 1 État de l'art

La nature générale d'une collision 'Run-Off-Road' (ROR) est que le véhicule est hors de contrôle et a au moins une collision avec soit l'équipement en bordure de la route, soit le bord de la route lui-même. Les collisions ROR représentent environ 10% du total des accidents de la route, alors que 45% des accidents mortels sont ROR. La présence des DDR peut réduire la sévérité des accidents (e.g. le DDR, barrière de sécurité routière, peut réduire les décès dans

les accidents routiers jusqu'à un facteur 4 par rapport aux collisions contre d'autres obstacles de la route). La conception des DDR, plus précisément, de la barrière de sécurité routière est étudiée dans le mémoire.

Contexte normatif --- EN1317

Les essais de chocs sont utilisés pour l'évaluation des performances des équipements routiers. La norme EN1317 définit les essais sur barrières. Les barrières ont classées en des niveaux de confinements différents selon l'utilisation des dispositifs. Les conditions d'impact sous les quelles les barrières de différentes niveaux doivent être testé ont définis dans la Table A- 4.

	Niveau de confinement	Essais	Conditions d'impact			
			Type de véhicule	Masse d'impact (kg)	Vitesse d'impact (km/h)	Angle d'impact (°)
Normal	N1	TB31	VL	1 500	80	20
	N2	TB11	VL	900	100	20
		TB32	VL	1 500	110	20
Elevé	H1	TB11	VL	900	100	20
		TB42	PL	10 000	70	15
	H2	TB11	VL	900	100	20
		TB51	Bus	13 000	70	20
	H3	TB11	VL	900	100	20
		TB61	PL	16 000	80	20
Très élevé	H4a	TB11	VL	900	100	20
		TB71	PL	30 000	65	20
	H4b	TB11	VL	900	100	20
		TB81	PL	38 000	65	20

Table A- 4 EN1317 Définition des conditions d'impact [13]

La Table A- 5 liste les indices de sévérité de choc : vitesse d'impact de la tête théorique (THIV) et Indice de gravité de l'accélération (ASI). La Table A- 6 done les classes de largeur de fonctionnement de la barrière (W). La performance globale d'un dispositif est présentée au niveau européen par une compilation de son niveau de retenue, de son niveau de largeur de fonctionnement et de sa classe de sévérité (e.g. N2-W2-A).

Sévérité	Critères		
A	ASI≤1,0	avec	THIV≤33 km/h
B	ASI≤1,4		
C	ASI≤1,9		

Table A- 5 EN1317 indices de sévérité [13]

W classes	Valeur (m)
W1	W≤0,6
W2	W≤0,8
W3	W≤1,0
W4	W≤1,3
W5	W≤1,7
W6	W≤2,1
W7	W≤2,5
W8	W≤3,5

Table A- 6 EN1317 Largeur de fonctionnement [13]

Simulation des essais de chocs sur les barrières

Les essais de chocs sont associés au développement d'un nouveau dispositif. La simulation numérique des chocs sert à: développer du nouveaux dispositifs ou optimiser des dispositifs existants ; certifier des produits modifiés.

Modèle du véhicule

Un véhicule peut contenir des milliers de composants et un temps très important peut être nécessaire à la modélisation détaillée de l'ensemble du véhicule. Des modèles détaillés avec des maillages fins augmenteront sans doute la précision de la simulation de choc. Pour réduire le coût de calcul, les modèles réduits sont avantageux dans le cas des simulations où les déformations du véhicule ne sont pas si influents et où un grand nombre d'exécution du modèle est nécessaire. Pour le cas des DDR, un grand nombre d'exécution du modèle est nécessaire pour les études de paramètres basés sur l'échantillonnage telles que l'analyse de l'incertitude du modèle et la conception structurale. Les modèles de véhicule doivent donc être simplifiés.

Modèle de la barrière de sécurité

La configuration de la barrière testée peut atteindre une centaine de mètres de longueur, et l'utilisation du modèle de l'ensemble du système est impraticable et inefficace du point de vue du calcul. Seules les composants au milieu de la barrière seront modélisées, et des contraintes sont appliquées aux deux extrémités de la barrière. Comme la barrière réoriente les véhicules principalement par la tension des lisses, des éléments de ressorts peuvent être fixés aux extrémités des lisses de la barrière pour simuler sa poursuite dans les deux directions et appliquer les contraintes.

Les composantes de la barrière (supports, lisses et écarteurs) sont reliés par des boulons à travers des trous oblongs. Dans l'essai de choc, certaines des connexions sont soumises à des forces élevées qui provoquent le cisaillement des boulons à travers les composants. Ce comportement est important pour la simulation de l'événement d'impact et influence considérablement la redirection du véhicule. Différentes approches sont disponibles pour simuler la connexion du boulon : modélisation des connexions en détail; simplification des

connexions en connectant les composants de la barrière avec les éléments de ressorts ou bien en fusionnant des noeuds des composants en-vis à-vis.

Les supports de la barrière sont fixés au sol. La simulation de l'interaction sol-support, qui joue un rôle vital dans la réponse de la barrière lors d'un choc, est complexe. Des matériaux solides ont définis dans LS-DYNA pour la modélisation du sol dans les simulations de chocs. Étant donné qu'il est coûteux en termes de temps de calculs, des éléments de ressort ont été utilisés pour simuler la réponse du sol lors de la simulation de choc de la barrière.

Figure A- 4 est un exemple du modèle d'essai de choc de la barrière, avec les conditions limites (i.e. extrémités de la barrière, connexion du boulon et sol) simplifiée par des éléments ressorts.

Figure A- 4 Un modèle d'essai de choc de la barrière [15]

Incertitude du modèle et Optimisation robuste

Les paramètres du modèle tels que les propriétés mécaniques des matériaux ne peuvent pas être définis exactement. Sous l'influence de la précision de fabrication, la tolérance des variables de conception contribue à l'incertitude d'un modèle. Presque tous les systèmes d'ingénierie sont sujets à des incertitudes, et la propagation de l'incertitude à travers le système donne lieu à des complexités correspondantes dans la simulation de la réponse structurelle. En fait, un modèle ne peut pas être validé au sens large, une bonne fois pour toutes. Au contraire, il est plus défendable et correct de dire qu'un modèle a été corroboré dans un cadre précis, ce qui signifie que le modèle a survécu à une série de tests. L'Analyse de Sensibilité (AS) consiste à étudier comment l'incertitude sur la performance d'un modèle peut être répartie entre différentes sources d'incertitude en entrée du modèle. L'AS permet l'analyse de la robustesse du modèle et la quantification des influences des incertitudes sur les entrées sur les variations de performance du modèle.

Un problème d'optimisation consiste à maximiser ou minimiser les sorties du modèle (objectifs) en choisissant des valeurs d'entrées (variables de conception) à partir d'un ensemble (contraintes). Les conceptions des dispositifs ont souvent plusieurs objectifs contradictoires, par exemple il est difficile de minimiser le coût économique et d'optimiser les performances d'un dispositif en même temps. Des facteurs incertains existent dans les systèmes d'ingénierie. Ces types d'optimisations sont appelées 'Multi-Objective Non-deterministic Optimization (MONO)'. Ils visent à obtenir des solutions de conception aussi 'meilleures' que possible, et en même temps limiter les variations dans leurs objectifs et les contraintes en raison d'incertitudes les paramètres d'entrée.

Conception de DDR

La conception d'une barrière de sécurité routière sera présenté dans ce mémoire. Les tâches principales sont les suivantes :

- Modélisation de la barrière et le véhicule: un modèle de l'essai de choc de la barrière avec un coût de calcul relativement faible est essentiel pour les études paramétriques fondées sur l'échantillonnage ;
- Les performances d'une barrière sont influencées par les facteurs incertains. L'AS de la barrière permet d'identifier les paramètres dont les incertitudes ont une grande influence sur les performances de la barrière et de quantifier ces influences. Seuls les facteurs influents seront ensuite utilisés lors de l'analyse robuste et de l'optimisation structurelle de la barrière. L'AS quantitative a besoin de milliers d'exécutions du modèle, et la recherche méthodologique pour l'AS des dispositifs compliqués tel que la barrière est une autre tâche importante de cette étude ;
- MONO pour augmenter les performances de la barrière en tenant compte des influences des facteurs incertains : les dimensions des composants de la barrière peuvent être traitées comme des variables de conception et l'optimisation de la barrière sera réalisée ;
- Les performances d'une barrière sont testées dans des conditions d'impact normalisées. Les conditions d'impact sont inconnues lors des accidents réels, la barrière optimisé doit donc être évalué dans des conditions d'impact différentes.

Chapitre 2 Méthodes de l'AS basée sur l'échantillonnage

Méthodes

Les approches d'analyse de sensibilité fondées sur l'échantillonnage sont à la fois efficaces et largement utilisées. La définition des distributions des entrées pour caractériser l'incertitude épistémique dans les données de sortie est l'une des parties les plus importantes pour l'AS car ces distributions influencent à la fois les incertitudes des sorties et la sensibilité des sorties aux entrées. De nombreuses méthodes d'échantillonnage sont disponibles, y compris l'échantillonnage aléatoire, l'échantillonnage factoriel fractionnaire, l'échantillonnage par hypercube latin, etc., et les stratégies du plan d'expériences (DOE) doivent être choisies en fonction de la demande des méthodes de l'AS. La propagation des échantillonnés du dispositif d'ingénierie contribue à créer la relation entre les entrées et sorties du modèle, et c'est souvent la partie la plus exigeante du point de vue informatique. Il faudra peut-être créer un métamodèle pour substituer le modèle complexe. La relation entre les entrées et les sorties sera étudiée par l'AS.

Les critères de choix pour la méthode d'AS sont résumés dans la Figure A- 5 [46]. La complexité du modèle (linéarité, monotonie, interactions, etc.) et le nombre de variables sont les deux facteurs à considérer.

Les avantages et les inconvénients des méthodes d'AS sont énumérés dans la Table A-7. Les méthodes graphiques donnent une vue intuitive de la complexité du modèle. Les AS avec corrélation et régression sont des méthodes qui peuvent être utilisées dans l'étude des relations entre les entrées et les sorties des modèles linéaires. Avec des biais acceptable, la méthode des transformations de rang linéarise des modèles 'non-linéaires mais monotones'. Les méthodes différentielles réduisent les échantillons en estimant la relation d'entrée et

sortie du modèle uniquement autour d'une position locale spécifiée. En général, nous n'avons pas beaucoup d'informations sur le comportement d'un dispositif d'ingénierie, les analyses de criblage utilisant des plans d'expérience à deux niveaux sont efficaces pour l'AS de modèle monotone. Le criblage multi-niveaux, l'analyse de Morris, peut être utilisé pour l'AS des dispositifs non monotones. Indépendamment de la linéarité et de la monotonie du dispositif, les méthodes fondées sur la variance (e.g. indices de Sobol) sont utilisées pour l'AS quantitative afin d'évaluer à la fois les effets principaux et les effets totaux des facteurs. Le calcul des indices de Sobol nécessite des milliers d'évaluations du modèle, et un métamodèle peut être nécessaire. L'AS par groupe permet d'isoler les paramètres influents, même avec un nombre d'échantillons inférieur au nombre de paramètres, et est proposé lorsque le nombre d'entrées est énorme.

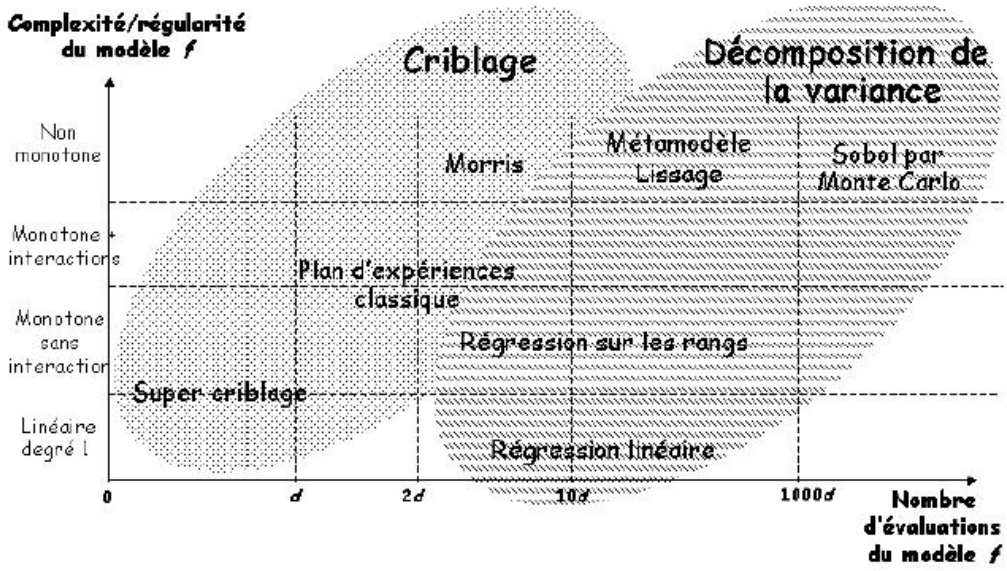

Figure A- 5 Synthèse des méthodes d'AS [46]

Méthodes	Avantages	Inconvénient
Méthodes graphiques	Méthode intuitive	Manque de critères d'évaluation
Régression / Corrélation	Efficacité pour l'évaluation de la corrélation des entrées et des sorties	Utiliser uniquement pour AS des modèles linéaires
Régression de rang	Linéarisation des modèles non linéaires mais monotones	Approximation avec sacrifice sur la précision du calcul
Différentielle	Efficacité pour l'étude des rapports entrée / sortie des modèles linéaires	Méthodes locales pour l'AS de modèle linéaire
Criblages à deux niveaux	Efficace pour l'AS de modèle monotone	Aucune information n'est obtenue sur la corrélation interne
Morris	Principales études d'effets d'interactions sur des modèles non monotoniques	Méthode qualitative avec un nombre élevé d'échantillons
Basées sur les variances	Méthodes quantitatives indépendamment des propriétés du modèle	Nombre élevé d'échantillons requis

Table A- 7 Comparaison des méthodes de l'AS différentes

Différentes méthodes peuvent être nécessaires pour l'AS d'un modèle complexe, la Figure A- 6 [48] illustre la stratégie pour l'AS d'un modèle complexe. Pour la barrière de sécurité routière étudiée : on ne peut pas faire d'hypothèses (linéarité, monotonie, interactions, etc.) sur le modèle ; une douzaine d'entrées doivent être analysés ; la simulation de modèle a un coût de calcul élevé. Les indices de Sobol peuvent être utilisés pour l'AS quantitatives de tels modèles, et l'analyse de criblage est préférable pour identifier les facteurs influents et réduire le nombre de facteurs d'entrée avant l'analyse quantitative.

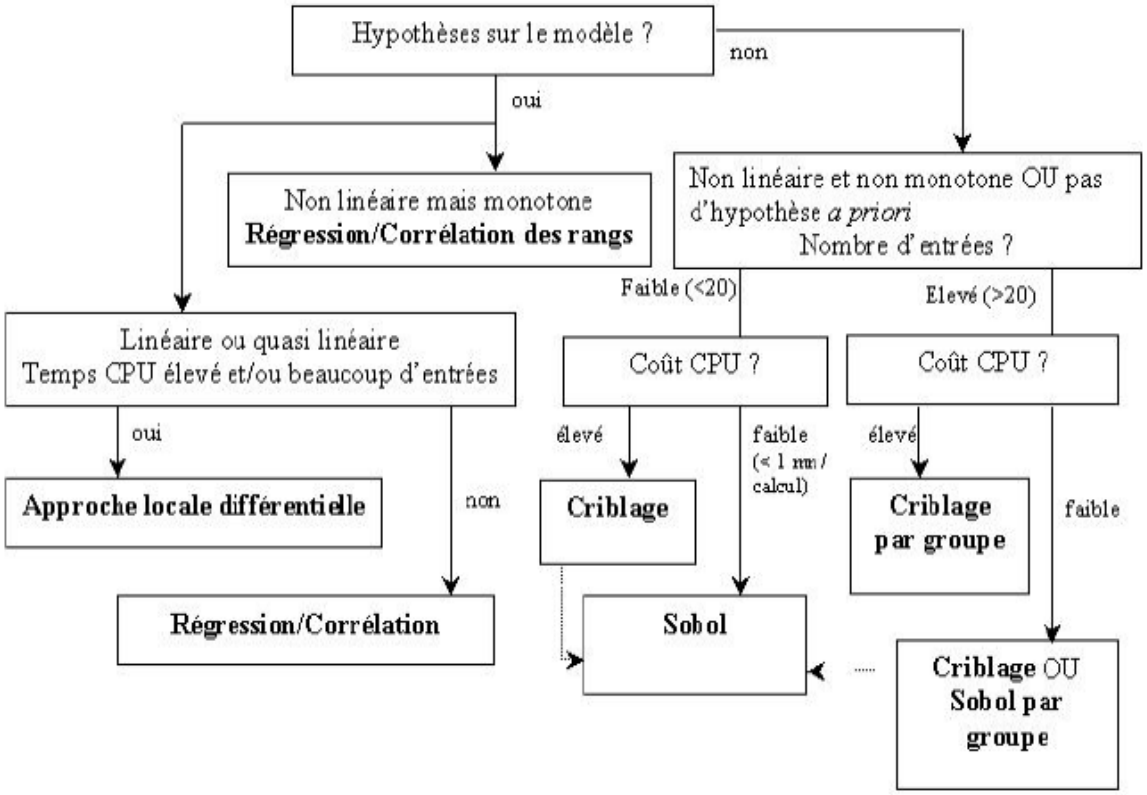

Figure A- 6 Diagramme de décision pour le choix de la méthode d'AS [48]

AS d'un modèle dynamiques de flexion trois points

Au lieu d'analyser directement le modèle de la barrière de sécurité routière dont le coût de simulation est élevé, différentes méthodes de criblages et les indices de Sobol sont utilisés pour tester les méthodes d'AS sur un modèle dynamique simple. L'efficacité et l'exactitude des méthodes de criblages sont étudiées et la stratégie pour l'AS de la barrière et d'autres dispositifs d'ingénierie complexes sont discutées. Le modèle simple étudié est un essai dynamique de flexion trois points d'une poutre en bois renforcé par un plat en acier (Figure A- 7) [49], qui représente un sous-ensemble d'une barrière. La simulation de d'essai est montré dans la Figure A- 8.

Les méthodes de criblages visent à identifier qualitativement les influences de l'entrée sur la sortie du modèle. L'analyse de Morris et le criblage à deux niveaux avec les plans fractionnaires sont proposés pour l'AS qualitatives des modèles de type boîtes noires.

- En prenant des valeurs multiples pour chaque facteur d'entrée, l'analyse de Morris peut être utilisée pour l'AS de modèle non monotone et l'effet d'interaction entre les

entrées peut être testé avec cette méthode.

- Des criblages à deux niveaux sont utilisés pour l'AS des modèles monotones, et différentes stratégies existent pour la sélection des échantillons. Pour prendre en compte toutes les combinaisons de tous les facteurs k à 2 niveaux, 2^k échantillons sont nécessaires en utilisant un plan factoriel complet. Par conséquent, le principal inconvénient du plan factoriel est l'énorme nombre de simulations requises, en particulier pour les modèles avec de nombreuses variables. Consistant en une fraction soigneusement choisie du plan factoriel complet, les plans fractionnaires peuvent considérablement diminuer le nombre d'échantillons. Le criblage à deux niveaux à l'aide des matrices orthogonales (un des plans fractionnaires) est l'une des méthodes de l'AS les plus efficaces.

Les facteurs influents sont identifiés après l'analyse de criblage et leurs influences peuvent être quantifiées avec les indices de Sobol.

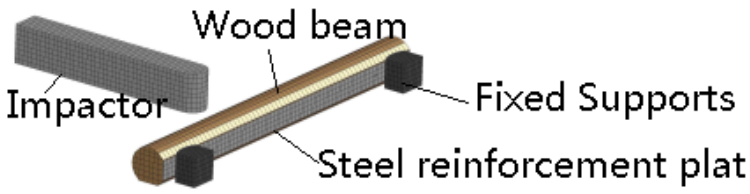

Figure A- 7 Le modèle numérique de l'essai de flexion [49]

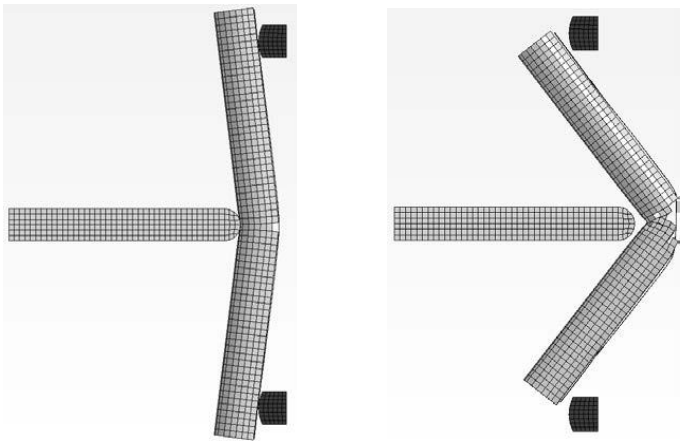

Figure A- 8 Simulation de l'essai de flexion : t = 0,02s (gauche) et rupture du poutre (droite)

Méthodologies pour l'AS de modèles complexes

Les étapes de l'AS quantitative des modèles d'ingénierie complexes sont résumées comme suit:

1) Le criblage avec le plan factoriel fractionnaire à deux-niveaux (e.g. matrices orthogonales)
2) Le criblage multi-niveaux (e.g. l'analyse de Morris)
3) L'analyse quantitative basée sur les variances (e.g. Indices de Sobol)

Un modèle complexe peut avoir des dizaines ou des centaines de facteurs d'entrée, mais

seulement quelques-uns d'entre eux peuvent avoir une influence importante sur la robustesse du modèle. En choisissant soigneusement les échantillons, bien qu'avec une précision faible pour l'AS, les criblage à deux niveaux sont les méthodes les plus efficaces. La contrainte de cette approche est que le modèle étudié doit être monotone.

Limité par la précision du calcul, le criblage à deux niveaux ne peut sélectionner que les variables influentes. Les variables non influentes seront alors considérées comme constantes, ce qui peut grandement faciliter le criblage à multi-niveaux. L'analyse de Morris peut être ensuite utilisée pour classer les variables influentes.

Les quelques variables ayant une grande influence sur les performances du modèle seront identifiées après le criblage à niveaux multiples. L'analyse quantitative basée sur la variance (e.g. indices de Sobol) sera ensuite utilisée pour quantifier les influences des variables influentes. Même pour un modèle avec peu de variables, des milliers d'exécutions de modèle pourraient être nécessaires pour l'AS quantitative, un métamodèle (modèle de substitution) peut être utilisé pour permettre des évaluations à moindre coût de calcul.

Chapitre 3 Analyse de sensibilité d'une barrière

Essai de choc de la barrière et modèle numérique

En suivant la norme Européenne EN1317 [12][13], l'essai de choc d'une barrière acier est réalisé par le laboratoire LIER[60]. La longueur du dispositif est de 60m. A chaque extrémité, la barrière comporte des lisses abaissées sur 12m. Le véhicule (BMW 520i), d'une masse de 1431 kg arrive sur le dispositif à la vitesse contrôlée de 113,6 km/h, sous un angle de 20 ° [61]. La Figure A- 9 montre la trajectoire du véhicule dans l'essai de choc. Le véhicule ne brise pas la barrière ; le véhicule ne se renverse pas sur la zone d'essai ; la barrière est de niveau de confinement N2, de largeur de fonctionnement W5 et de niveau de sévérité de choc A d'après la norme EN1317.

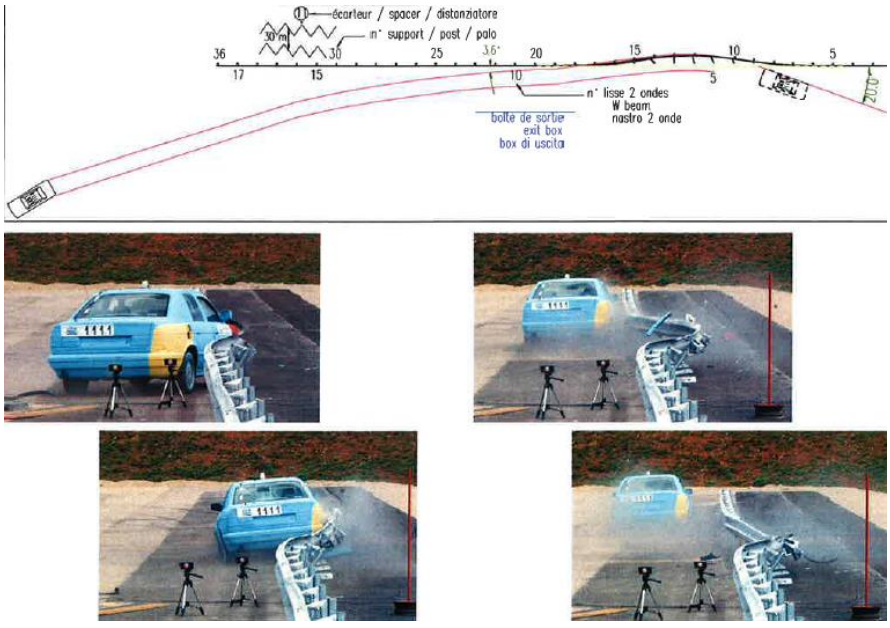

Figure A- 9 L'essai de choc de la barrière et la trajectoire du véhicule [61]

La Figure A- 10 montre les profils des composants de la barrière et leurs maillages :

a) Les lisses (rails) sont des profilés 2 ondes de longueur 4315mm, avec *E*=81mm, *H*=310mm ;
b) Les supports (post) sont de longueur 1500 mm, avec *A*=100mm, B=50mm ;
c) Les écarteurs (spacers) mécanosoudés sont fixés aux supports par vis & écrou ;
d) Les supports sont fichés dans le sol

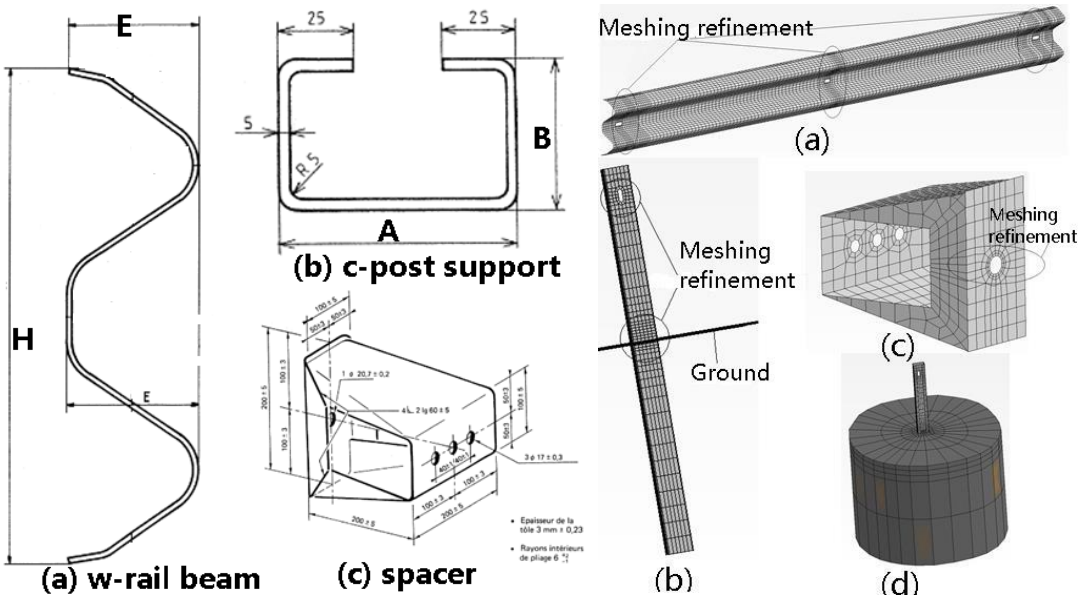

Figure A- 10 Profils des composants de la barrière et les maillages des composants

Le modèle réduit du véhicule avec des maillages grossier est fourni par LIER. Les maillages des parties qui sont en contact avec la barrière pendant l'impact est raffiné (voir Figure A- 11).

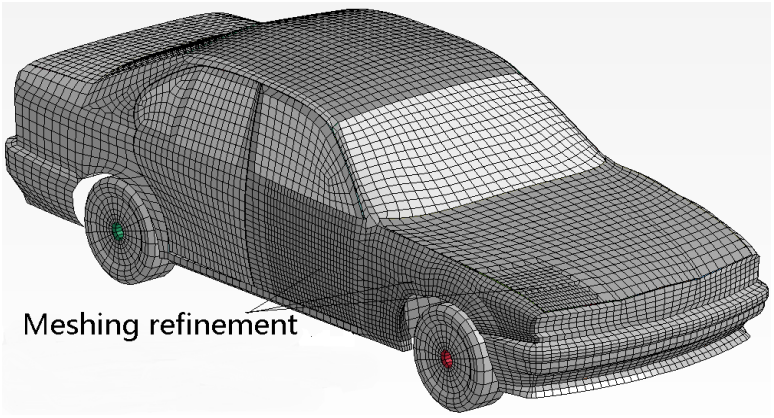

Figure A- 11 Modèle du véhicule de LIER et zones raffinées

Compte tenu de l'amplitude des déformations des composants lors de l'essai de choc de la barrière, le modèle numérique de la barrière a été simplifié:

- Modèle réduit avec raffinement de maillage pour les pièces de déformation remarquable;

- Applications des conditions aux limites dans le prolongement de la barrière à l'aide d'éléments ressort aux extrémités de la lisse;
- Modélisation détaillée du sol avec des éléments solides pour les pièces de déformation évidente et remplacement par des éléments ressort pour les autres parties de sol ;
- Simplification des composants de connexions pour les connexions lisse-lisse et modélisation détaillée pour les connexions support-écarteur et écarteur-lisse compte tenu de la magnitude de déformation et des degrés de liberté des composants.

Le modèle d'essai de choc est montré dans la Figure A- 12. La comparaison entre essai et simulation des déroulements temporels de l'impact est illustré par la Figure A- 13. Les critères de performance de la barrière mesurés par l'essai et par la simulation sont listés dans la Table A- 8.

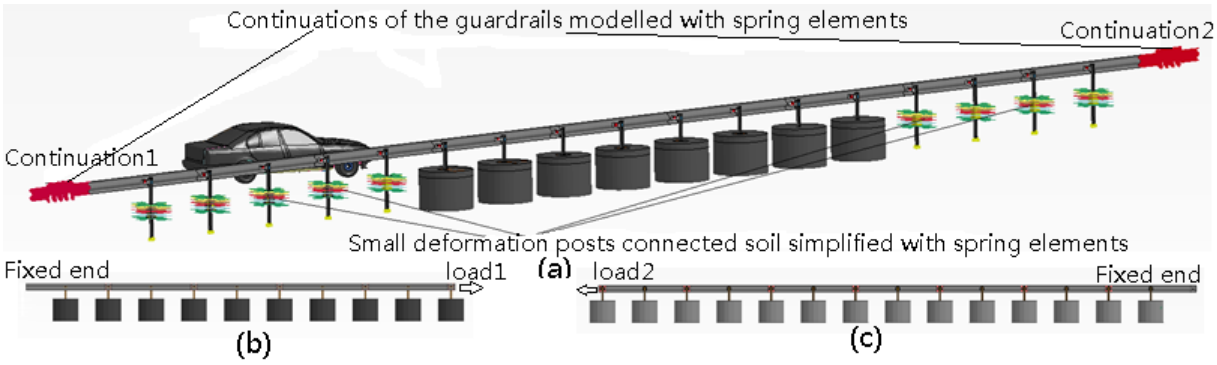

Figure A- 12 Le modèle d'essai de choc de la barrière

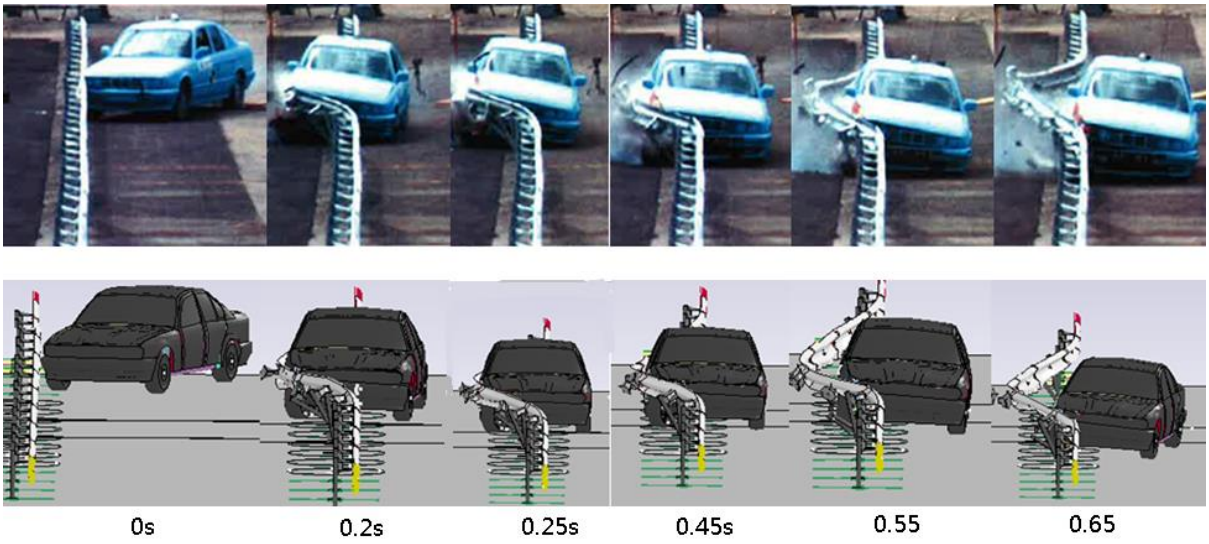

Figure A- 13 L'essai de choc et la simulation

	ASI	THIV(km/h)	W(m)
Essai	0,8	24	1,5
Simulation	0,8	22	1,5

Table A- 8 Comparaison des résultats de l'essai et de la simulation

AS de la barrière

La barrière est fabriquée en acier S235. Les incertitudes sur l'acier influencent les propriétés mécaniques des composants de la barrière. Des tolérances existent dans l'épaisseur des composants. Des incertitudes existent pour l'installation de la barrière. Supposons que les facteurs incertains ont des distributions normales, 11 variables sont choisies et leur distributions sont listées dans la Table A- 9.

Incertitudes	Composants	Variables	Abr.	Unité	moyenne	Écart-type
Propriétés mécaniques de l'acier S235	Lisses	Limite d'élasticité	*RY*	MPa	284,5	21,5
		Module d'Young	*RM*	GPa	203	12,6
	Écarteurs	Limite d'élasticité	*SY*	MPa	284,5	21,5
		Module d'Young	*SM*	GPa	203	12,6
	Supports	Limite d'élasticité	*PY*	MPa	284,5	21,5
		Module d'Young	*PM*	GPa	203	12,6
Tolérances de fabrication	Lisses	Épaisseur	*RT*	mm	3	0,15
	Écarteurs	Épaisseur	*ST*	mm	3	0,15
	Supports	Épaisseur	*PT*	mm	5	0,25
Conditions d'installation	Sol	Module en vrac	*SoilM*	MPa	400	100
	Boulon	Préchargement	*BP*	N	12432	4144

Table A- 9 Les facteurs incertains de la barrière

La vitesse d'impact théorique de la tête (*THIV*) et la déformation dynamique (*D*) de la barrière sont choisis comme les critères de performance de la barrière. L'AS de la barrière est réalisée en trois étapes :

- Les résultats du criblage à deux-niveaux avec matrices orthogonales (OA) sont montrés dans la Table A- 10. Les effets principaux (*ME*) des 11 facteurs sont calculés. Six facteurs sont influents d'après le criblage avec OA ;
- Les six facteurs choisis après le criblage de OA sont recriblés avec l'analyse de Morris et les résultats sont montrés dans la Figure A- 14. Les effets principaux *ME* et les effets d'interaction (*Inter*) sont calculés, et les trois facteurs les plus influents d'après l'analyse de Morris sont *PY*, *RT* et *PT*.
- Les influences des trois facteurs *PY*, *RT*, *PT* sont quantifées avec les indices de Sobol et les résultats sont montrés dans la Figure A- 15.

Les résultats sont résumés dans la Table A- 11. Trois variables ont été identifiées comme influentes après les analyses de criblage OA et Morris (avec respectivement 12 et 42 évaluations du modèle). 120 évaluations sont utilisées pour créer le métamodèle avec une interpolation de type Krigeage, et les sensibilités des trois variables sélectionnées ont été quantifiées avec les indices de Sobol en utilisant le métamodèle. Deux des trois variables influentes ont été classées comme ayant des influences critiques sur les performances de la barrière : la tolérance sur l'épaisseur de support (*PT*) et l'incertitude sur la résistance de l'acier du support (*PY*). Il est coûteux de mesurer la densité de probabilité de tous les 11 variables. Les hypothèses aident à définir les distributions de probabilité des paramètres incertains dans l'AS de la barrière et les deux paramètres les plus influents sont identifiés

après l'analyse. Des efforts supplémentaires sont nécessaires pour mesurer la densité de probabilité réelle des deux paramètres incertains influents, et cela permet d'augmenter la précision du modèle numérique.

Le moyen le plus efficace pour augmenter la robustesse du modèle est de diminuer la tolérance de fabrication sur l'épaisseur de support. Une autre façon pour augmenter la robustesse du modèle est de construire les supports avec un acier fabriqué par le même fabricant dans les mêmes conditions de fabrication (i.e. diminuer l'incertitude de *PY*). L'AS peut également fournir des informations utiles pour la conception de la barrière. En raison de leur grande influence sur les performances du modèle, les incertitudes des deux variables *PT* et *PY* doivent être prises en compte dans l'optimisation de la barrière.

Parameters	*THIV*		*D*	
	ME (km/h)	Rank	*ME* (mm)	Rank
RY	**-0.4029**	**1**	**-9.8**	**4**
RM	**0.1227**	**8**	**9.8**	**4**
SY	0.1281	7	-9.7	6
SM	0.1446	6	0	11
PY	**0.2896**	**3**	**-33.5**	**1**
PM	0.2315	5	-1.2	10
RT	**0.1222**	**9**	**-14.7**	**3**
ST	**-0.2402**	**4**	**-7.8**	**8**
PT	**0.3971**	**2**	**-32.2**	**2**
SoilM	-0.0116	11	-9.7	6
BP	0.0840	10	-2.2	9

Table A- 10 *ME* des facteurs criblés par OA

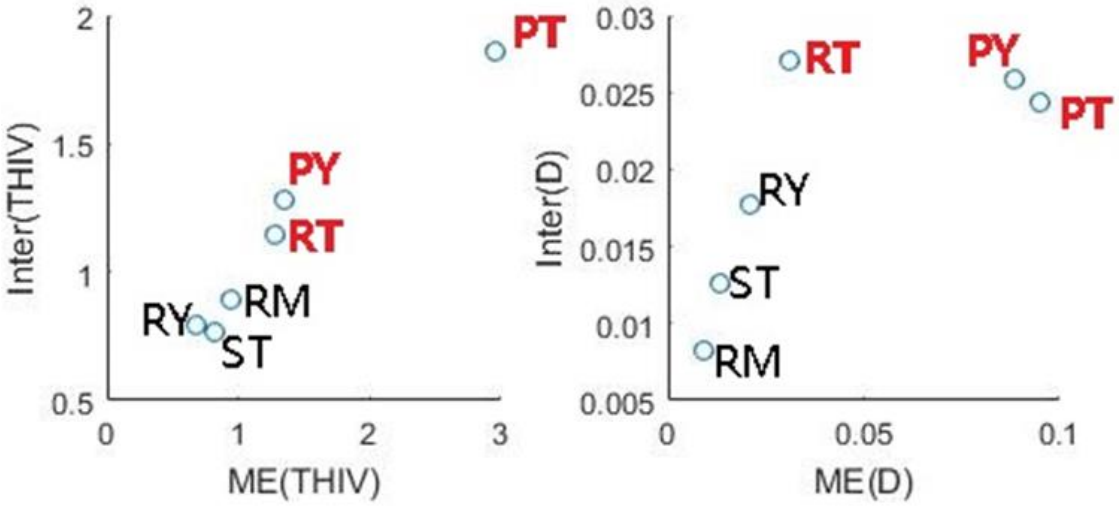

Figure A- 14 *ME* et *Inter* avec *THIV* et *D* comme critères pour le criblage de Morris

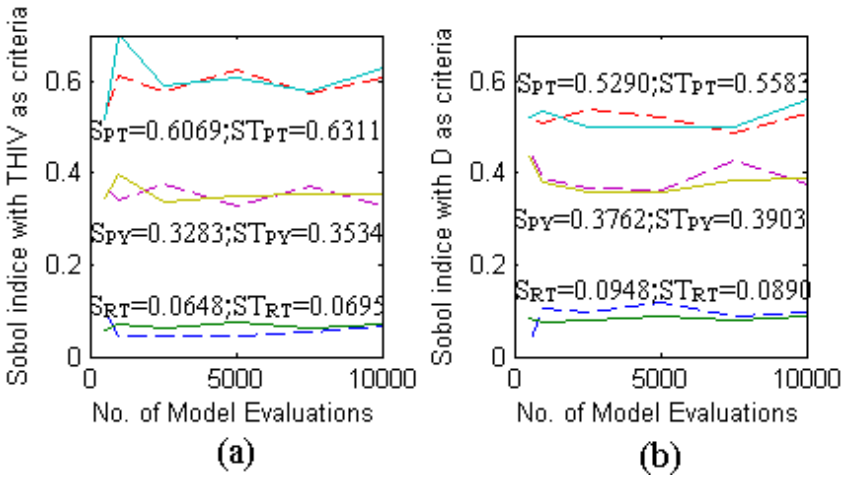

Figure A- 15 Évolution des indices de Sobol (a) critère *THIV* (b) critère *D*

11 facteurs incertains	***RY, RM, SY, SM, PY, PM, RT, ST, PT, SoilM, BP***
Étape 1: criblage de OA	12 échantillons
Facteurs choisis après OA	***RY, RM, PY, RT, ST, PT***
Étape 2: criblage de Morris	42 échantillons
Facteurs choisis après Morris	***PY, RT, PT***
Étape 3: Indices de Sobol	120 échantillons pour la création du métamodèle
Facteurs critiques	***PY, PT***

Table A- 11 Résumé AS de la barrière effectuée en trois étapes

Chapitre 4 Optimisation de la barrière

Optimisation non déterministe multi-objectifs (MONO)

De nombreux problèmes de conception ont des objectifs multiples et des contraintes non linéaires. De plus, les incertitudes des paramètres d'entrée sont inévitables et peuvent considérablement dégrader les performances d'une conception. Ces problèmes et les méthodes de solution correspondantes forment le champ de recherche appelé optimisation non déterministe multi-objectifs (MONO). L'optimisation multi-objectifs est également connue sous le nom d'optimisation de Pareto. Un optimum de Pareto est une allocation des ressources pour laquelle il n'existe pas d'alternative dans laquelle tous les acteurs seraient dans une meilleure position. L'ensemble des optimums de Pareto est la "frontière d'efficacité de Pareto", à partir de laquelle la solution optimale pourrait être choisie en fonction des exigences du concepteur. Les tendances des problèmes d'optimisations sont de minimiser les objets **F**, puisque la maximisation de l'objet **F** équivaut à minimiser **-F**.

Les défis pour la MONO des dispositifs d'ingénierie complexes comme la barrière de sécurité routière incluent: le coût de calcul élevé de la simulation ; les nombreux facteurs incertains dans le modèle ; le manque d'information sur l'espace de conception et sur les incertitudes du modèle. L'essai de choc d'une barrière en acier a été réalisé par LIER. Dans les études précédentes :

- L'essai de choc a été simulé avec un modèle simplifié sur LS-DYNA, qui nécessite un temps de simulation relativement faible (5 heures par simulation);
- 11 facteurs incertains sont initialement sélectionnés. Après l'AS de la barrière, 2 des facteurs incertains, i.e. la tolérance de l'épaisseur de support (*PT*) et l'incertitude de la résistance de l'acier du support (*PY*), ont été identifiés comme ayant des grandes influences sur les performances de la barrière et leurs influences ont été quantifiées. Au lieu de considérer les incertitudes des 11 facteurs, seules les incertitudes de *PY* et de *PT* seront considérées dans la MONO de la barrière.

Pré-étude de l'optimisation

Les composants de la barrière sont illustrés dans la Figure A- 10. Les paramètres de dimensions *H*, *E*, *A*, *B* sont utilisés comme variables de conception. La limite inférieure et la limite supérieure de chaque variable sont prédéfinies comme diminution et augmentation de la valeur initiale de 20%. 50 échantillons ont été prélevés avec DOE et les performances de la barrière ont été analysées dans l'espace de conception prédéfini : la diminution des dimensions des lisses, en particulier la valeur de *E*, dégrade la capacité de réorientation de la barrière (voir Figure A- 16) ; la diminution des dimensions des supports augmente considérablement la déformation de la barrière. Les intervalles de conception sont mis à jour et répertoriés dans la Table A- 12.

Considérant les influences des deux facteurs incertains, ainsi que la masse du dispositif (i.e. le coût de production), la robustesse du dispositif est définie comme des contraintes de la conception. Les intervalles de variation des contraintes sont étudiées et le vecteur des limites supérieures des contraintes $\mathbf{\Lambda}$ sont définies d'après les variations de contraintes.

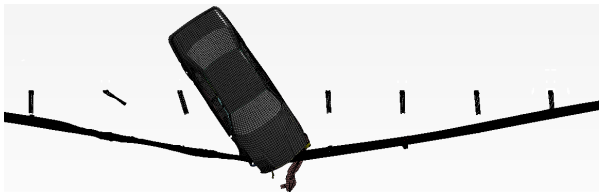

Figure A- 16 Échec de la réorientation du véhicule : *H* et *E* diminuent considérablement

Variables	inférieure	Initiale (mm)	supérieure
H	-15%	310	25%
E	-10%	81	25%
A	-20%	100	25%
B	-15%	50	25%

Table A- 12 Les intervalles des variables de conception

Le métamodèle est utilisé pour remplacer le modèle de simulation d'impact dans l'optimisation, la précision du métamodèle doit être assurée. Au lieu d'évaluer le métamodèle à travers l'espace des entrées, nous avons proposé une nouvelle approche pour affiner les échantillons autour des solutions optimales potentielles, ce qui réduit considérablement les échantillons supplémentaires nécessaires pour créer le métamodèle. Environs 260 exécutions sont utilisées pour la création du métamodèle avec le Krigeage.

Conceptions optimales

L'algorithme génétique est utilisé pour l'optimisation multi-objectifs. Les objectifs de l'optimisation sont de minimiser la vitesse d'impact théorique de la tête (*THIV*) et la déformation dynamique (*Dd*) de la barrière. Les performances des solutions optimales et de la conception initiale sont illustrées Figure A- 17. Les valeurs des entrées des solutions optimales sont dans la Figure A- 18.

- Les entrées *E* et *B* sont proposées d'être augmentées avec leurs valeurs d'échelle modifiées dans l'intervalle [1,16 1,24] et dans l'intervalle [1,16 1,25] respectivement ;
- On propose de diminuer la valeur de l'entrée *A* (conception *b*, *c*, *d*, *e*) lorsque la minimisation de *Dd* n'est pas d'importance critique; *A* est proposé d'être augmenté et *H* est proposé d'être diminué où l'objet principal de la conception est de minimiser la déformation et d'augmenter le niveau de confinement du dispositif.

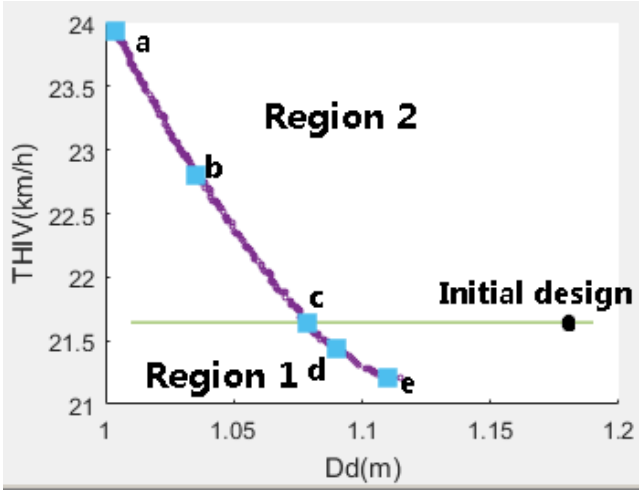

Figure A- 17 Les solutions optimales de MONO de la barrière

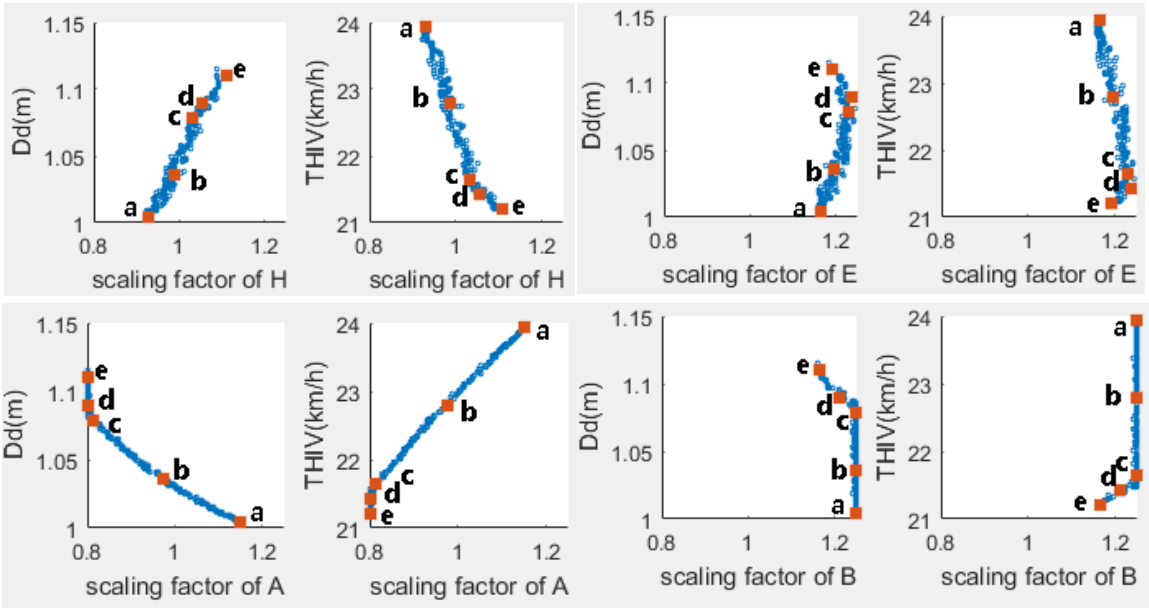

Figure A- 18 Les valeurs d'entrée des solutions optimales

En résumé, les dimensions de la lisse, en particulier pour la variable *E*, doivent être augmentées afin d'augmenter la capacité d'absorption d'énergie de la barrière; le composant support est de forme rectangulaire (voir Figure A- 10) avec *A*=100mm, *B*=50mm. La variable *A* est proposée d'être diminuée et l'entrée *B* est proposée d'être augmentée ; de plus, il faut plus de matière pour augmenter la rigidité de la barrière et diminuer la sortie *Dd*.

Géneralisation des conditions d'impacts

La barrière est optimisée sous des conditions d'impact fixées (i.e. TB32 défini dans la norme EN1317). En réalité, les véritables accidents sont plus complexes:

- Les conditions d'installation de l'équipement routier sont innombrables : la barrière longitudinale droite est étudiée bien que les installations courbes existent ; un sol plat est recommandé même si les installations sont parfois situées sur une rampe d'accès ;
- Le véhicule peut être de types différents (bus, camion, voiture, etc.) ; la vitesse et l'angle d'impact, le point d'impact, le coefficient de frottement de la route et le pneu, etc. ne sont pas des facteurs fixes.

Les performances de la barrière optimisée ont été évaluées dans des conditions d'impact généralisées. Contraintes par le modèle numérique, seule la vitesse et l'angle d'impact ont été considérés. Pour optimiser à la fois le *THIV* et le *Dd*, la conception *e* (voir Figure A- 17) est choisie. Les vitesses (*v*) et les angles (*a*) d'impact avec *THIV* aux valeurs [18 21 24 27 30] km/h et avec déformation *W* au niveau [W2 W3 W4 W5 W6] (voir Table A- 6) sont créées dans Figure A- 19 et dans Figure A- 20 :

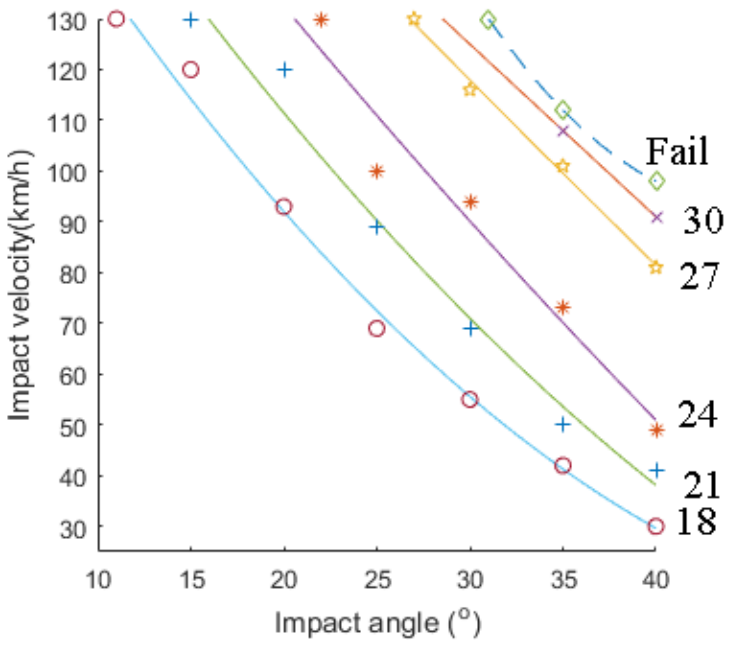

Figure A- 19 Évolution du THIV en fonction de l'angle et de la vitesse d'impact du véhicule

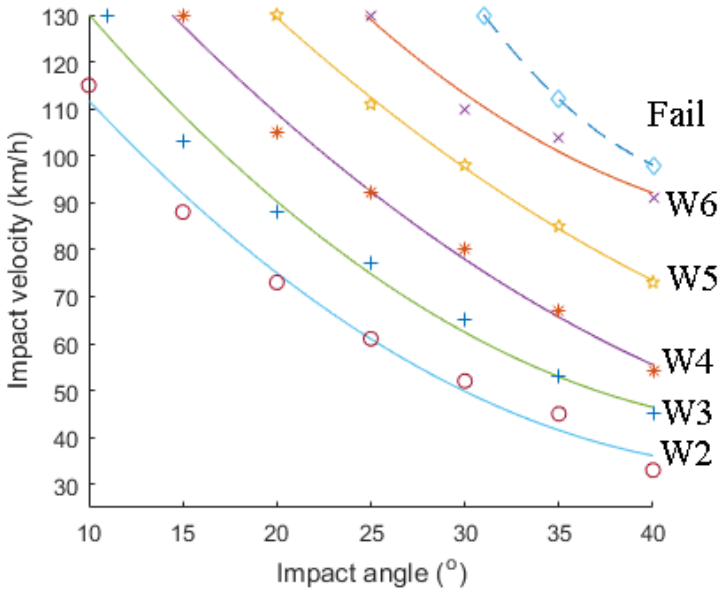

Figure A- 20 Évolution de la largeur de fonctionnement en fonction de l'angle et de la vitesse d'impact du véhicule

- La barrière ne réoriente pas le véhicule dans les conditions extrêmes de choc pour des valeurs importantes de l'angle et de la vitesse, e.g. v=130km/h, a> 32 ° ou v>100km/h, a=32 °. La ligne de défaillance sous laquel le dispositif a bien redirigé le véhicule est représentée en traits interrompus sur la Figure A- 19 et sur la Figure A- 20 ;
- Sous toutes les conditions d'accident possibles, la gravité de l'accident est de niveau **A** (voir Table A- 5). Les indices de gravité sont limités au niveau acceptable.
- Le dispositif fonctionne bien pour une petite valeur de l'angle d'impact: nous avons *THIV*<18km/h et *Wm*<*W*3 quand a=10 °, même pour v=130km/h, qui est la limitation de vitesse sur la plupart des autoroutes. L'augmentation de l'angle d'impact peut grandement augmenter la gravité de l'impact et les déformations de la barrière.

Conclusion générale

Des incertitudes existent dans les DDR, et un essai de choc d'un DDR ne peut pas être répété sous des mêmes conditions d'impact strictement identiques. En ce qui concerne les simulations numériques, un modèle est parfois difficile à valider à cause des facteurs incertains. Dans la conception robuste du DDR :

- La simulation numérique est utilisée pour l'étude structurelle du DDR, et le modèle doit être simplifié car les études paramétriques du DDR nécessitent des centaines d'exécutions des modèles.
- L'AS aide à identifier les facteurs incertains influents. Les simulations en tenant compte des variations des facteurs incertains influents aident à évaluer la robustesse d'une conception et donnent un nuage de résultats dans lequel le résultat d'essai expérimental est contenu avec une probabilité donnée. Les efforts pour mesurer les densités de probabilité des facteurs influents peuvent améliorer la précision de la simulation, et les réductions des incertitudes des facteurs influents aident à accroître la robustesse de la conception.
- Les conceptions optimales robustes peuvent être obtenues en tenant compte des

variations des facteurs incertains influents.

La norme européenne, EN1317, a normalisé les conditions d'essai de choc pour les DDR de niveaux de confinement différents et a défini les critères qualitatifs et quantitatifs de performance des dispositifs. Il fournit une ligne directrice pour la conception de DDR, mais pourrait encore être révisé:

- Les études statistiques des données sur les accidents de la circulation aident à préciser les conditions d'impact de l'accident. Les sensibilités des performances du DDR aux conditions d'impact pourraient être étudiées par des simulations numériques. Les conditions d'impact normalisées dans EN1317 doivent être définies en fonction de l'objectif des essais de chocs. Par exemple pour l'évaluation des performances de la barrière du niveau de confinement N2 qui a été discutée dans cette étude, supposons que les conditions d'impact TB32 définies dans EN1317 représentent les accidents les plus courants d'après les études statistiques. La barrière pourrait subir des conditions d'impact plus fatales. Ses performances sont sensibles à l'angle d'impact selon l'étude numérique, l'essai de choc de la barrière avec un angle d'impact plus important permettrait d'évaluer ses performances lors d'accidents graves et les conditions d'impact relatives pourraient être ajoutées à EN1317 ;
- EN1317 ne tient pas compte des facteurs incertains. Les analyses d'incertitude et de sensibilité aident non seulement à évaluer les intervalles possibles des performances d'une conception, mais aussi à la conception robuste de l'appareil.
- Même un DDR bien conçu pourrait ne pas sauver des vies dans les accidents. Bien que le niveau de sévérité de l'essai de choc d'un DDR avec des conditions d'essai normalisées pourrait être **A**. Il est important à déterminer les conditions d'impact sous lesquelles plus de blessures pourraient être causées aux passagers et le niveau de sévérité **B,** et sous lesquelles les accidents mortels se produisent.

Bien qu'ils ne puissent pas être évalués directement avec des essais de chocs, la robustesse du DDR et l'influence des conditions d'impact sur les performances du DDR pourraient être étudiées par les simulations et les critères relatifs pourraient être ajoutés à EN1317.

Les limitations principales de cette étude sont:

- Environ 500 d'exécutions de modèle ont été réalisés dans l'ensemble pour les analyses. Des efforts sont nécessaires pour simplifier le modèle de la simulation afin de réduire le temps d'exécution d'un seul modèle.
- La barrière a été analysé dans des conditions d'essai normalisées et tous les paramètres ne sont pas pris en considération. En dehors de la vitesse et de l'angle d'impact, de nombreux autres facteurs comme le type du véhicule, la position d'impact, la force de frottement entre le pneu et la route peuvent influencer la réorientation du véhicule ;
- Seuls les dimensions des composants de la barrière sont considérés comme facteurs. Il existe de nombreux autres facteurs de conception. Les études de ces facteurs pourraient faire l'objet d'étude ultérieures.